The early stages of stellar cluster formation

Aina Palau Puigvert
Instituto de Radioastronomía y Astrofísica
Universidad Nacional Autónoma de México

The early stages of stellar cluster formation

R. Estalella, P. T. P. Ho, J. M. Girart, A. Fuente, Q. Zhang, Á. Sánchez-Monge, G. Busquet,
B. Commerçon, P. Hennebelle, E. Vázquez-Semadeni, J. Ballesteros-Paredes, L. Zapata

Introduction

Inside 0.1 pc: method + first results

Density and T structure

Role of rotation, turbulence and B

Inside 0.01 pc: ALMA

Introduction

Inside 0.1 pc: method + first results

Density and T structure

Role of rotation, turbulence and B

Inside 0.01 pc: ALMA


Orion Nebula, HAWK-I infrared camera on VLT, ESO, H. Drass et al.


Pipe Nebula. Ezequiel Bellocchio
Approach: the first stages of cluster formation should start at cloud fragmentation

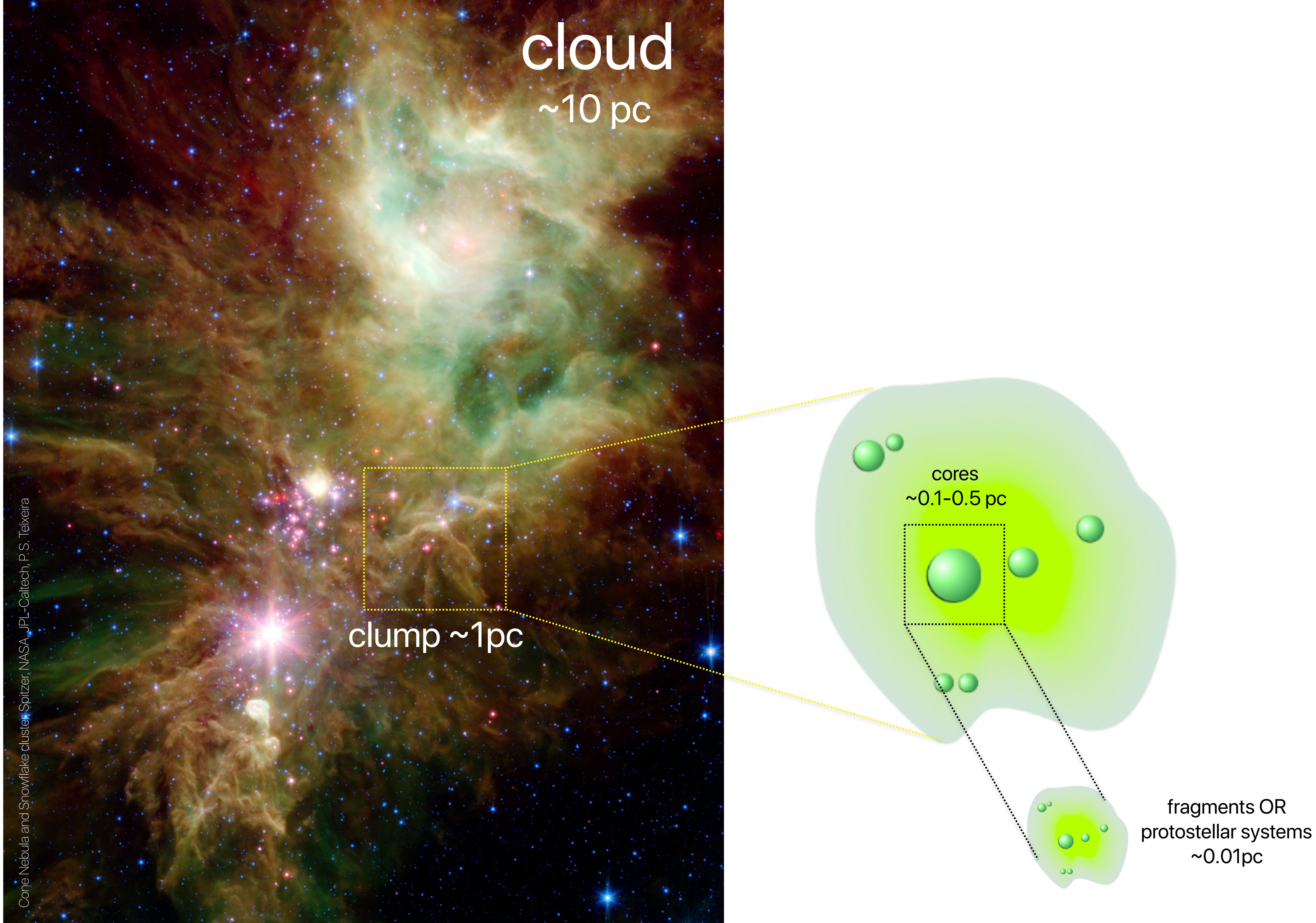
cloud
~10 pc
clump ~1pc
Cone Nebula and Snowflake cluster, Spitzer, NASA, JPL-Caltech, P. S. Teixeira
cores
~0.1-0.5 pc
fragments OR
protostellar systems
~0.01pc

Jeans criterion (1902): a fragment will collapse if its gravitational energy overcomes its thermal energy

Core: T, n

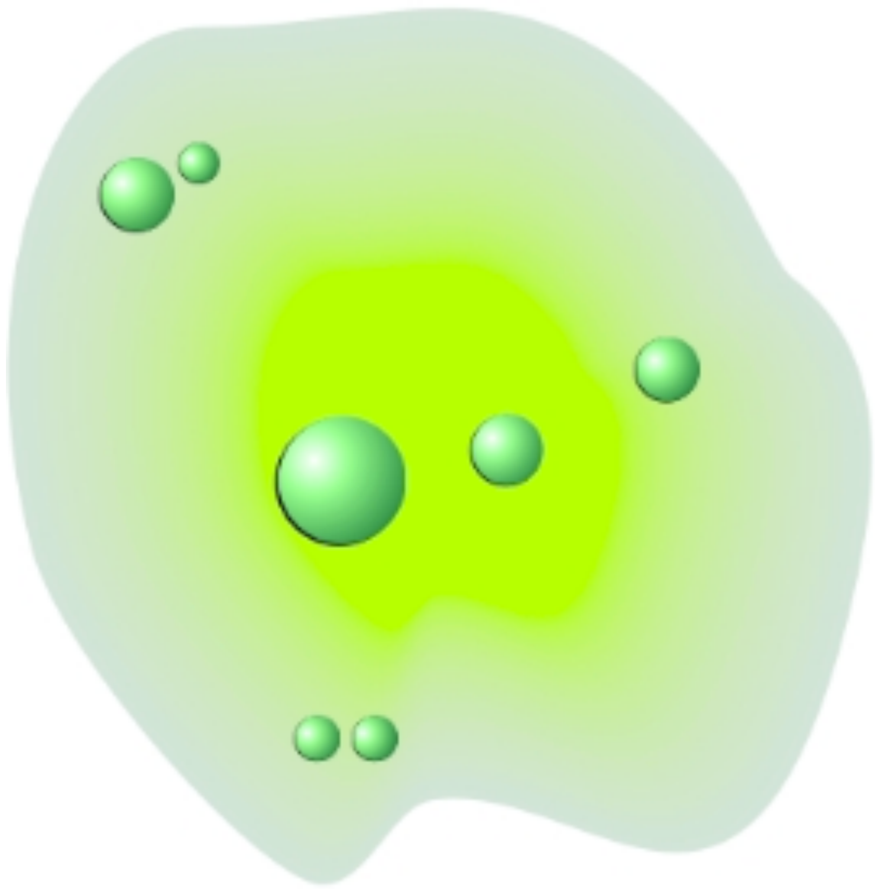

$$\left[\frac{M^{\rm th}_{\rm Jeans}}{M_\odot}\right] = 0.6285\left[\frac{T}{10\,{\rm K}}\right]^{3/2}\left[\frac{n_{\rm H_2}}{10^5\,{\rm cm^{-3}}}\right]^{-1/2}$$

Thermal Jeans fragmentation: efficient at producing low-mass fragments

Up to here: only gravity and thermal pressure taken into account

"Generalized" Jeans criterion: adapted to take into account other forms of support: turbulence

Core: Δv, n

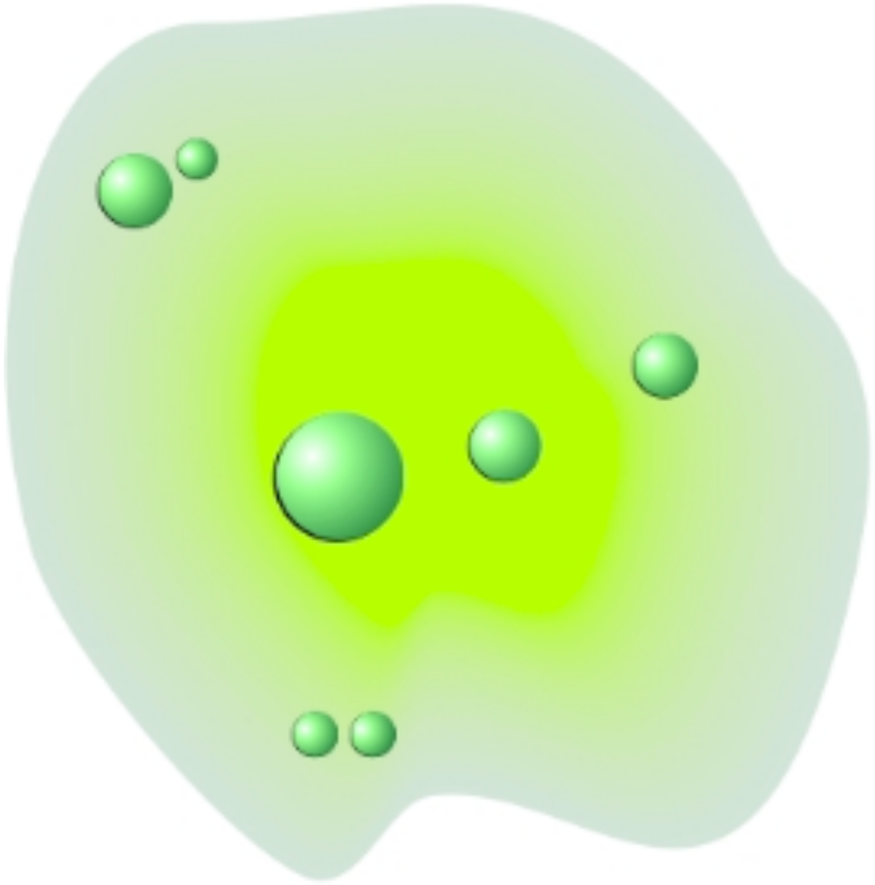

$$\left[\frac{M_{\rm Jeans}^{\rm nth}}{M_\odot}\right] = 0.8255 \left[\frac{\sigma_{\rm 1D,nth}}{0.188\,{\rm km\,s^{-1}}}\right]^3 \left[\frac{n_{\rm H_2}}{10^5\,{\rm cm^{-3}}}\right]^{-1/2}$$

Chandrasekhar 53

Turbulent Jeans fragmentation -> M_J ~ 120 M_{sun} (sigma ~ 1km/s) -> naturally yields massive fragments, but only a few

"Generalized" Jeans criterion: adapted to take into account other forms of support: magnetic field

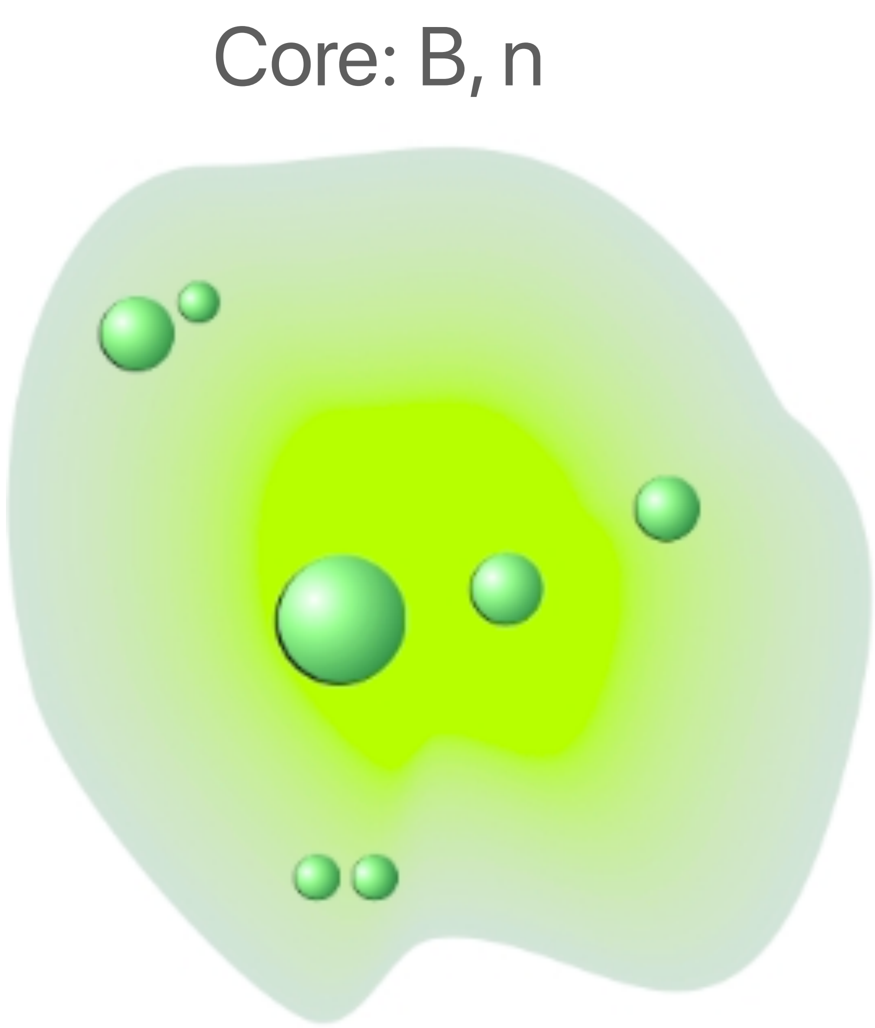

$$\left[\frac{M_{\rm crit}}{M_\odot}\right] = 1020 \left[\frac{R}{Z}\right]^2 \left[\frac{B}{30\,\mu{\rm G}}\right]^3 \left[\frac{n_{\rm H}}{10^3\ {\rm cm}^{-3}}\right]^{-2}$$

Bertoldi & McKee 92, McKee & Ostriker 07

Magnetic Jeans fragmentation -> M_{crit} ~ 150 M_{sun} (0.1x0.5 pc, 1 mG, 10^5 cm^{-3}) -> naturally yields massive fragments, but only a few

Turbulence: initial kinetic energy (Mach number), turbulence mode (compressive, solenoidal)

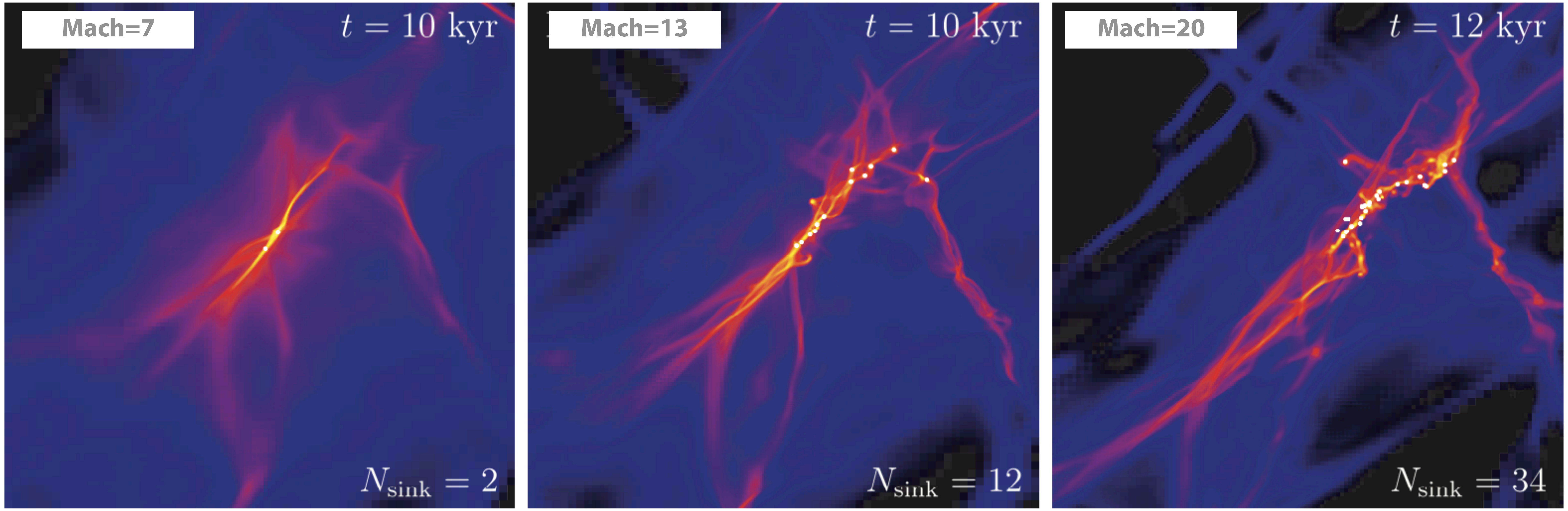

Girichidis et al. 2011; also: Vázquez-Semadeni et al. 1996, Padoan & Nordlund 2002, Schmeja & Klessen 2004, Federrath et al. 2008...

Magnetic field (B): higher B suppresses fragmentation

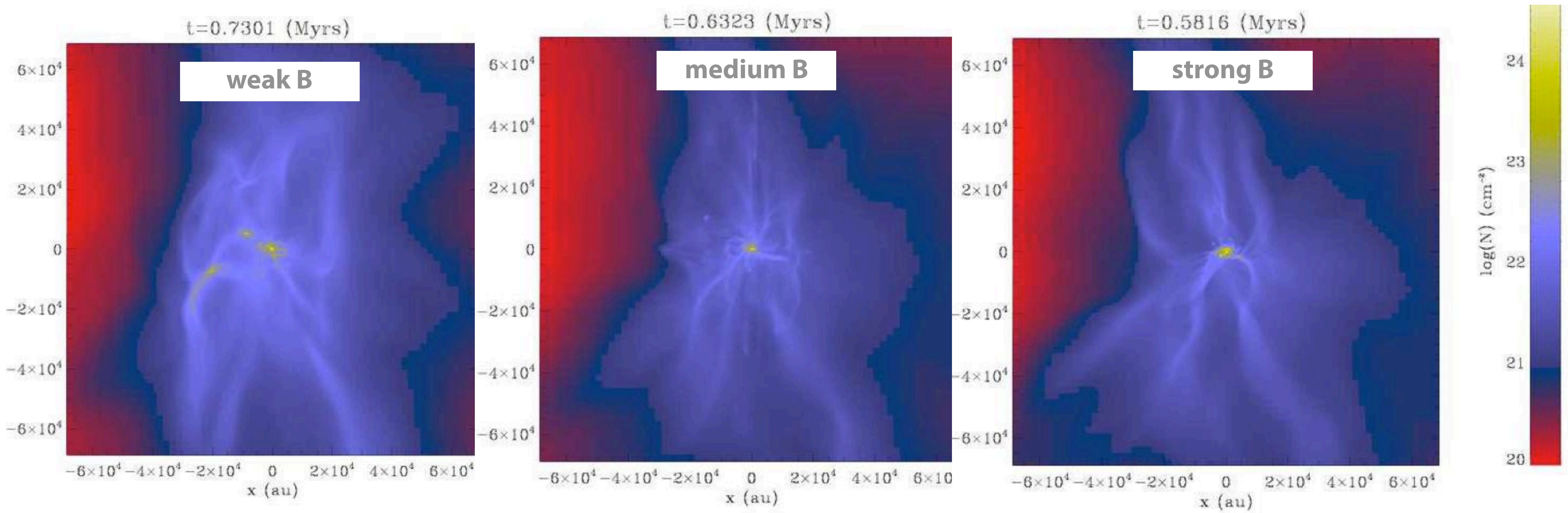

Hennebelle et al. 2011, Commerçon et al. 2011; also: Vázquez-Semadeni et al. 2005, 2011, Ziegler et al. 2005, Banerjee & Pudritz 2006, Price & Bate 2007, Peters et al. 2011, Myers et al. 2013...

Initial angular momentum: critical β for which fragmentation occurs: $\beta_{\rm rot} = \frac{E_{\rm rot}}{U} > 0.01$

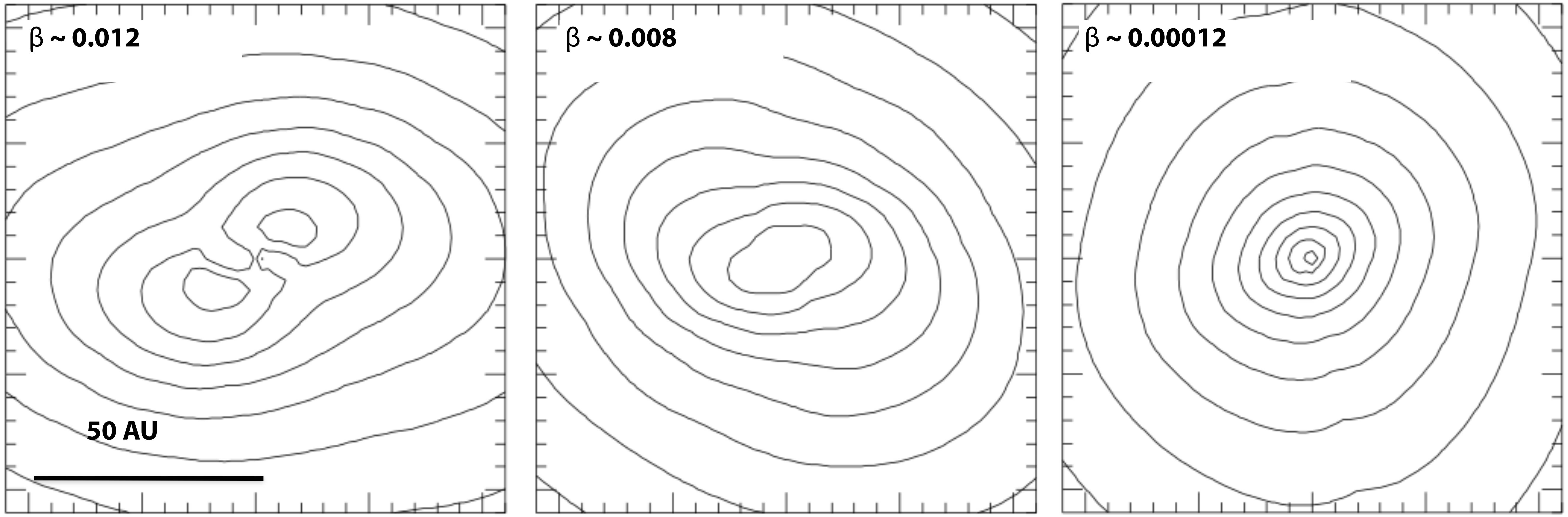

Boss 1999; also: Boss & Bodenheimer 1979, Hennebelle et al. 2004, Machida et al. 2005, Forgan & Rice 2012, Chen et al. 2012...

Density structure: higher fragmentation for flatter density profiles (n ~ r^{-1})

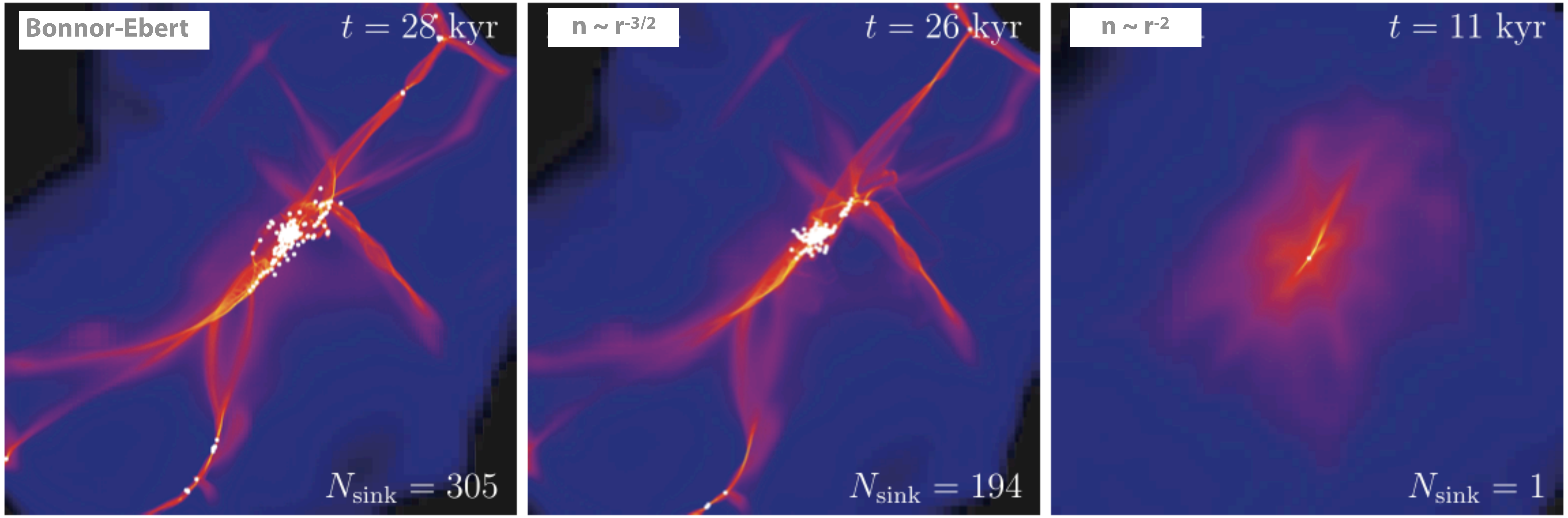

Girichidis et al. 2011; also: Myhill & Kaula 1992, Burkert et al. 1997...

The fragmentation process might be determined by...

- Initial angular momentum
- Initial density profile/Mass
- Initial magnetic field
- Radiative feedback
- Turbulence
- ...

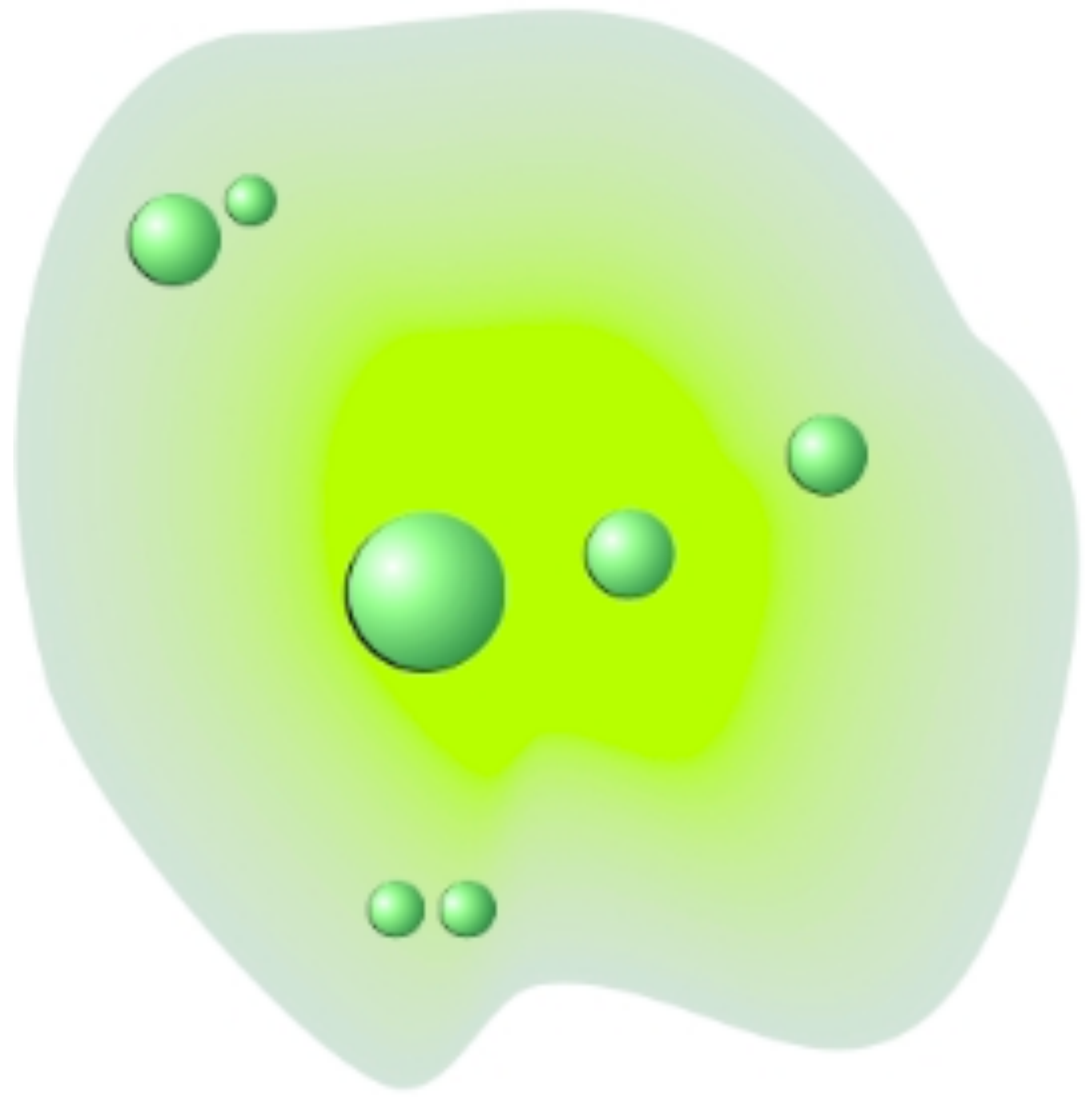

Is any of these ingredients dominating?

Introduction

Inside 0.1 pc: method + first results

Density and T structure

Role of rotation, turbulence and B

Inside 0.01 pc: ALMA

Wealth of theoretical and numerical work

But lack of observational constraints

Observational approach: observe massive dense cores down to ~1000 AU and ~0.5 M_{sun} at millimeter wavelengths

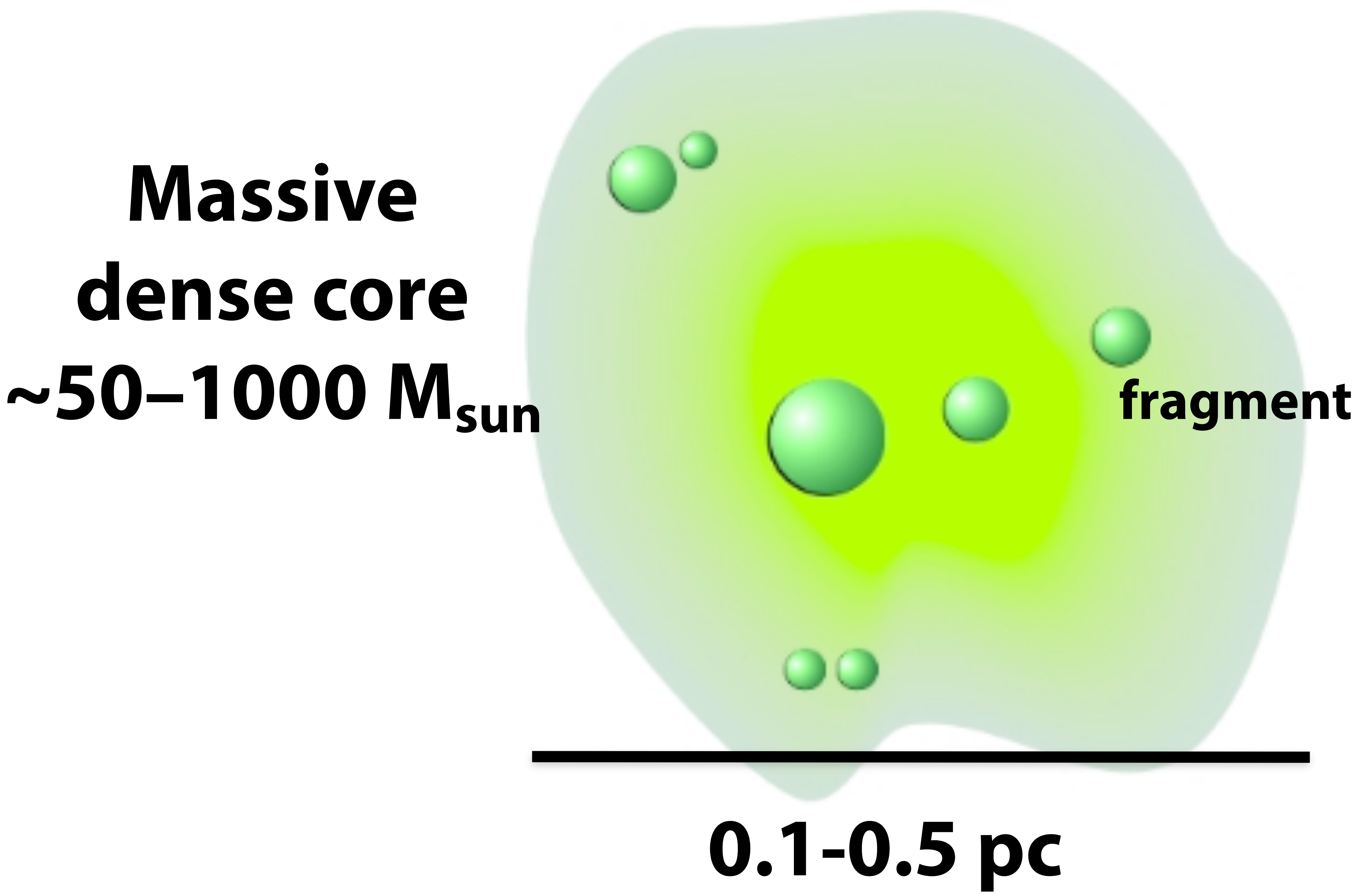

Plateau de Bure Interferometer: most extended configuration, beam ~0.4''

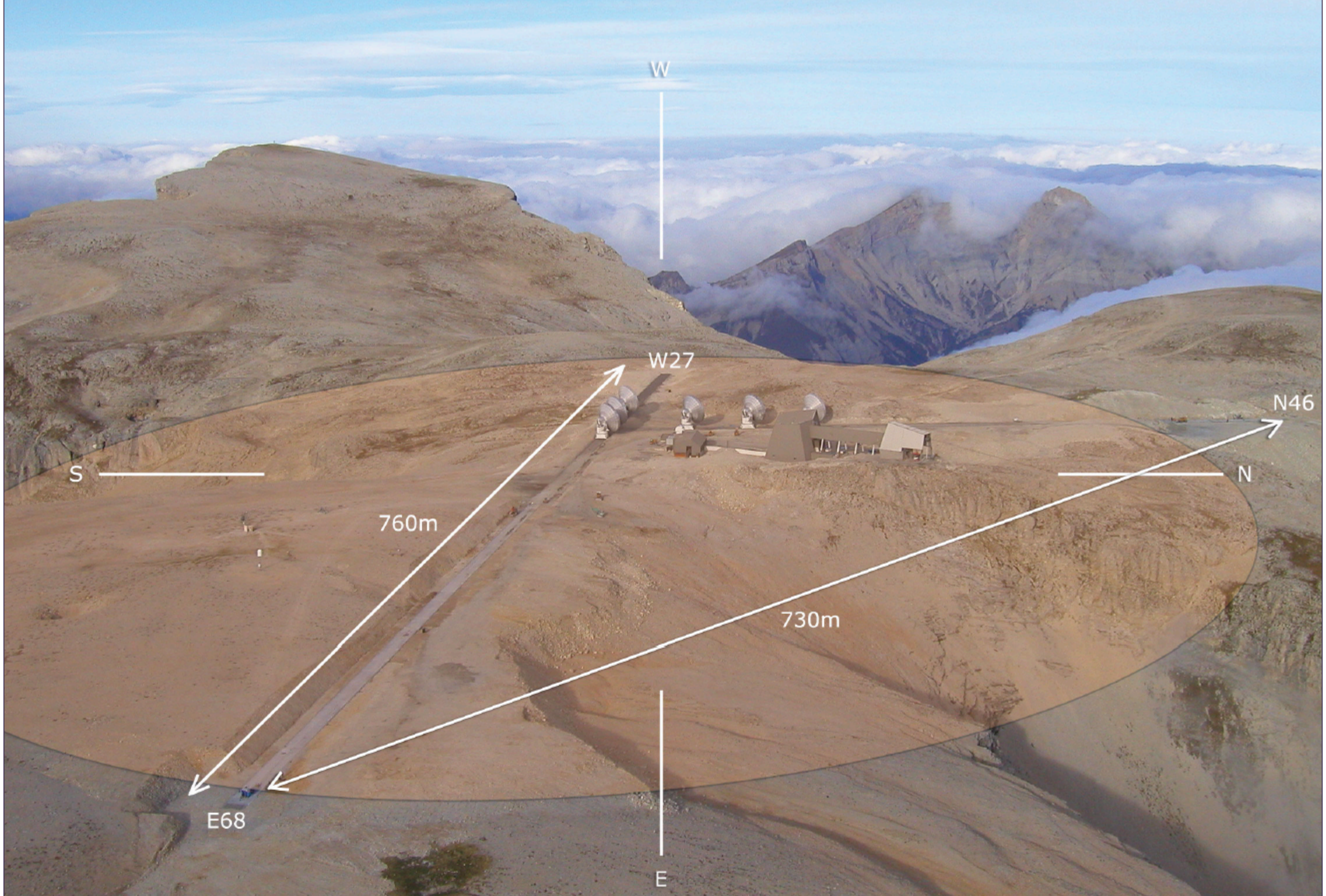

Single-dish submm/mm continuum archive observations of dense cores of all the sample:

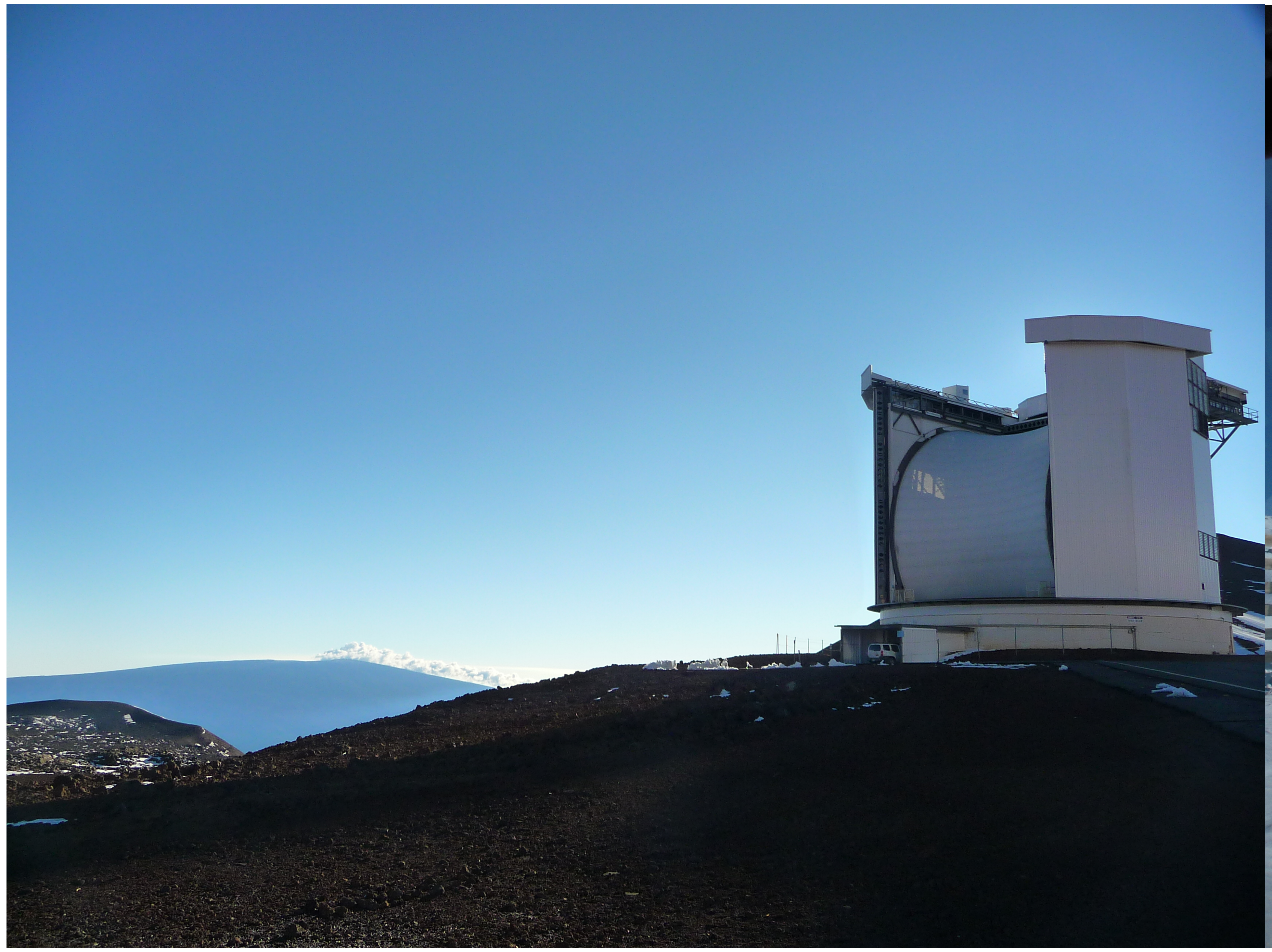

JCMT, Hawaii, USA
SCUBA bolometer, 450 & 850 μm
Di Francesco et al. 2008

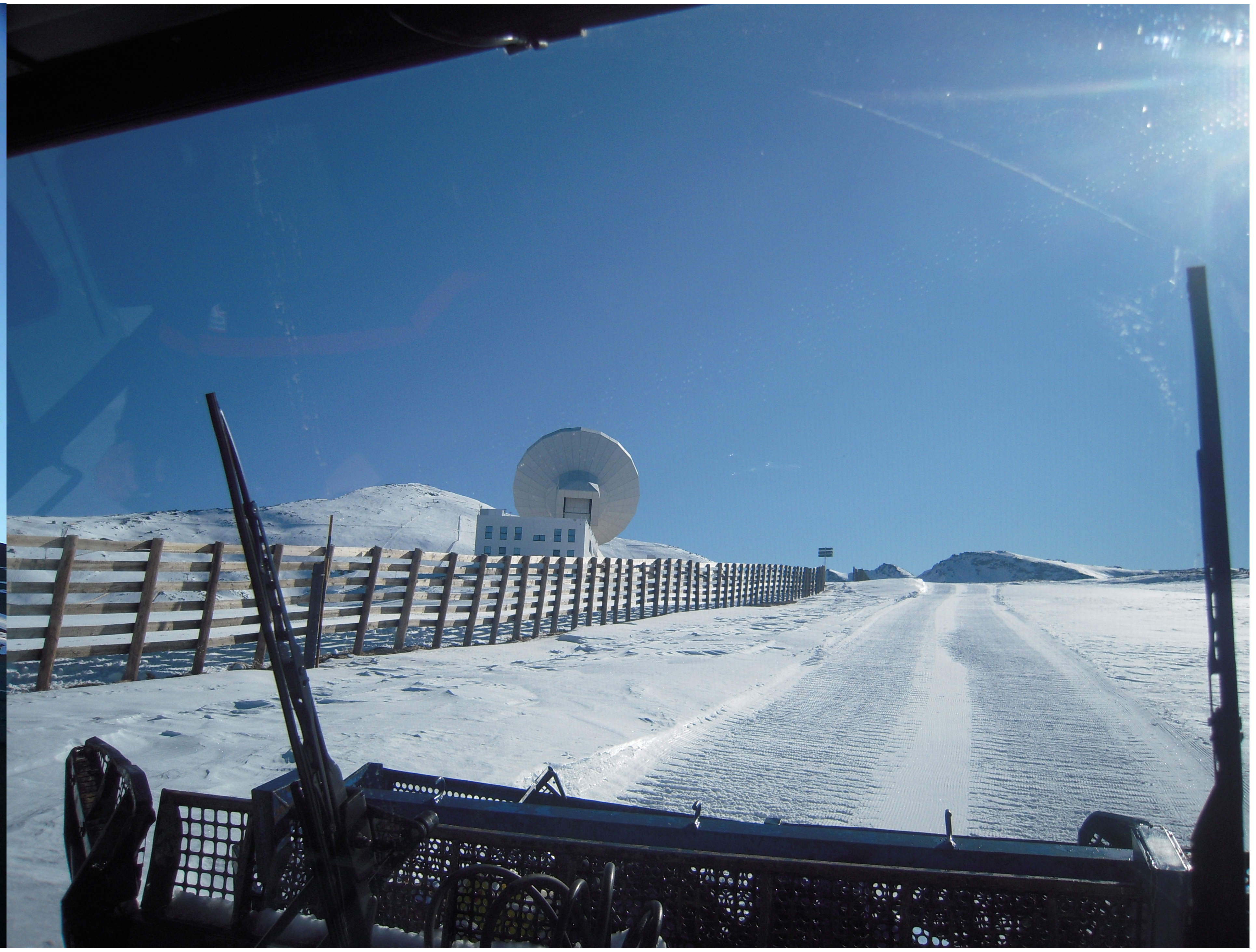

IRAM30m Granada, Spain
MAMBO bolometer, 1.2 mm
Motte et al. 2007

19 massive dense cores taken from literature + own observations with the PdBI:

- < 3 kpc
- associated with strong mm emission, outflows (similar evolutionary stages)
- $M_{min} < 1\ M_{sun}$
- Spatial resolution <~1000 AU
- $L_{bol} > 300\ L_{sun}$

19 massive dense cores taken from literature + own observations with the PdBI:

Table 3

Massive Dense Cores Studied with Interferometers at 1.3 mm with High Sensitivity and Down to a Spatial Resolution $\lesssim$1000 AU

ID-Source[a]	D (kpc)	L_{bol} ($L_\odot$)	T_{bol}[b] (K)	rms[c] (mJy)	M_{min}[c] ($M_\odot$)	Spat. Res.[d] (AU)	LAS[d] (AU)	N_{mm}[e]	N_{mm+IR}[e]	N_{IR}/N_{mm}	st. dens.[f] (10^4 pc^{-3})	Separation[f] (AU)
1-IC1396N	0.75	290	52	0.52	0.03	340	900	4	8	1.00	69	1800
2-I22198	0.76	340	59	2.0	0.13	300	700	1.5	2	0.33	3	...
3-NGC 2071-IRS1[g]	0.42	440	98	0.50	0.20	200	5500	4	14	2.50	16	2900
4-NGC 7129-FIRS2	1.25	460	58	2.9	0.49	750	1500	1	2	1.00	3	...
5-CB3-mm	2.50	700	49	0.43	0.29	875	2500	2	$\gtrsim$2	$\gtrsim$0.00	$\gtrsim$3	...
6-I22172N-IRS1	2.40	830	195	0.55	0.34	1000	2100	3	6	1.00	6	4400
7-OMC-1S-136	0.45	2000	...	30	0.66	540	3300	9	21	1.33	9	3000
8-A5142	1.80	2200	55	2.8	0.99	700	1600	7	11	0.57	7	3700
9-I05358+3543NE	1.80	3100	67	1.5	0.53	900	2100	4	7	0.75	10	3500
10-I20126+4104	1.64	8900	61	2.6	0.76	1400	4000	1	3	2.00	23	2700
11-I22134-IRS1	2.60	11800	93	0.30	0.22	1300	2300	3.5	7	1.00	4	4600
12-HH80-81	1.70	21900	81	3.0	0.94	830	4000	3	6	1.00	6	4200
13-W3IRS5	1.95	140000	114	1.2	0.50	720	2300	3.5	$\gtrsim$5.5	$\gtrsim$0.57	$\gtrsim$46	2300
14-AFGL 2591	3.00	190000	226	0.51	0.49	1000	1900	1.5	$\gtrsim$1.5	$\gtrsim$0.00	$\gtrsim$3	...
15-CygX-N53	1.40	300	33	1.9	0.41	1400	6900	4	7	0.75	11	3400
16-CygX-N12	1.40	320	58	1.9	0.41	1400	6900	2.5	5	1.00	23	2800
17-CygX-N63	1.40	470	39	4.2	0.90	1400	6900	2.5	4	0.60	72	2000
18-CygX-N48	1.40	4400	48	2.2	0.47	1400	6900	4	5	0.25	11	3600

Single-dish@850μm **Single-dish@450μm** **Interferometer@1mm**

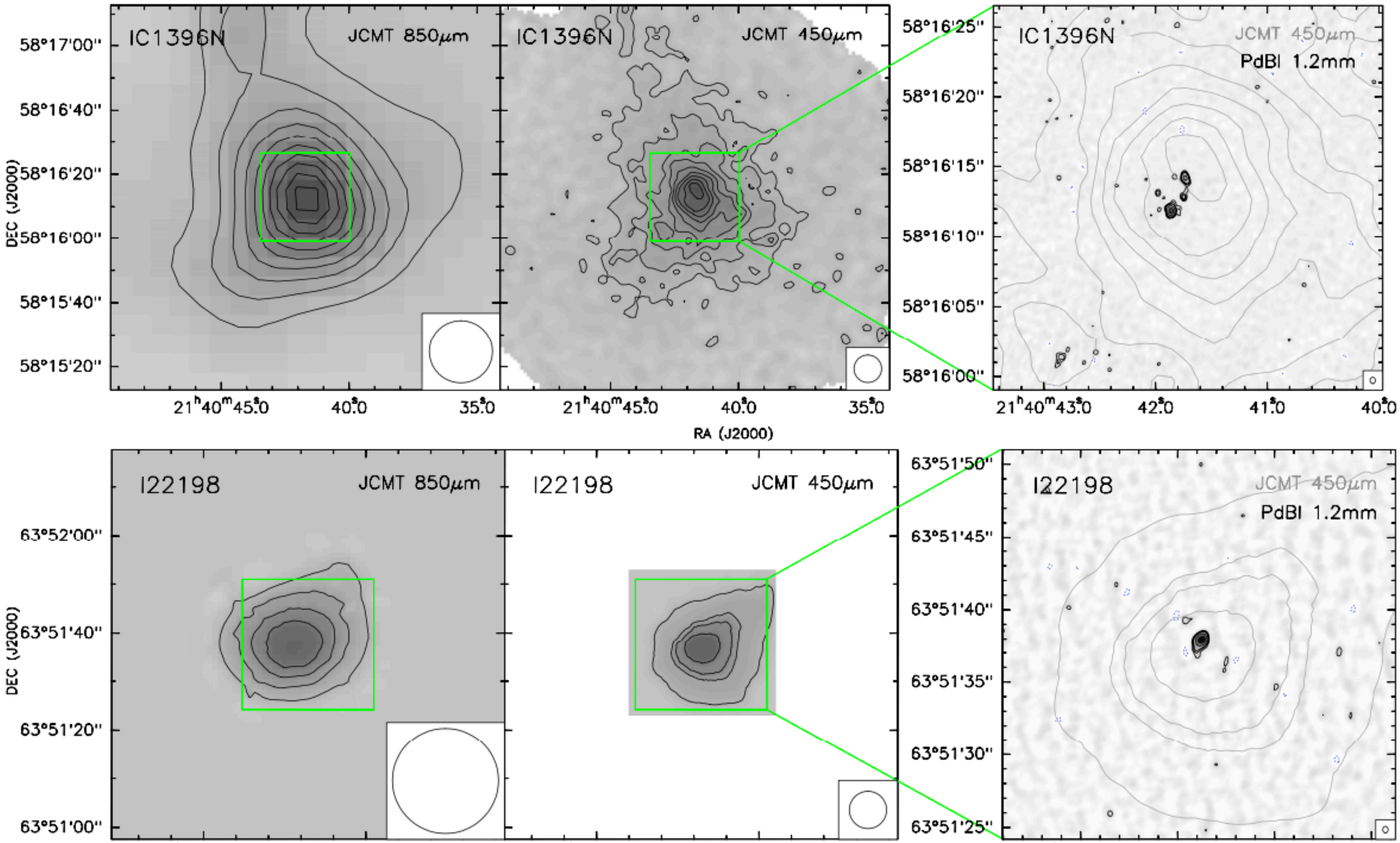

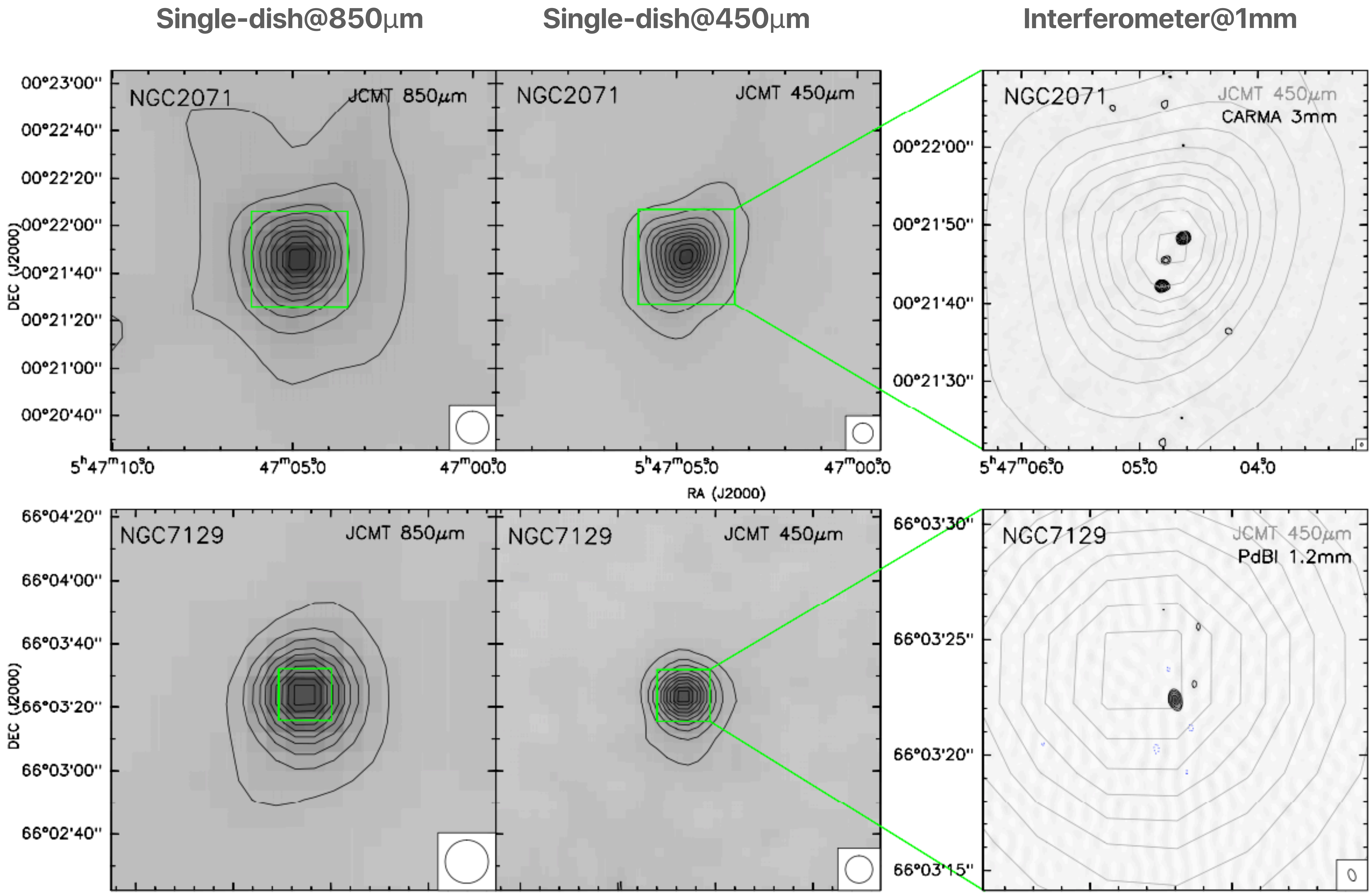

Single-dish@850μm
Single-dish@450μm
Interferometer@1mm
NGC2071
JCMT 850μm
JCMT 450μm
CARMA 3mm
NGC7129
PdBI 1.2mm
DEC (J2000)
RA (J2000)
00°23'00''
00°22'40''
00°22'20''
00°22'00''
00°21'40''
00°21'20''
00°21'00''
00°20'40''
00°21'50''
00°21'30''
5h47m10.0s
47m05.0s
47m00.0s
5h47m05.0s
5h47m06.0s
05.0s
04.0s
66°04'20''
66°04'00''
66°03'40''
66°03'20''
66°03'00''
66°02'40''
66°03'30''
66°03'25''
66°03'15''

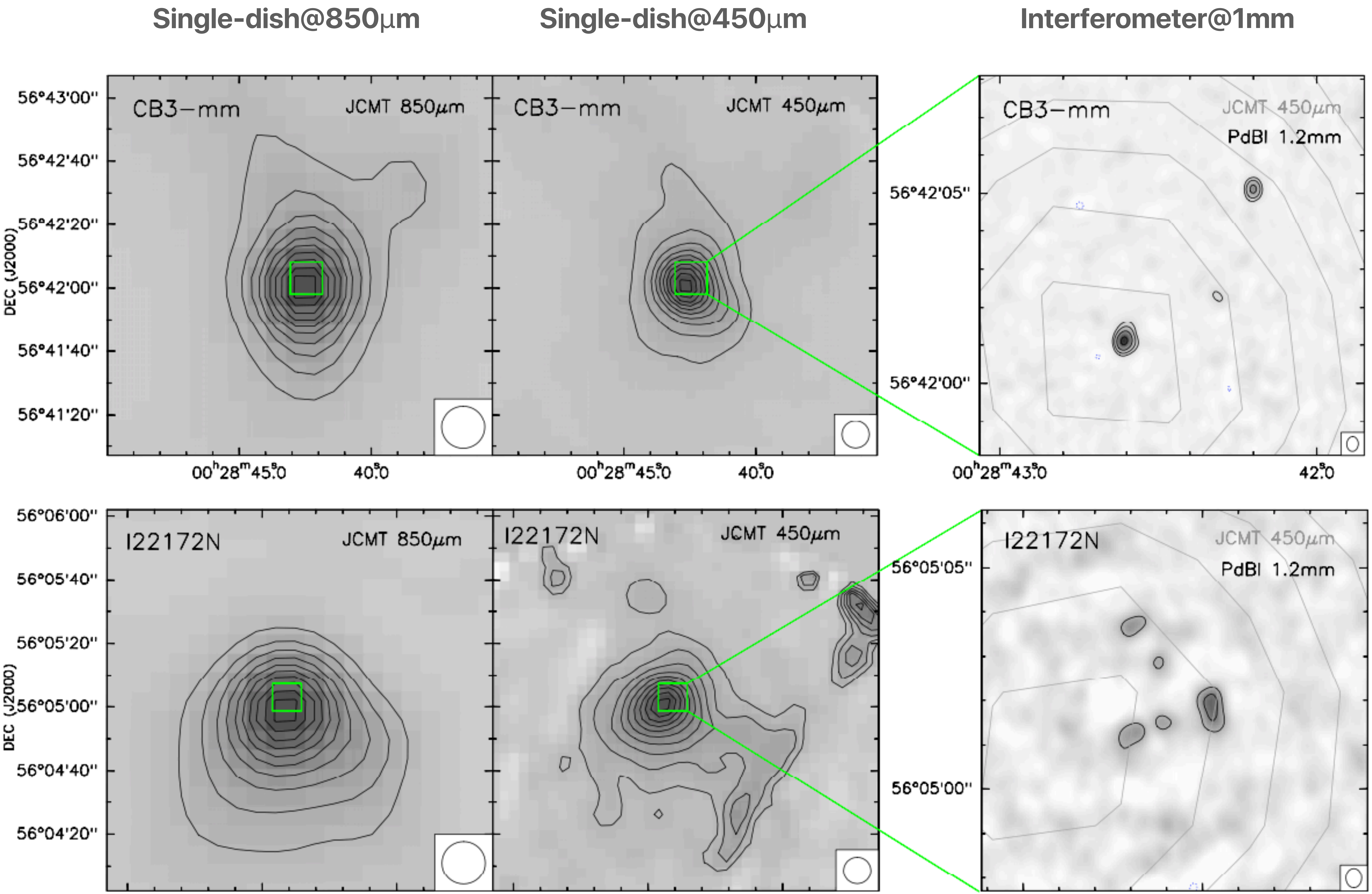

Single-dish@850μm
Single-dish@450μm
Interferometer@1mm
CB3−mm
JCMT 850μm
JCMT 450μm
PdBI 1.2mm
I22172N
DEC (J2000)
56°43'00"
56°42'40"
56°42'20"
56°42'00"
56°41'40"
56°41'20"
56°42'05"
56°42'00"
00h28m45.0s
40.0s
00h28m43.0s
42.0s
56°06'00"
56°05'40"
56°05'20"
56°05'00"
56°04'40"
56°04'20"
56°05'05"
56°05'00"

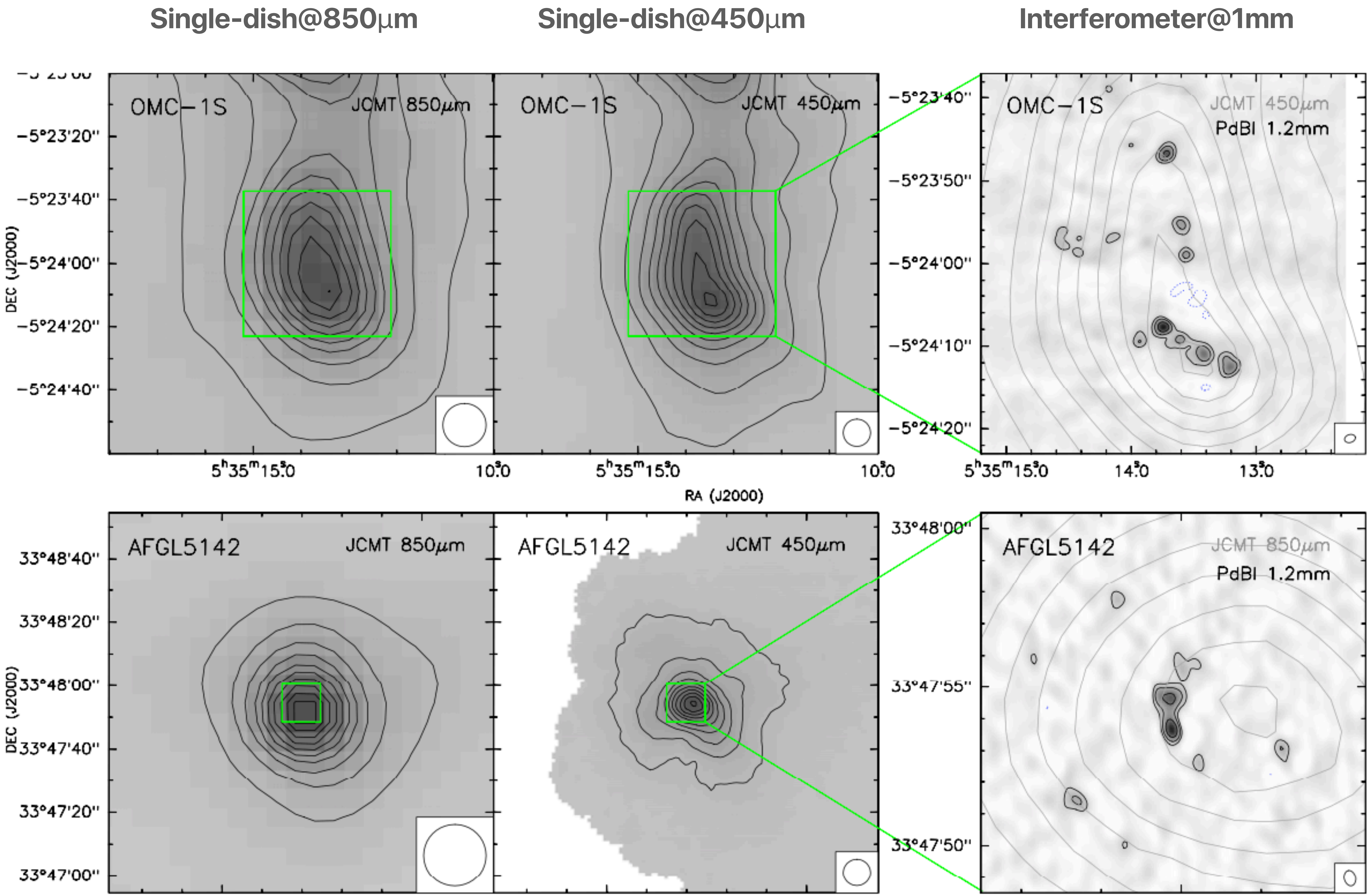
Single-dish@850μm
Single-dish@450μm
Interferometer@1mm
OMC−1S
JCMT 850μm
JCMT 450μm
PdBI 1.2mm
AFGL5142
DEC (J2000)
RA (J2000)
-5°23'20"
-5°23'40"
-5°24'00"
-5°24'20"
-5°24'40"
-5°23'50"
-5°24'10"
5h35m15.0s
10.0s
14.0s
13.0s
33°48'40"
33°48'20"
33°48'00"
33°47'40"
33°47'20"
33°47'00"
33°47'55"
33°47'50"

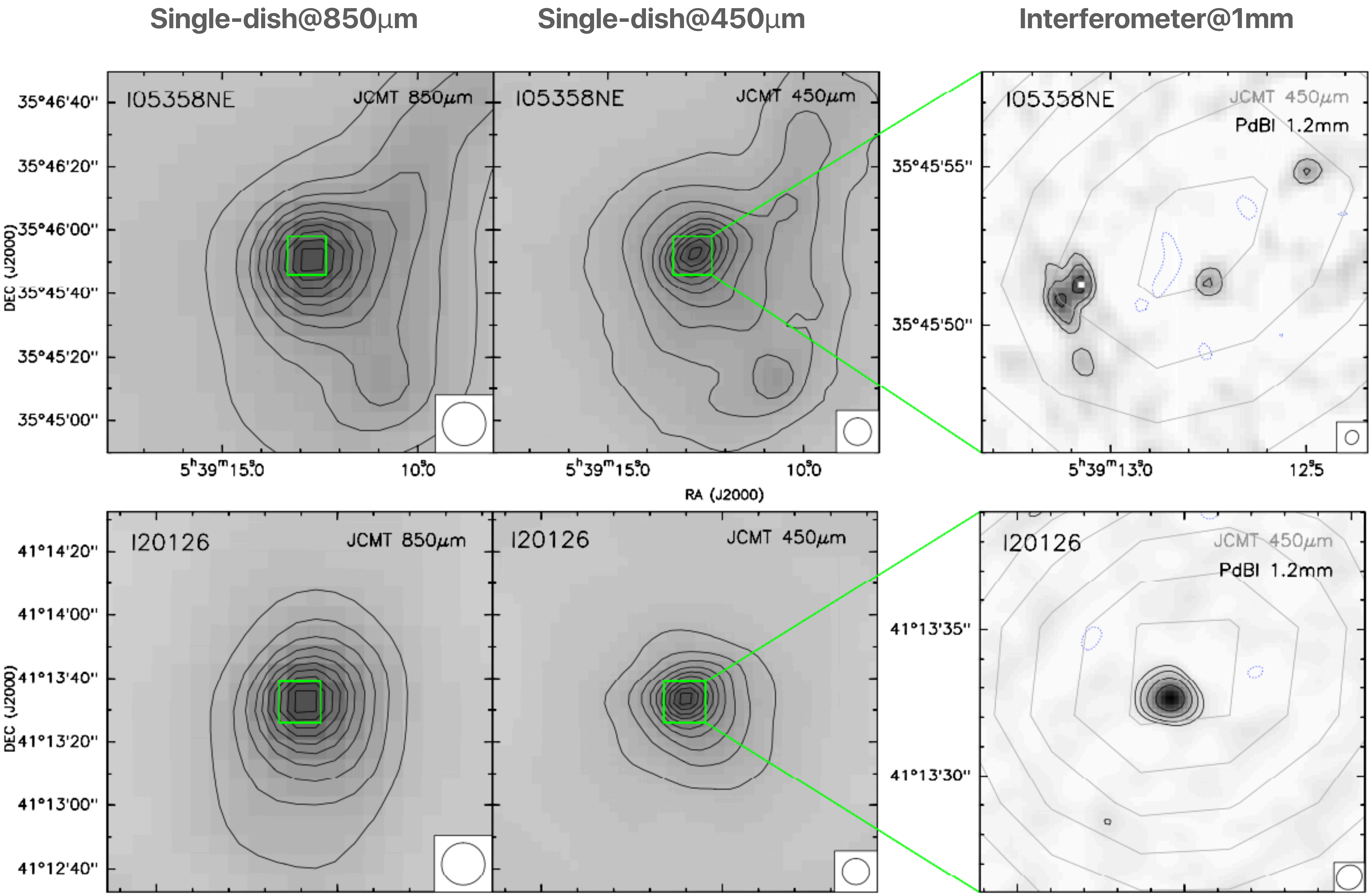

Single-dish@850μm
Single-dish@450μm
Interferometer@1mm
I05358NE
JCMT 850μm
I05358NE
JCMT 450μm
I05358NE
JCMT 450μm
PdBI 1.2mm
35°46'40"
35°46'20"
35°46'00"
35°45'40"
35°45'20"
35°45'00"
DEC (J2000)
35°45'55"
35°45'50"
5h39m15.0s
10.0s
5h39m15.0s
10.0s
5h39m13.0s
12.5s
RA (J2000)
I20126
JCMT 850μm
I20126
JCMT 450μm
I20126
JCMT 450μm
PdBI 1.2mm
41°14'20"
41°14'00"
41°13'40"
41°13'20"
41°13'00"
41°12'40"
DEC (J2000)
41°13'35"
41°13'30"

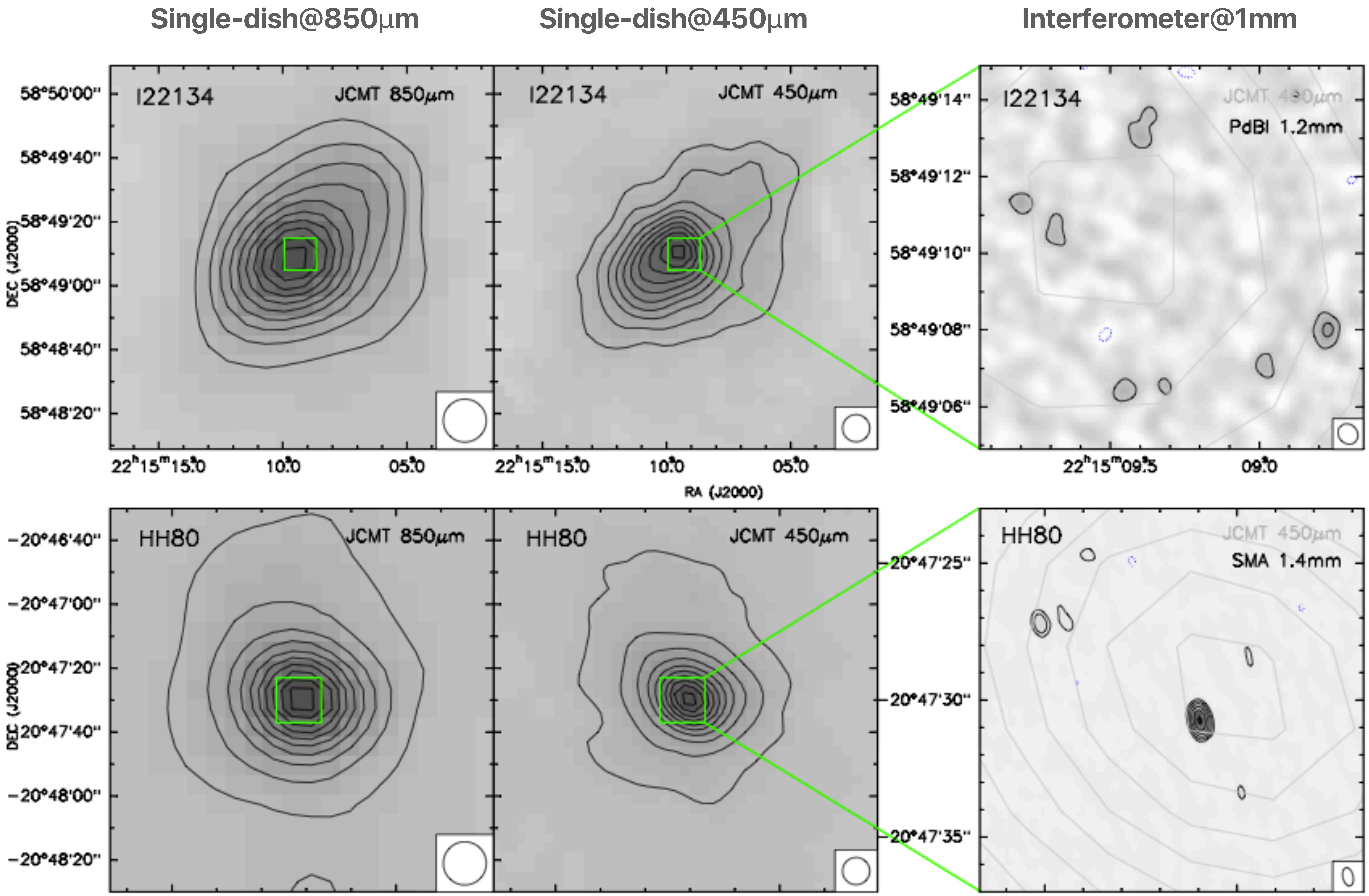
Single-dish@850μm
Single-dish@450μm
Interferometer@1mm
I22134
JCMT 850μm
JCMT 450μm
PdBI 1.2mm
HH80
SMA 1.4mm
DEC (J2000)
RA (J2000)
58°50'00"
58°49'40"
58°49'20"
58°49'00"
58°48'40"
58°48'20"
22h15m15.0s
10.0s
05.0s
58°49'14"
58°49'12"
58°49'10"
58°49'08"
58°49'06"
22h15m09.5s
09.0s
-20°46'40"
-20°47'00"
-20°47'20"
-20°47'40"
-20°48'00"
-20°48'20"
-20°47'25"
-20°47'30"
-20°47'35"

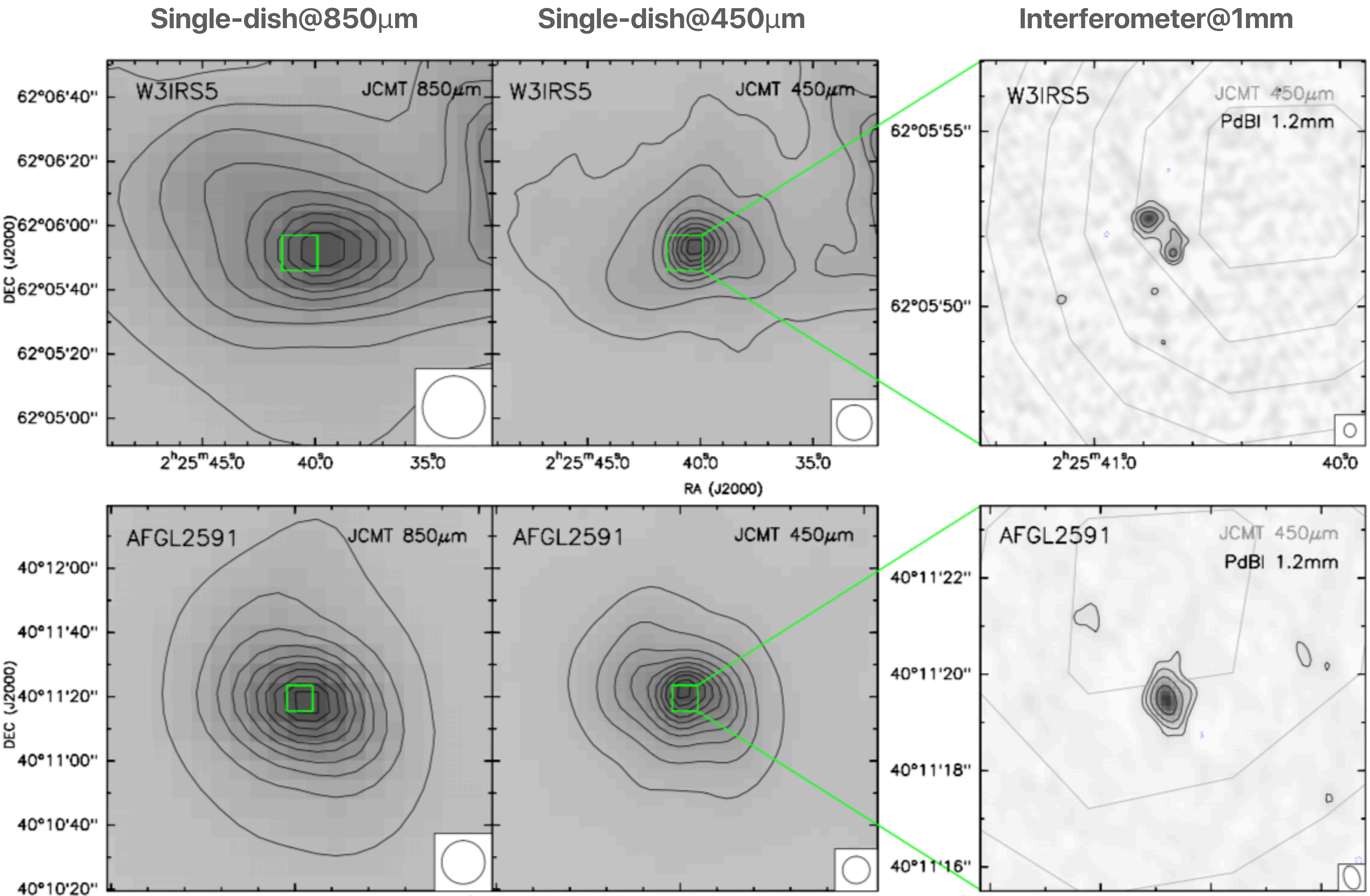

Single-dish@850μm
Single-dish@450μm
Interferometer@1mm
W3IRS5
JCMT 850μm
JCMT 450μm
PdBI 1.2mm
AFGL2591
62°06'40"
62°06'20"
62°06'00"
62°05'40"
62°05'20"
62°05'00"
62°05'55"
62°05'50"
DEC (J2000)
RA (J2000)
2h25m45.0s
40.0s
35.0s
2h25m41.0s
40°12'00"
40°11'40"
40°11'20"
40°11'00"
40°10'40"
40°10'20"
40°11'22"
40°11'20"
40°11'18"
40°11'16"

Single-dish@850μm **Single-dish@450μm** **Interferometer@1mm**

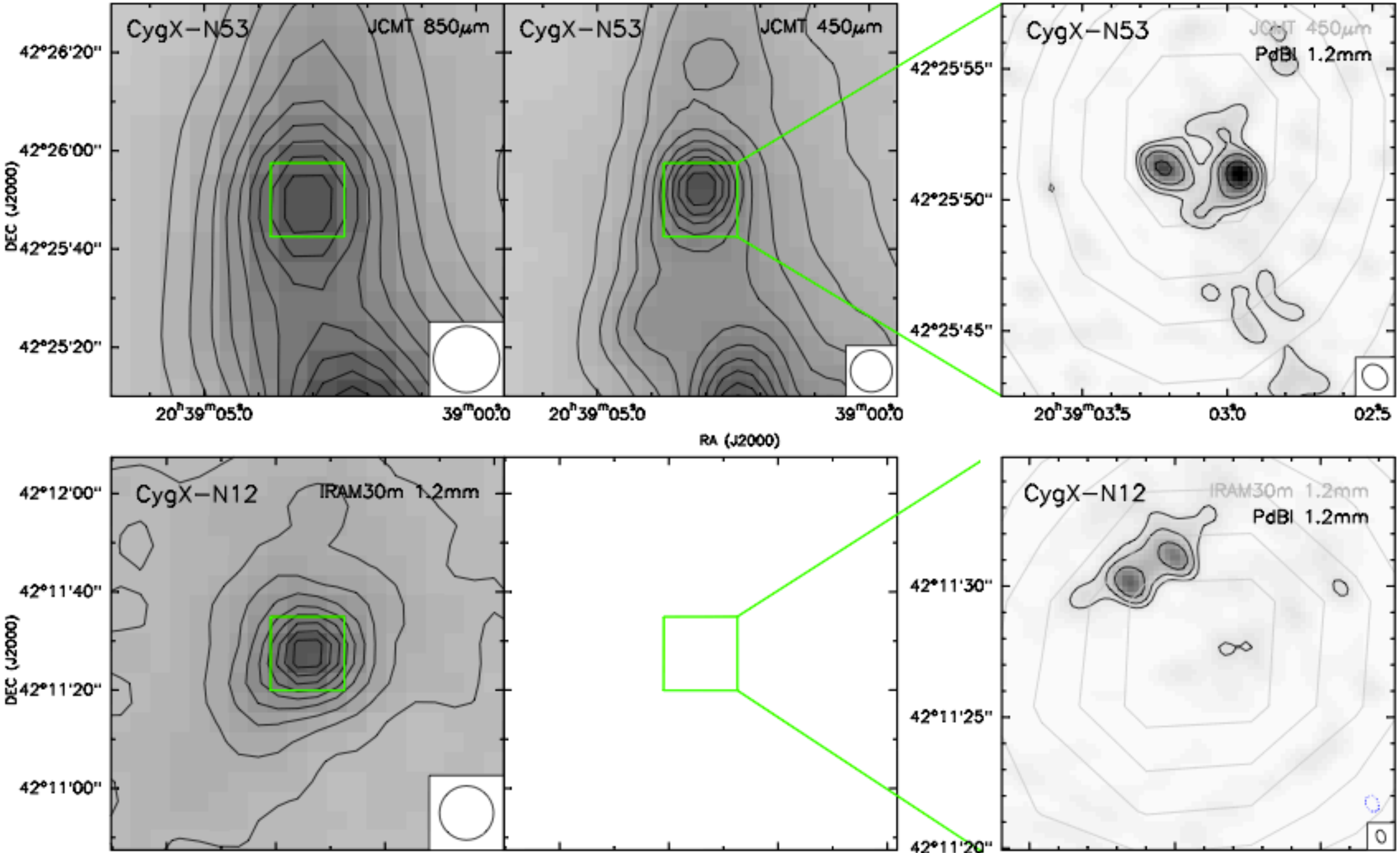

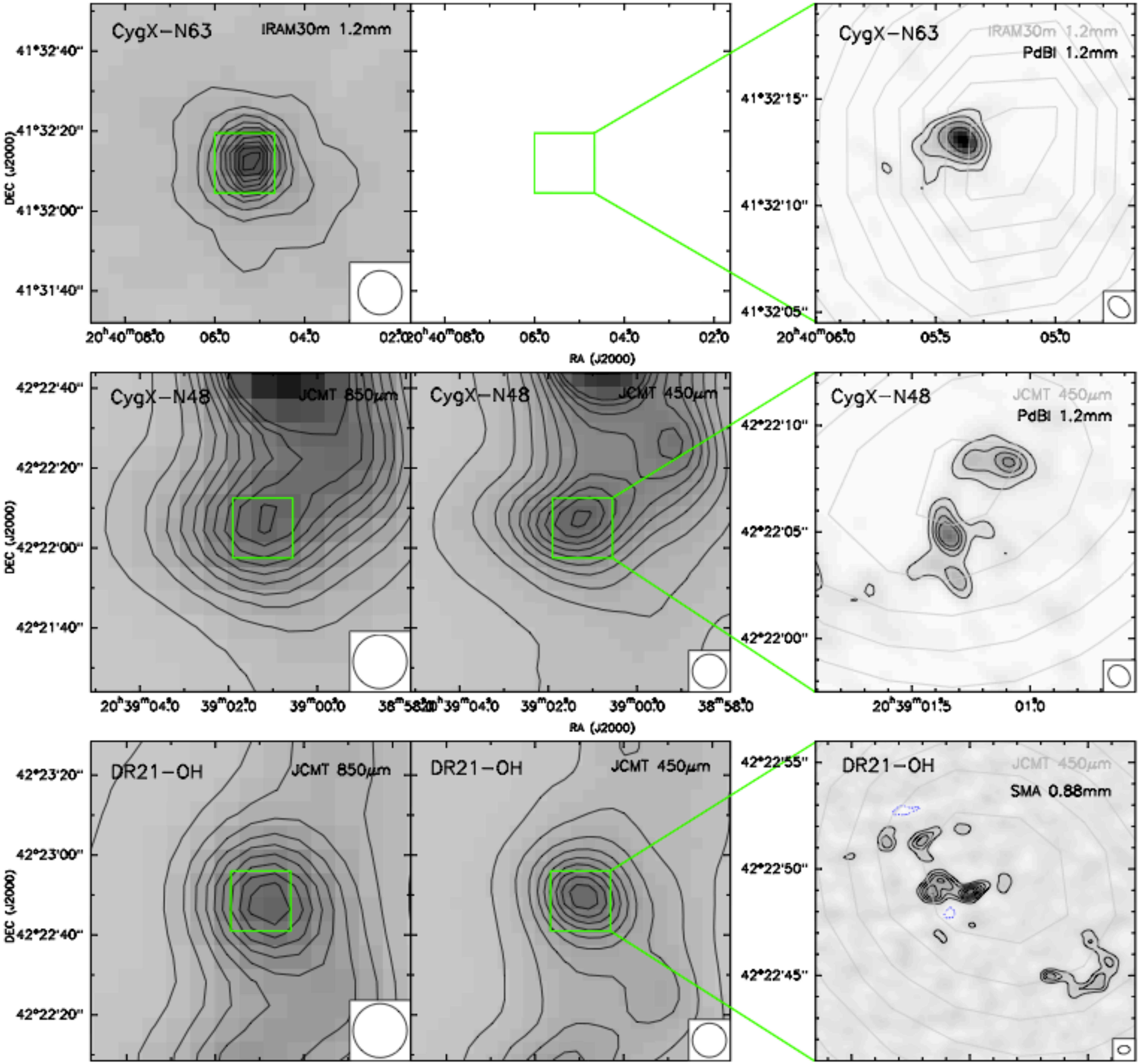

CygX-N63
IRAM30m 1.2mm
PdBI 1.2mm
CygX-N48
JCMT 850μm
JCMT 450μm
DR21-OH
SMA 0.88mm
DEC (J2000)
RA (J2000)
41°32'40"
41°32'20"
41°32'00"
41°31'40"
41°32'15"
41°32'10"
41°32'05"
20h40m08.0
06.0
04.0
02.0
20h40m06.0
05.5
05.0
42°22'40"
42°22'20"
42°22'00"
42°21'40"
42°22'10"
42°22'05"
42°22'00"
20h39m04.0
39m02.0
39m00.0
38m58.0
20h39m01.5
01.0
42°23'20"
42°23'00"
42°22'40"
42°22'20"
42°22'55"
42°22'50"
42°22'45"

Fragmentation level N_{mm}: number of millimeter sources above 6σ within 0.1 pc with extended only configs (~1000 AU) and mass sensit. <1 M_{sun}

Palau+13 main result: 30% low fragmentation; 50% high fragmentation

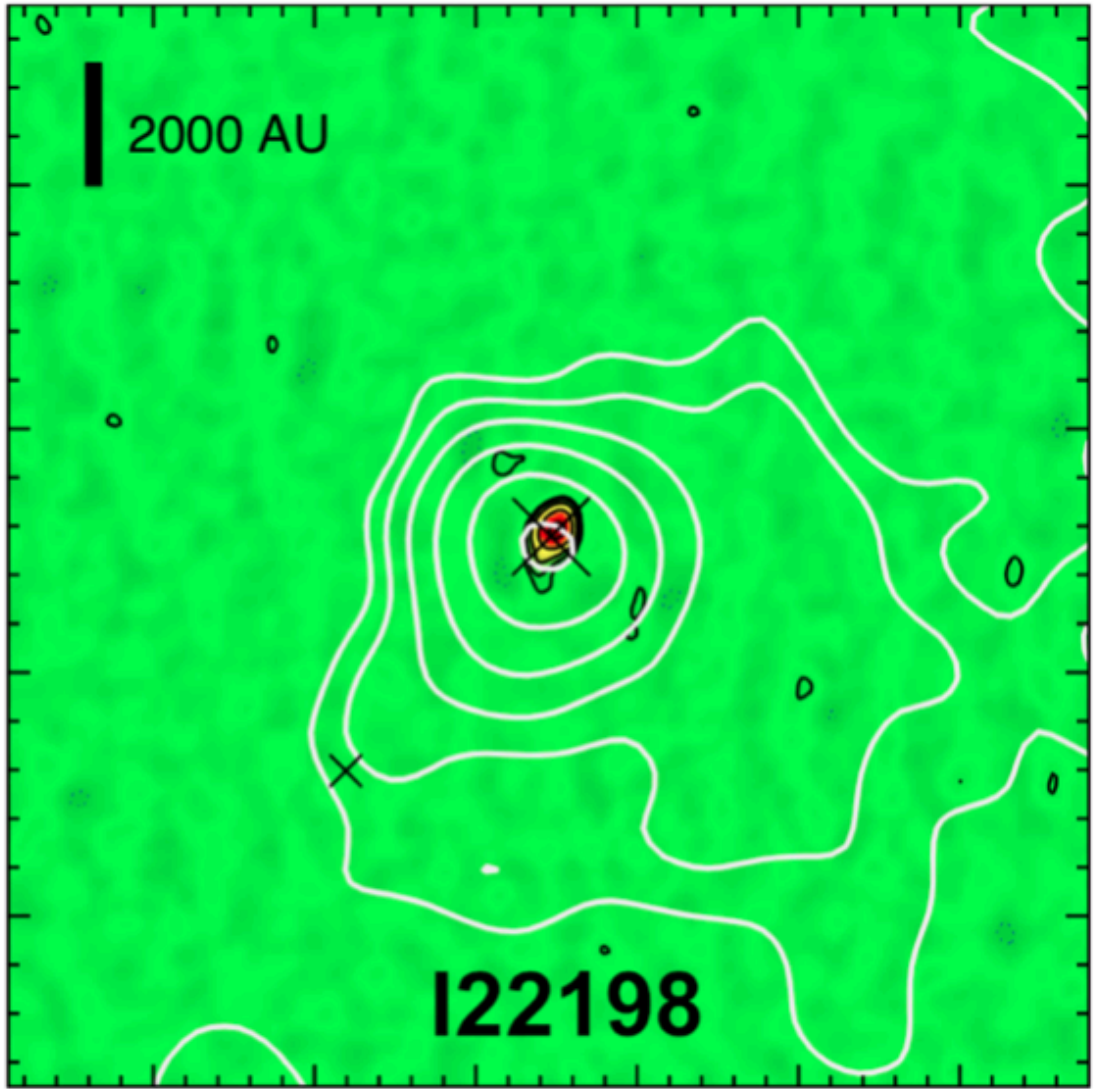

spatial resolution: 300 AU
mass sensitivity: 0.1 M_{sun}

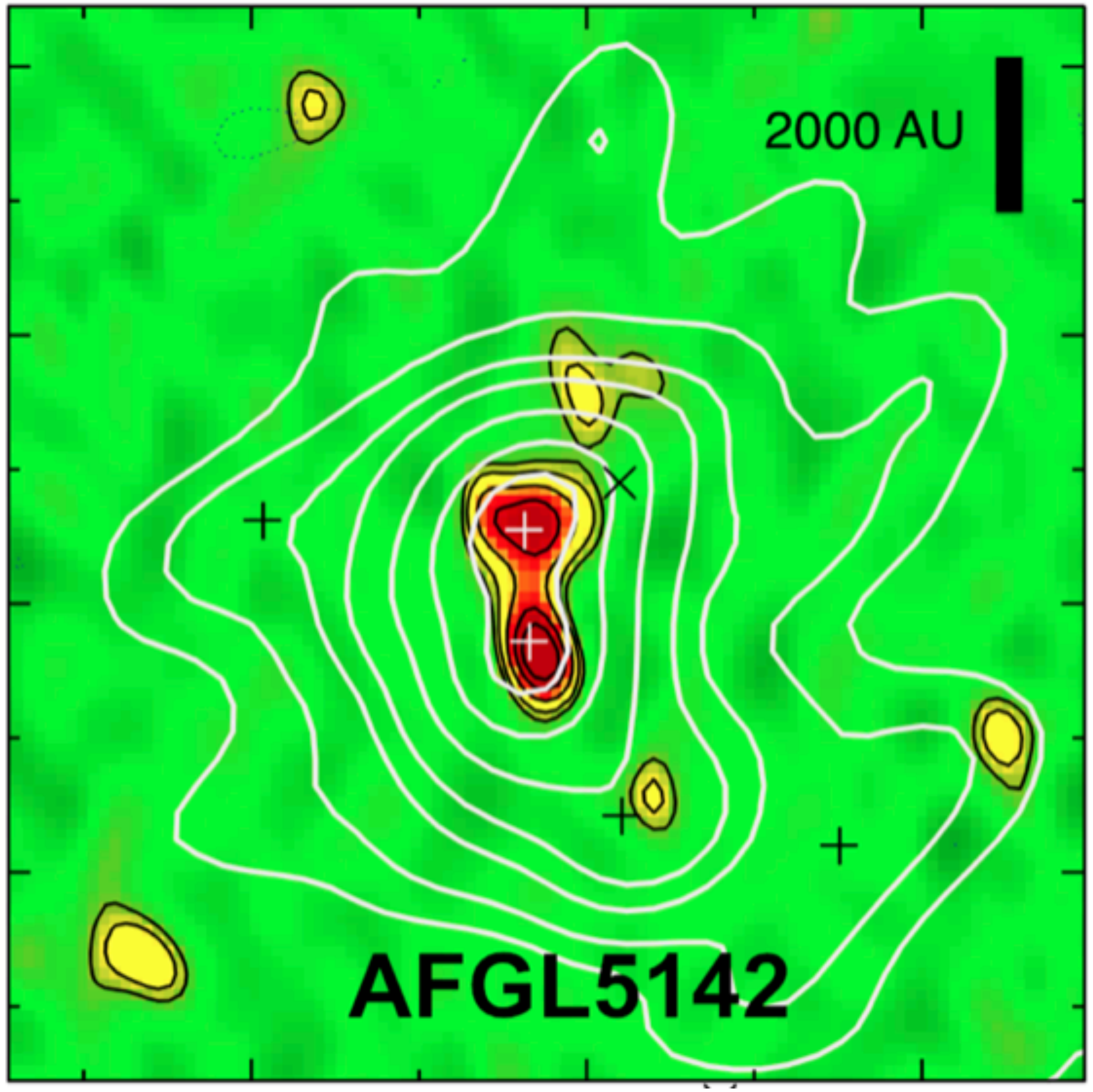

spatial resolution: 700 AU
mass sensitivity: 0.9 M_{sun}

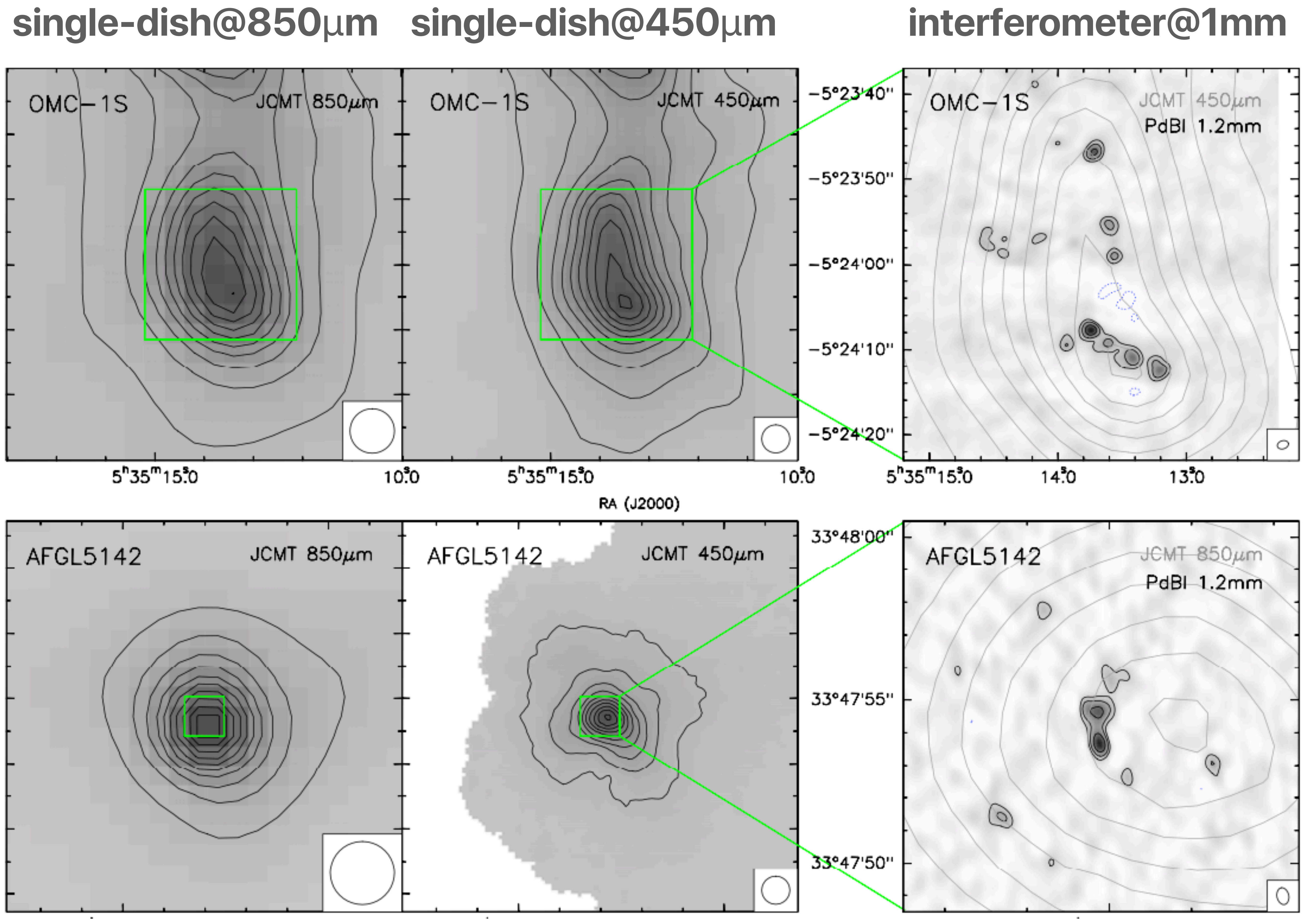

Calculate:

- single-dish: Mass (T_d, opacity), avg surface density ($M/\pi R^2$), avg density entire core ($3M/4\pi R^3$)
- interferometer: Mass of each fragment, CFE = $\Sigma m_{i\text{-}interf} / M_{sd}$

Build SED using: IRAC, MIPS, MSX, IRAS, AKARI, SCUBA...

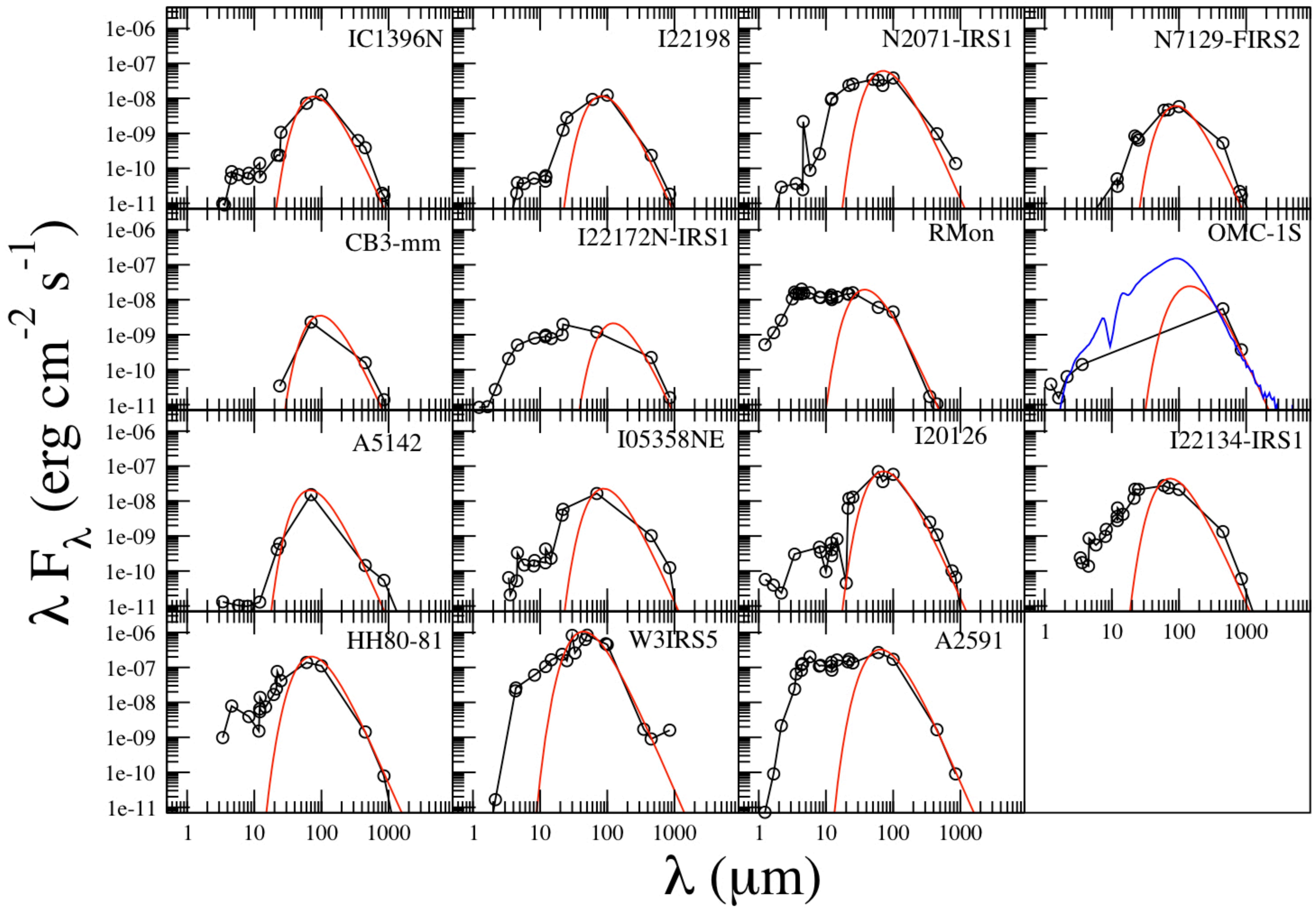

Calculate: L_{bol} and L_{bol}/M_{sd}

N_{mm} vs L_{bol}, M_{sd}

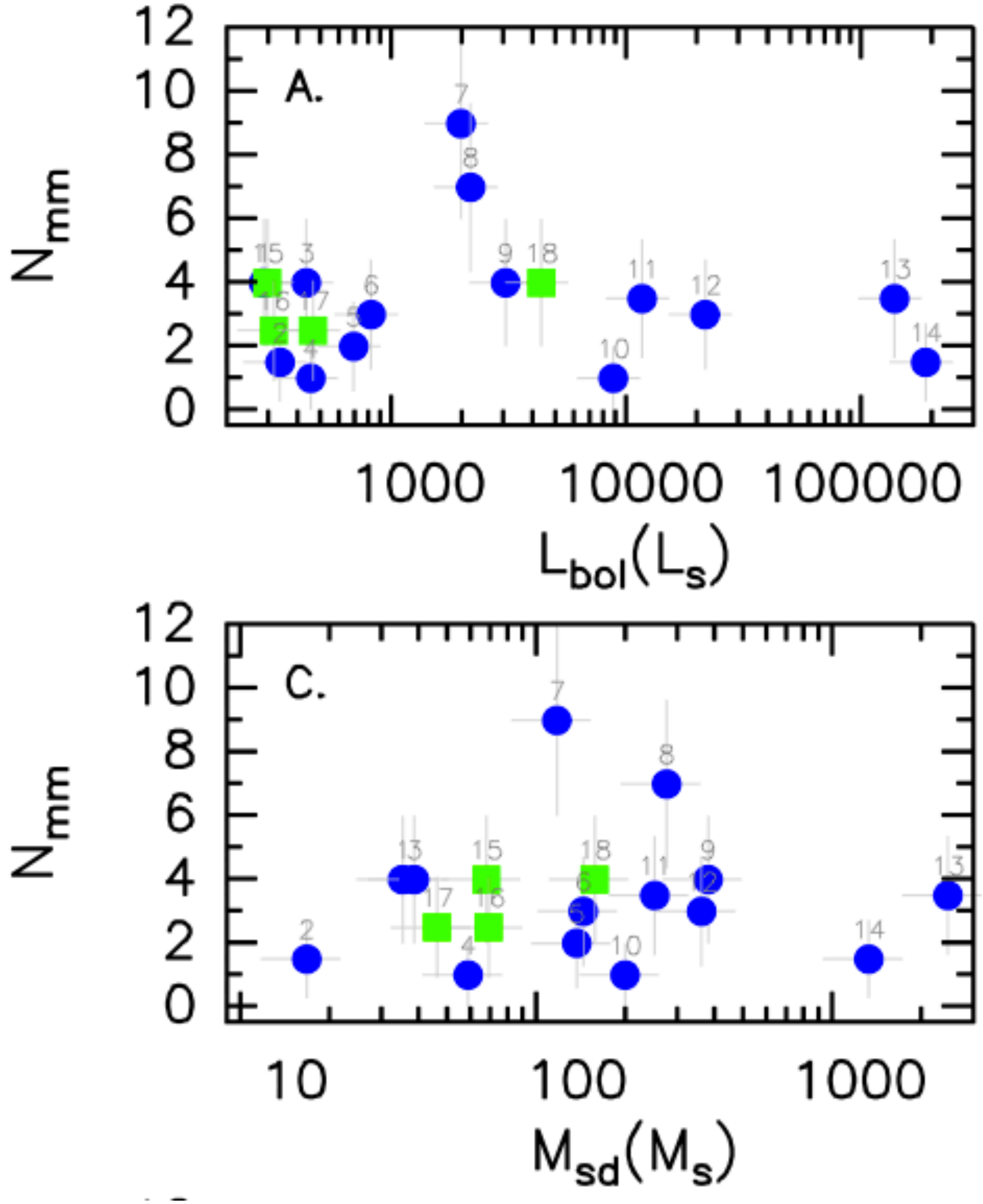

N_{mm} vs evolutionary stage, density of entire core, CFE

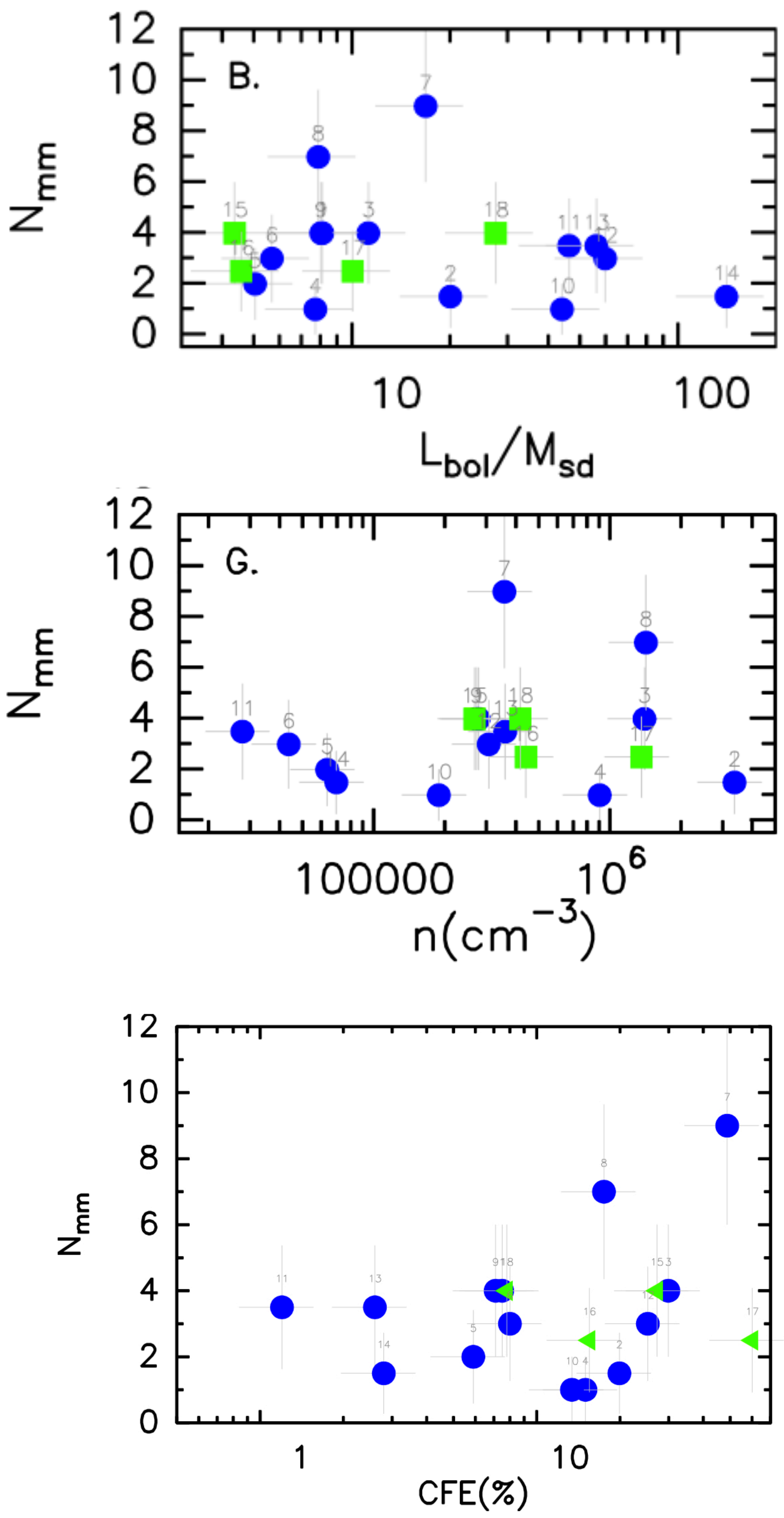

Palau et al. 2013, ApJ, 762, 120

Introduction

Inside 0.1 pc: method + first results

Density and T structure

Role of rotation, turbulence and B

Inside 0.01 pc: ALMA

Next step: study **density structure** of the massive dense cores

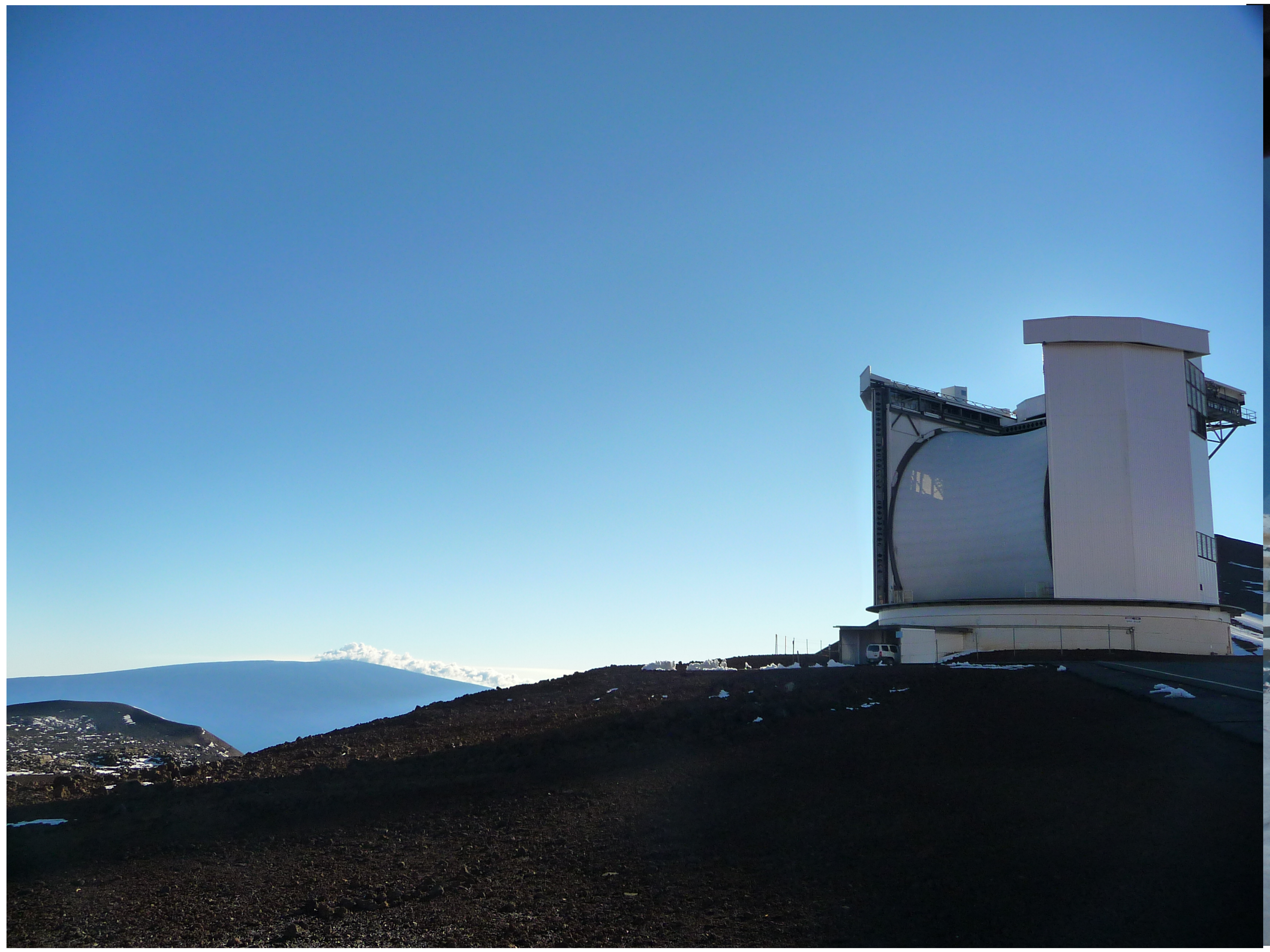

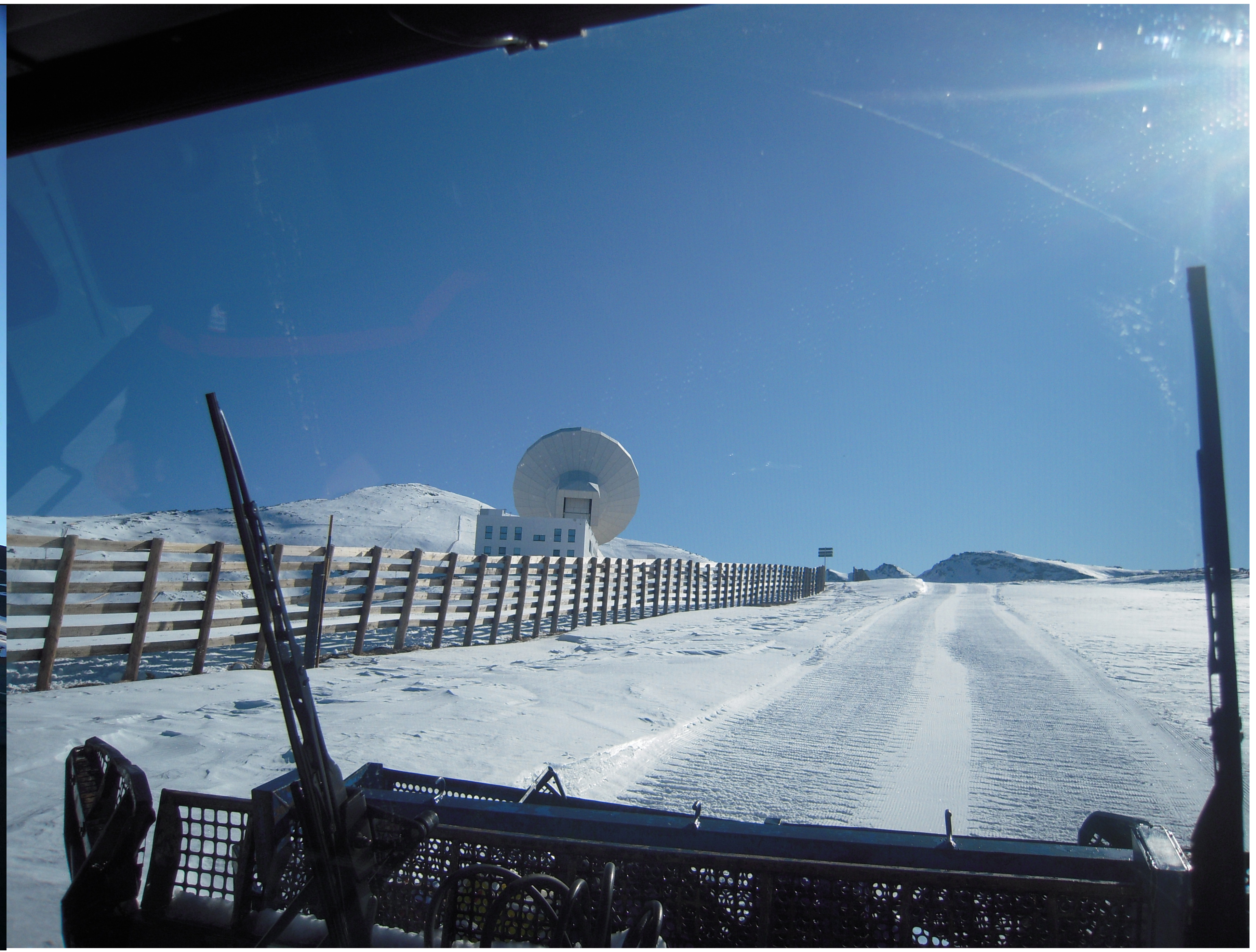

JCMT, Hawaii, USA
SCUBA bolometer, 450 & 850 µm
Di Francesco et al. 2008

IRAM30m Granada, Spain
MAMBO bolometer, 1.2 mm
Motte et al. 2007

Model density and temperature profiles of the dense cores

Assumptions:

- spherically symmetric envelope
- dust opacity $\kappa_\nu \propto \nu^\beta$
- **density profile $\rho = \rho_0\ (r/r_0)^{-p}$**
- **temperature profile $T = T_0\ (r/r_0)^{-q}$**, with $q = 2/(4+\beta)$
- external heating: T = 10 K in the outer envelope
- no assumption of optically thin emission
- no R-J approximation

Fit simultaneously:

- **intensity profiles at 850 and 450 µm**
- **SED from cm to 60 µm wavelengths** (sensitive to T)

Model density and temperature profiles of the dense cores

Assumptions:

- spherically symmetric envelope
- dust opacity $\kappa_\nu \propto \nu^\beta$
- **density profile $\rho = \rho_0 (r/r_0)^{-p}$**
- **temperature profile $T = T_0 (r/r_0)^{-q}$** with $q = 2/(4+\beta)$
- external heating: T = 10 K in the outer envelope
- no assumption of optically thin emission
- no R-J approximation

4 free parameters

Fit simultaneously:

- **intensity profiles at 850 and 450 μm**
- **SED from cm to 60 μm wavelengths** (sensitive to T)

Modeling of radial intensity profiles and Spectral Energy Distributions (Palau+14a)

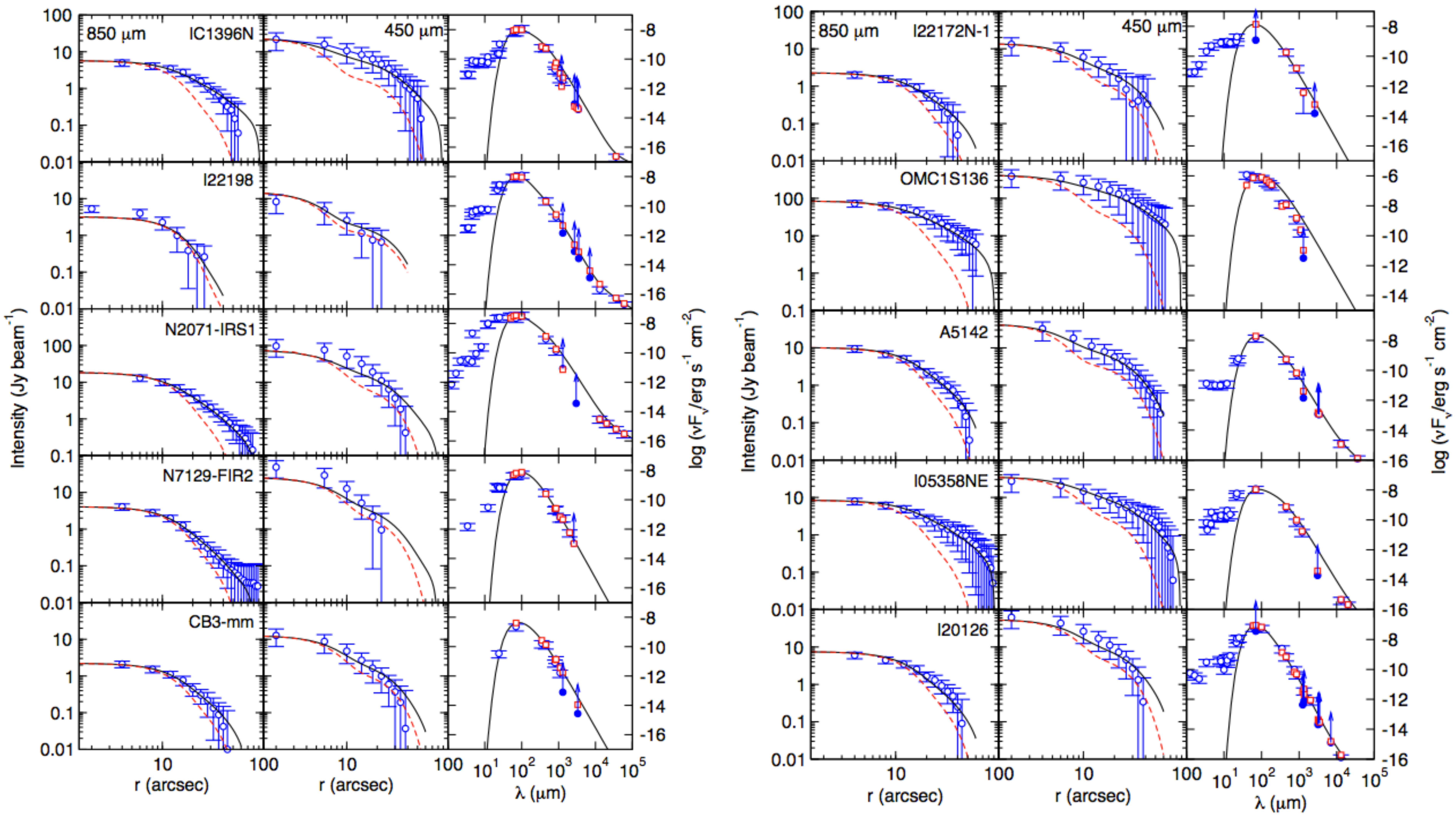

Palau et al. 2014, ApJ, 785, 42

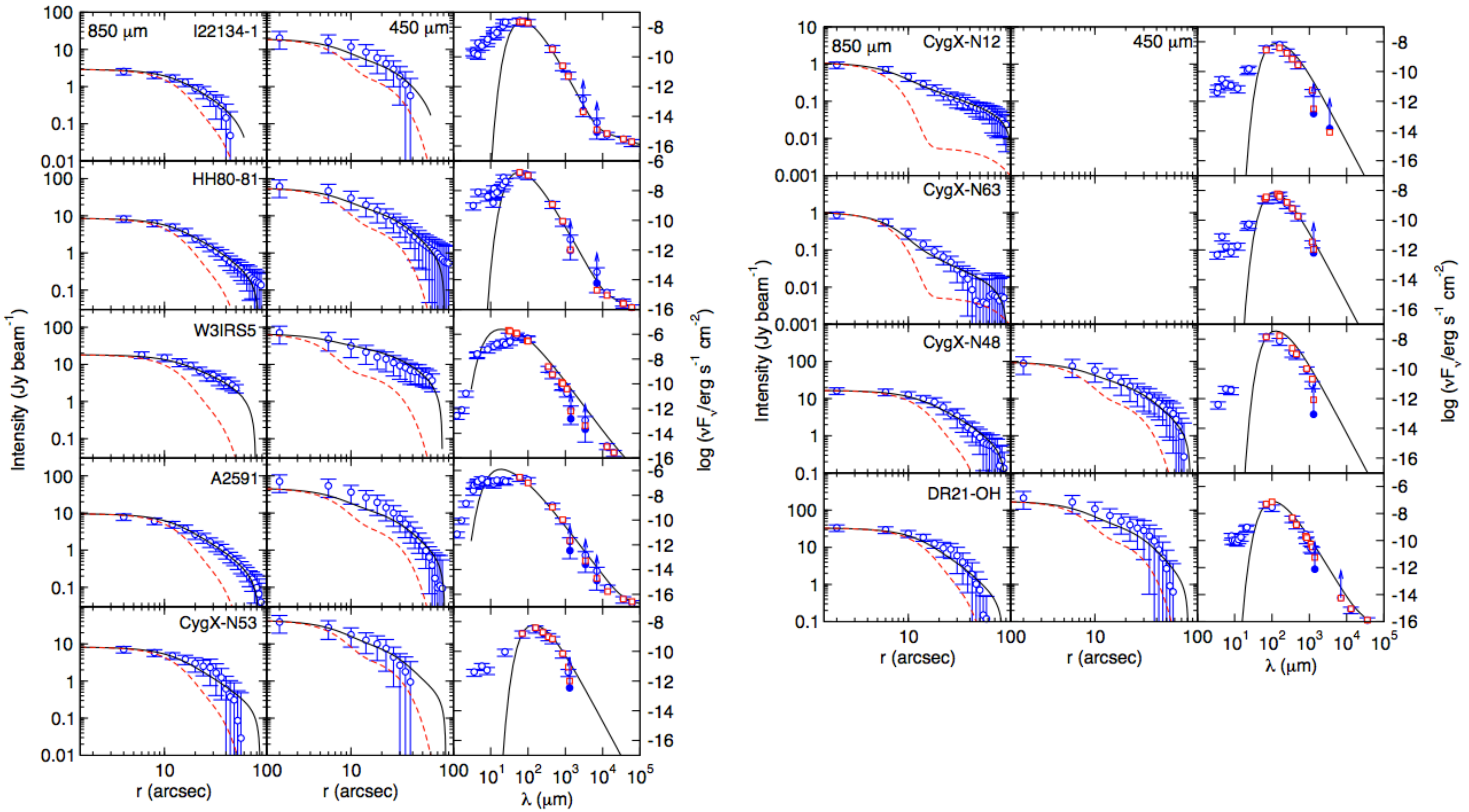

Palau et al. 2014, ApJ, 785, 42

Modeling of radial intensity profiles and Spectral Energy Distributions (Palau+14a): obtain density and temperature structure

THE ASTROPHYSICAL JOURNAL, 785:42 (18pp), 2014 April 10

Table 1
Best-fit Parameters to the Radial Profiles and SED of the Massive Dense Cores

ID-Source	D (kpc)	L_{bol}[a] ($L_\odot$)	N_{mm}[a]	β[b]	T_0[b] (K)	ρ_0[b] (g cm^{-3})	p[b]	χ_r[b]	p_{lit}[c]	References[c]
1-IC1396N	0.75	290	4	1.41 ± 0.19	43 ± 4	$(2.8 \pm 0.4) \times 10^{-17}$	1.62 ± 0.08	0.580	1.2	1
2-I22198[d]	0.76	340	1.5	1.46 ± 0.31	43 ± 5	$(2.8 \pm 1.0) \times 10^{-17}$	2.45 ± 0.16	0.885	...	...
3-NGC 2071-IRS1	0.42	440	4	1.09 ± 0.21	40 ± 3	$(6.1 \pm 1.0) \times 10^{-17}$	1.83 ± 0.09	0.534	...	...
4-NGC 7129-FIRS2	1.25	460	1	1.55 ± 0.28	47 ± 4	$(5.9 \pm 1.1) \times 10^{-17}$	2.14 ± 0.11	0.454	1.4	1
5-CB3-mm	2.50	700	2	1.42 ± 0.24	58 ± 7	$(7.4 \pm 1.5) \times 10^{-17}$	2.04 ± 0.10	0.552	2.2	1
6-I22172N-IRS1	2.40	830	3	1.49 ± 0.23	75 ± 10	$(3.7 \pm 0.7) \times 10^{-17}$	1.89 ± 0.08	0.283	...	...
7-OMC-1S	0.45	2000	9	1.42 ± 0.20	86 ± 9	$(8.8 \pm 1.8) \times 10^{-17}$	1.56 ± 0.10	0.319	??	2
8-AFGL 5142	1.80	2200	7	1.25 ± 0.20	70 ± 7	$(1.8 \pm 0.2) \times 10^{-16}$	2.00 ± 0.05	0.361	...	...
9-I05358+3543NE	1.80	3100	4	1.28 ± 0.18	62 ± 6	$(6.4 \pm 1.0) \times 10^{-17}$	1.55 ± 0.05	0.229	>0.8, 1.5	3, 7
10-I20126+4104	1.64	8900	1	1.82 ± 0.24	86 ± 9	$(8.4 \pm 1.6) \times 10^{-17}$	2.21 ± 0.11	0.607	1.6, 1.8, 2.2	3, 4, 5
11-I22134-IRS1	2.60	11800	3.5	1.70 ± 0.19	82 ± 8	$(3.1 \pm 0.5) \times 10^{-17}$	1.76 ± 0.06	0.477	1.3	3
12-HH80-81	1.70	21900	3	1.56 ± 0.14	108 ± 10	$(4.2 \pm 0.6) \times 10^{-17}$	1.78 ± 0.04	0.473	...	...
13-W3IRS5	1.95	140000	3.5	1.04 ± 0.12	260 ± 30	$(2.4 \pm 0.3) \times 10^{-17}$	1.46 ± 0.04	0.602	1.5, 1.4	4, 7
14-AFGL 2591	3.00	190000	1.5	0.96 ± 0.12	250 ± 20	$(5.4 \pm 0.7) \times 10^{-17}$	1.80 ± 0.03	0.549	1.0, 2.0, 1.0	4, 6, 7
15-CygX-N53	1.40	300	6	1.55 ± 0.22	45 ± 4	$(9.7 \pm 1.8) \times 10^{-17}$	1.76 ± 0.07	0.487	...	...
16-CygX-N12[e]	1.40	320	2.5	1.75 ± 0.26	50 ± 4	$(3.3 \pm 0.3) \times 10^{-17}$	1.52 ± 0.03	0.376	...	...
17-CygX-N63[e]	1.40	470	1	1.80 ± 0.33	45 ± 3	$(6.5 \pm 1.1) \times 10^{-17}$	2.03 ± 0.07	0.570	...	...
18-CygX-N48	1.40	4400	5	1.88 ± 0.18	58 ± 5	$(1.0 \pm 0.2) \times 10^{-16}$	1.71 ± 0.05	0.459	...	...
19-DR21-OH	1.40	10000	11	1.60 ± 0.26	73 ± 7	$(3.1 \pm 0.6) \times 10^{-16}$	1.98 ± 0.08	0.808	1.8, 1.4	4, 7

N_{mm} vs density power law index "p"

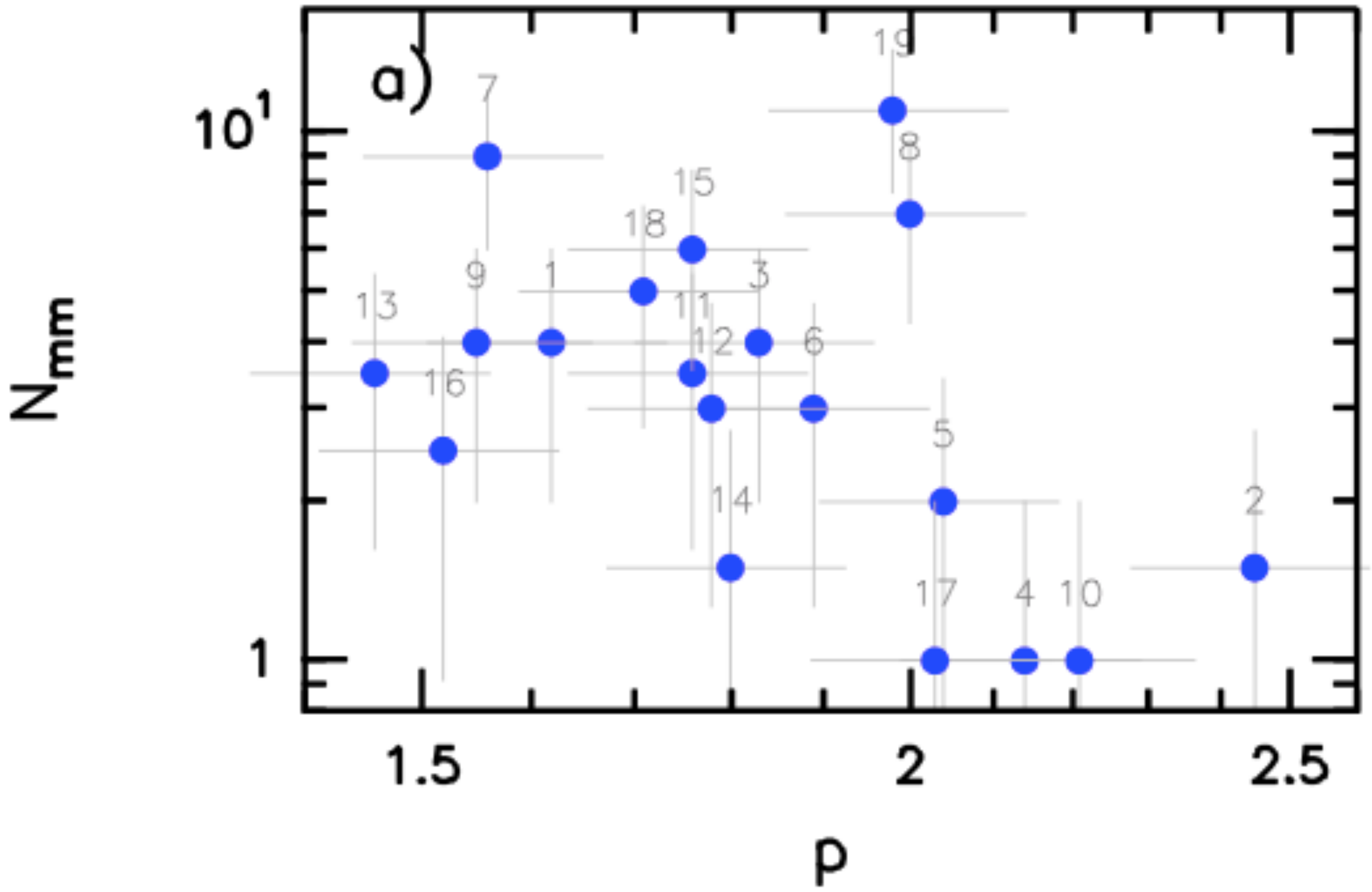

N_{mm} vs central density

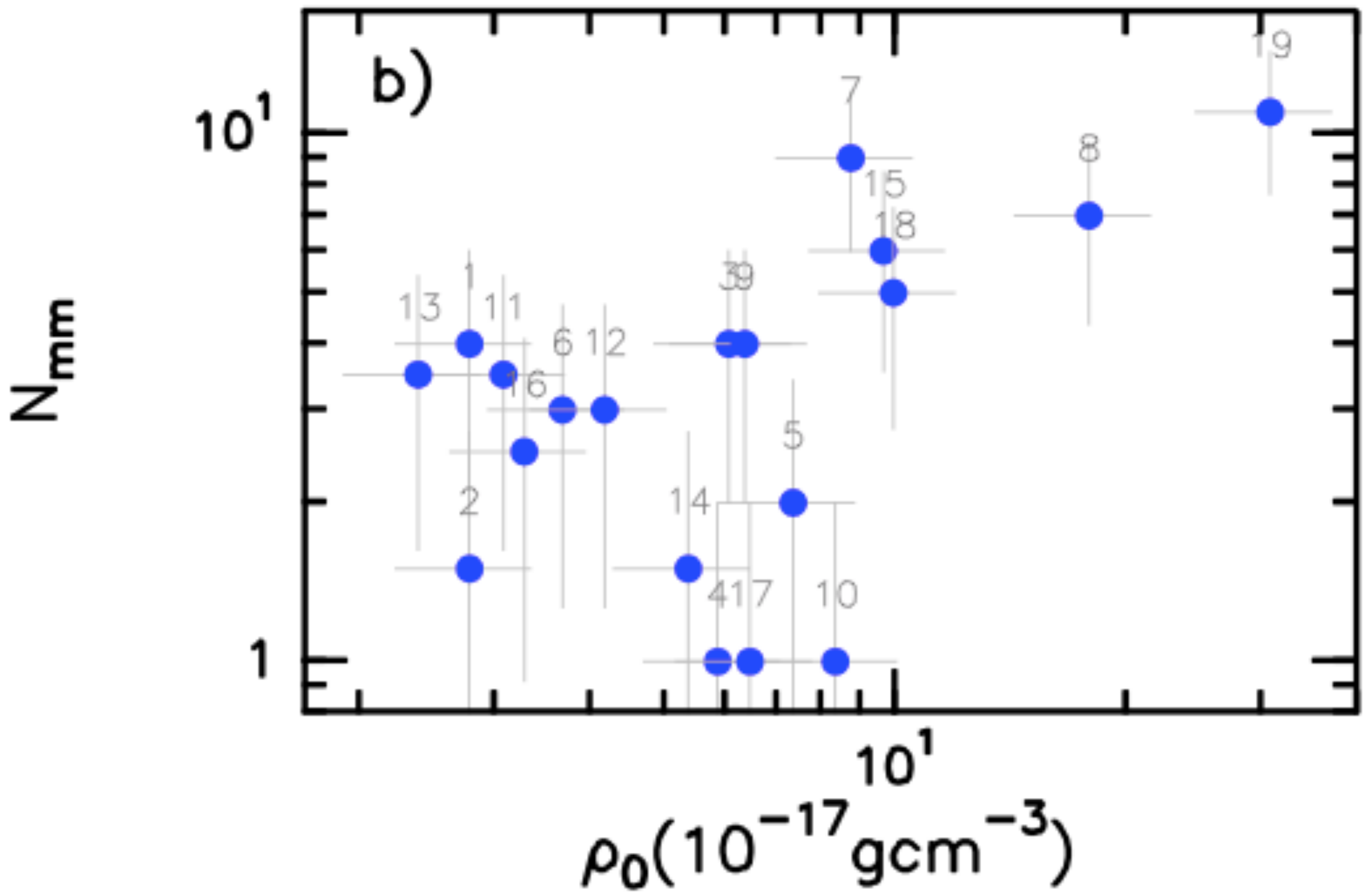

Palau et al. 2014, ApJ, 785, 42

N_{mm} vs density within 0.1 pc

0.1 pc is the region where fragmentation (N_{mm}) was assessed

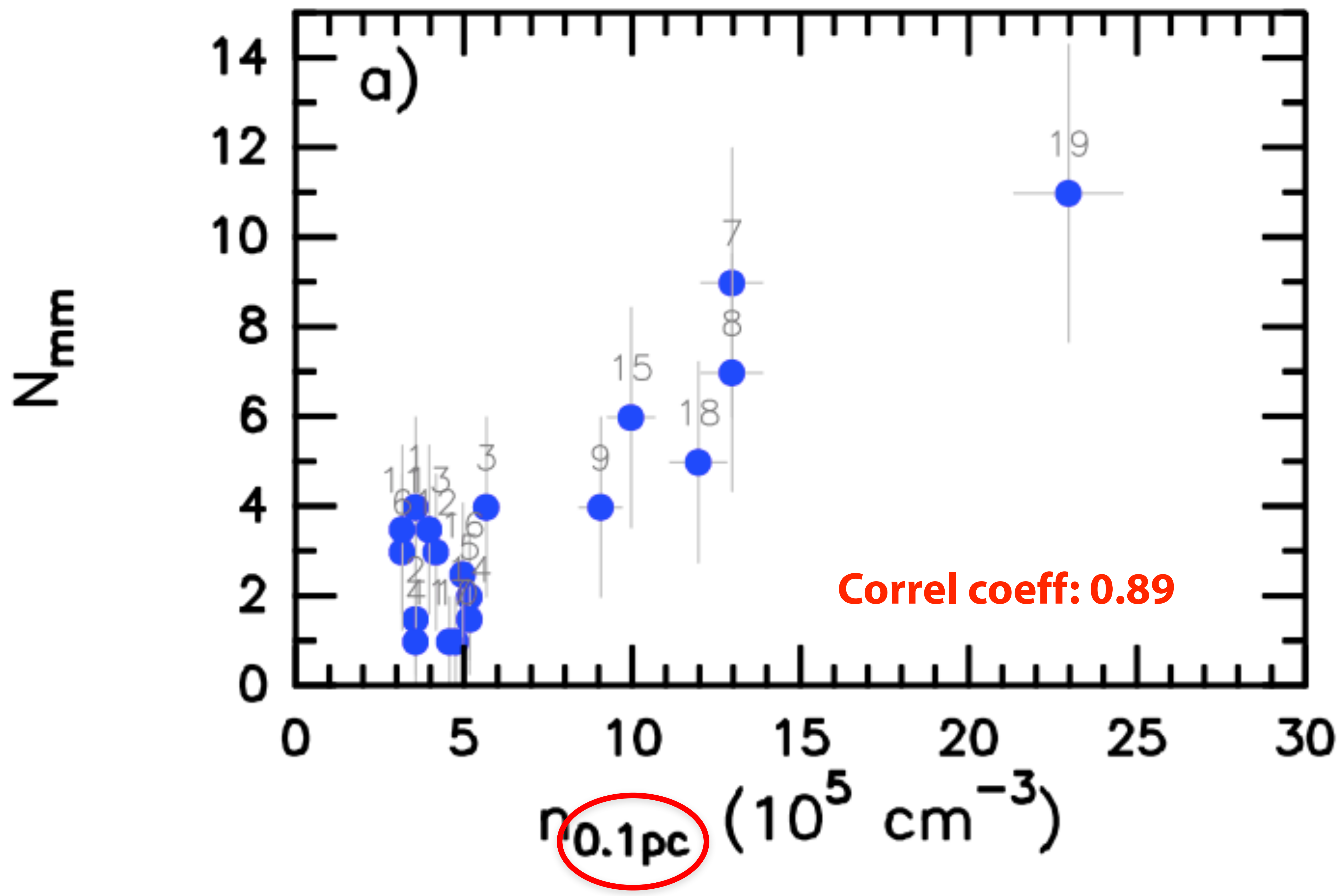

Palau et al. 2014, ApJ, 785, 42
Palau et al. 2015, MNRAS, 453, 3785

Introduction

Inside 0.1 pc: method + first results

Density and T structure

Role of rotation, turbulence and B

Inside 0.01 pc: ALMA

Velocity information of the massive dense cores

VLA, USA
NH_3(1,1): imaging, beam~5'', largest ang. scale~30''
SánchezMonge, Palau+13 + archive + literature

IRAM30m, Spain
N_2H^+(1-0): single pointings, beam~26''
Fontani+11 + literature

NH3(1,1) emission with the VLA

study the kinematics of massive dense cores

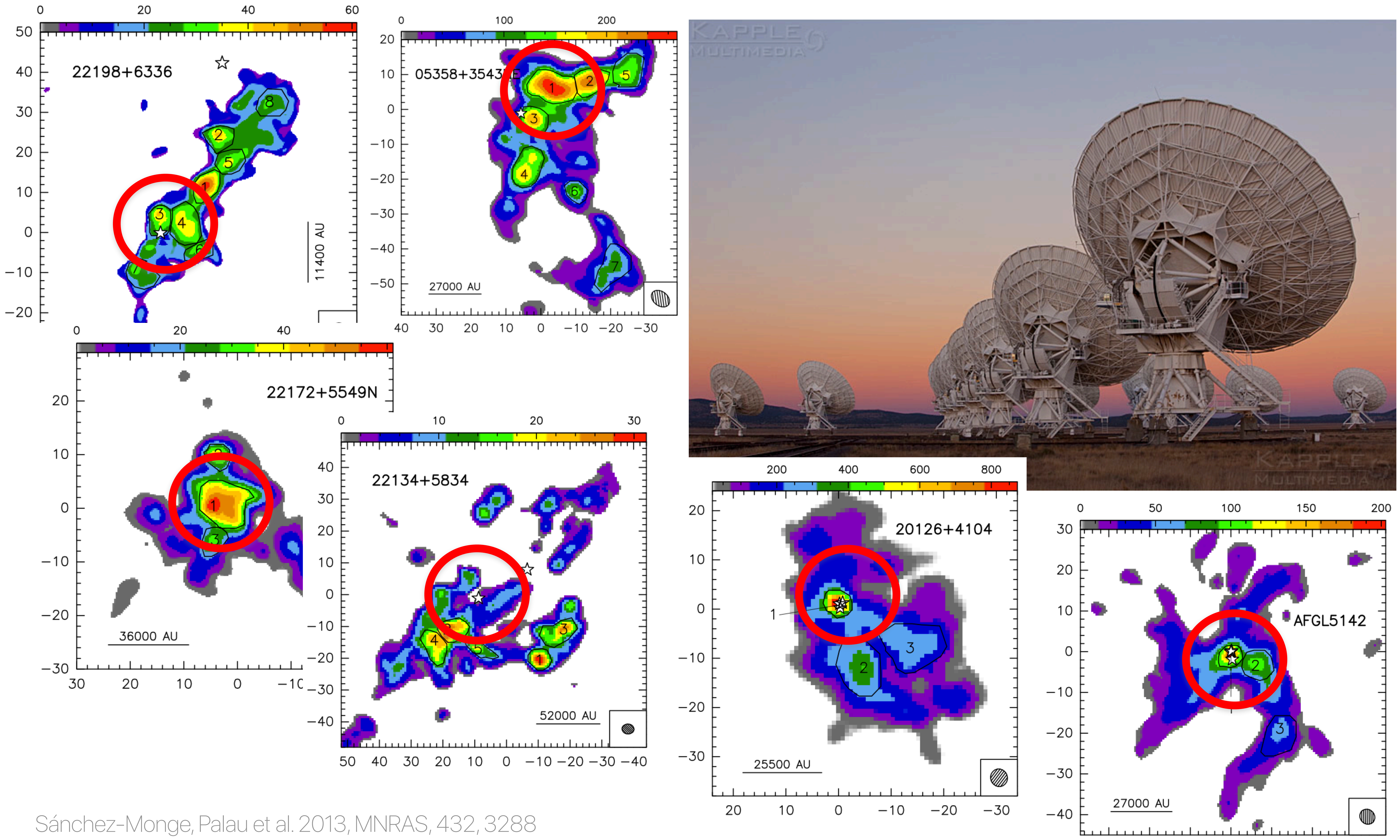

Sánchez-Monge, Palau et al. 2013, MNRAS, 432, 3288

NH3(1,1) emission with the VLA

moment 1 maps: velocity gradients

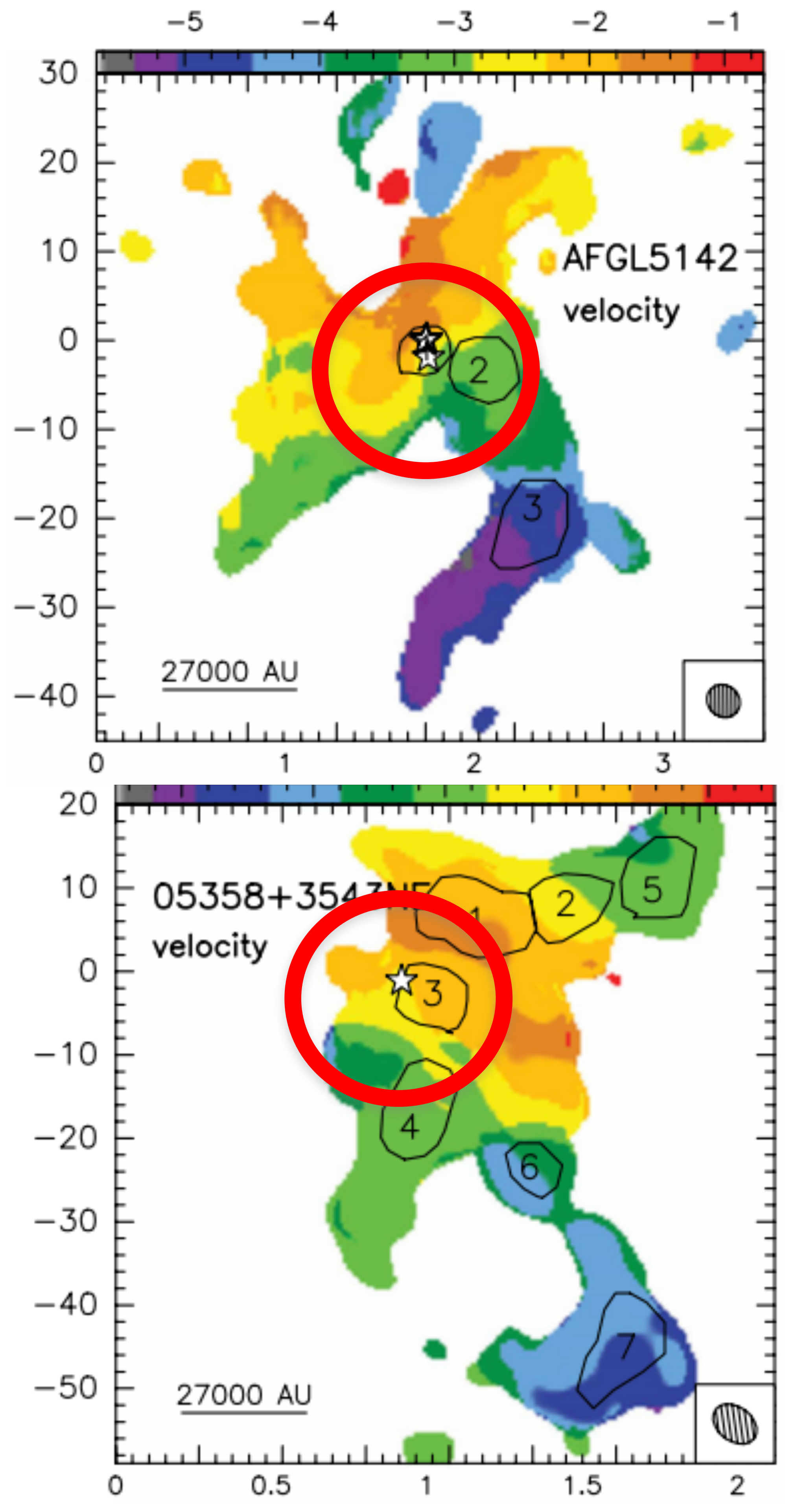

$$\beta_{\rm rot} = \frac{E_{\rm rot}}{U}$$

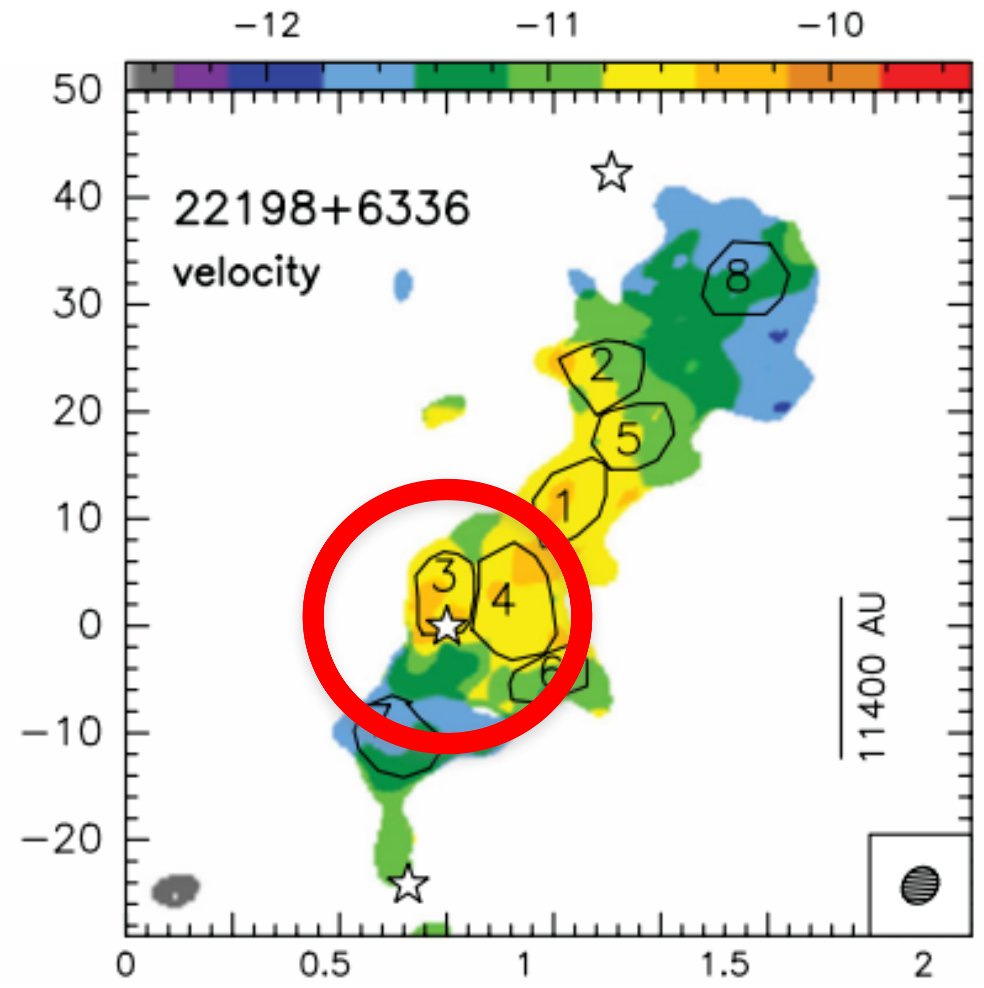

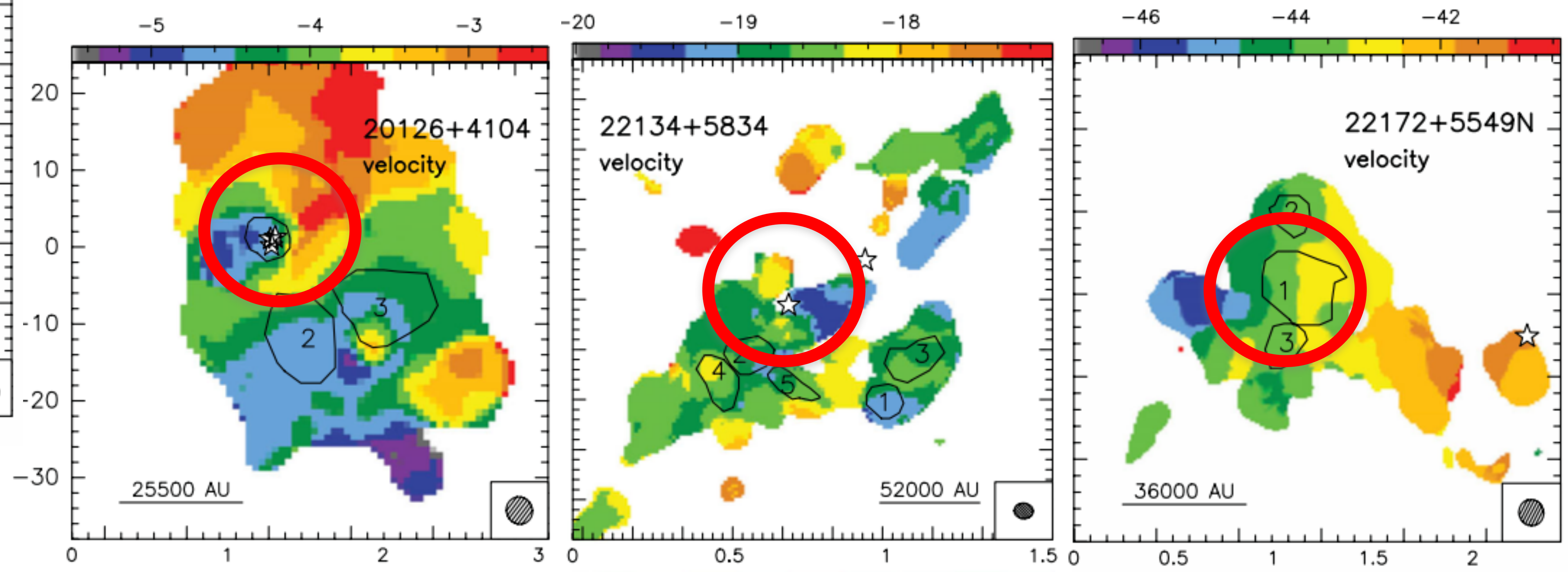

Sánchez-Monge, Palau et al. 2013, MNRAS, 432, 3288

No correlation between fragmentation level and rotation: $\beta_{\rm rot} = \frac{E_{\rm rot}}{U} > 0.01$

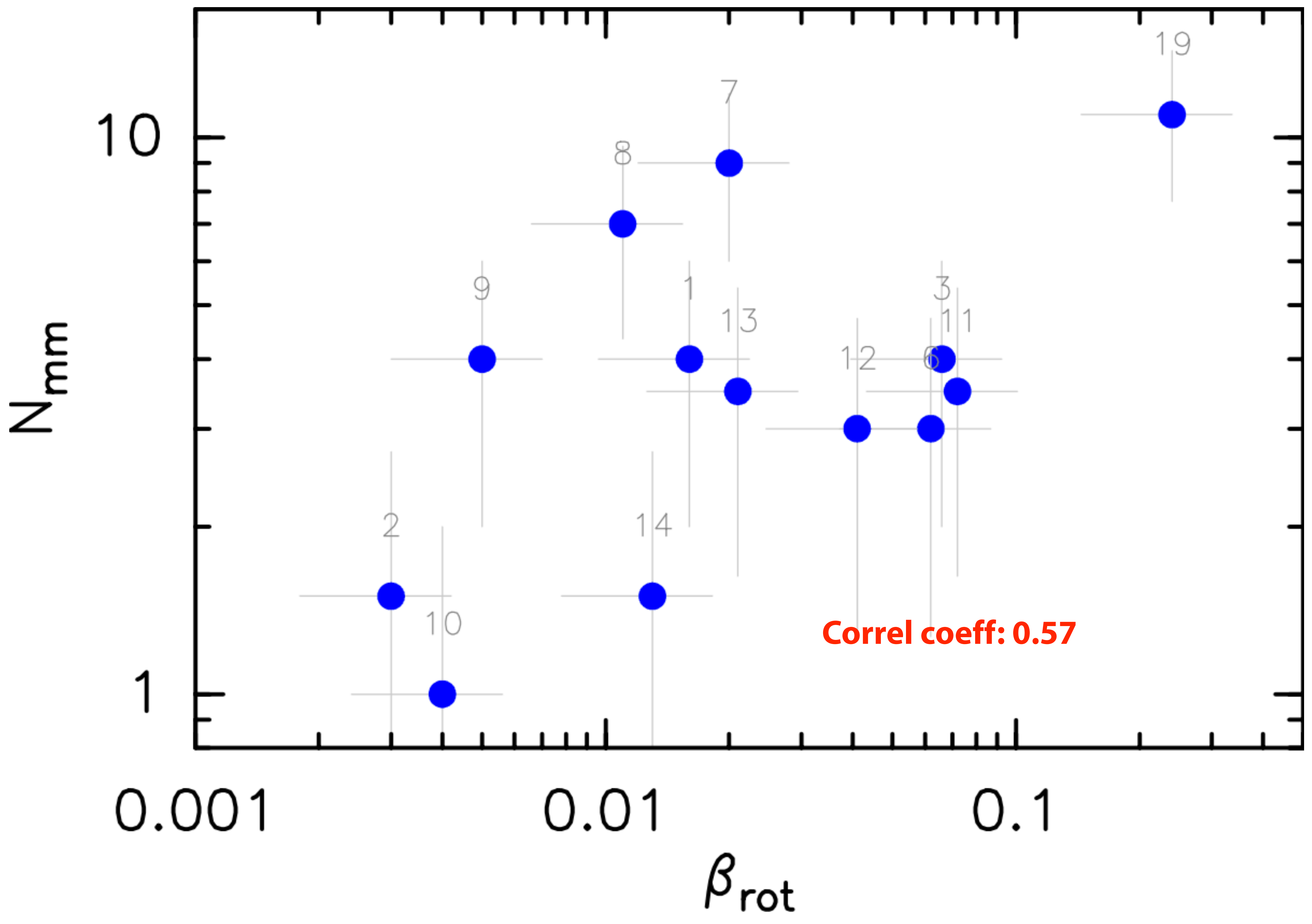

Palau et al. 2014, ApJ, 785, 42

NH_3(1,1) and N_2H^+ emission with VLA and IRAM30m

measure linewidths fitting the hyperfine structure

NH_3(1,1) with the VLA

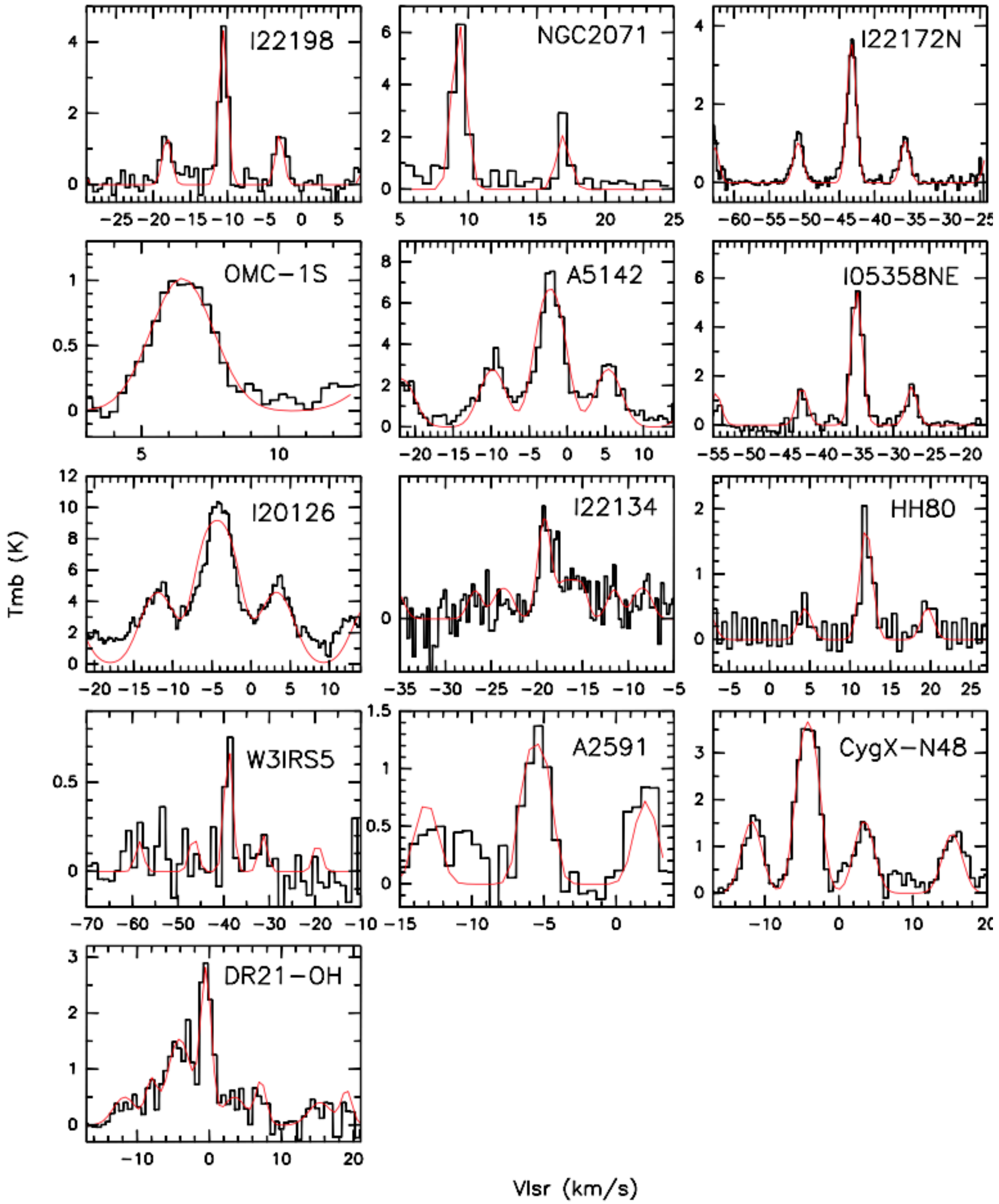

Palau et al. 2015, MNRAS, 453, 3785

N_2H^+(1-0) with IRAM30m

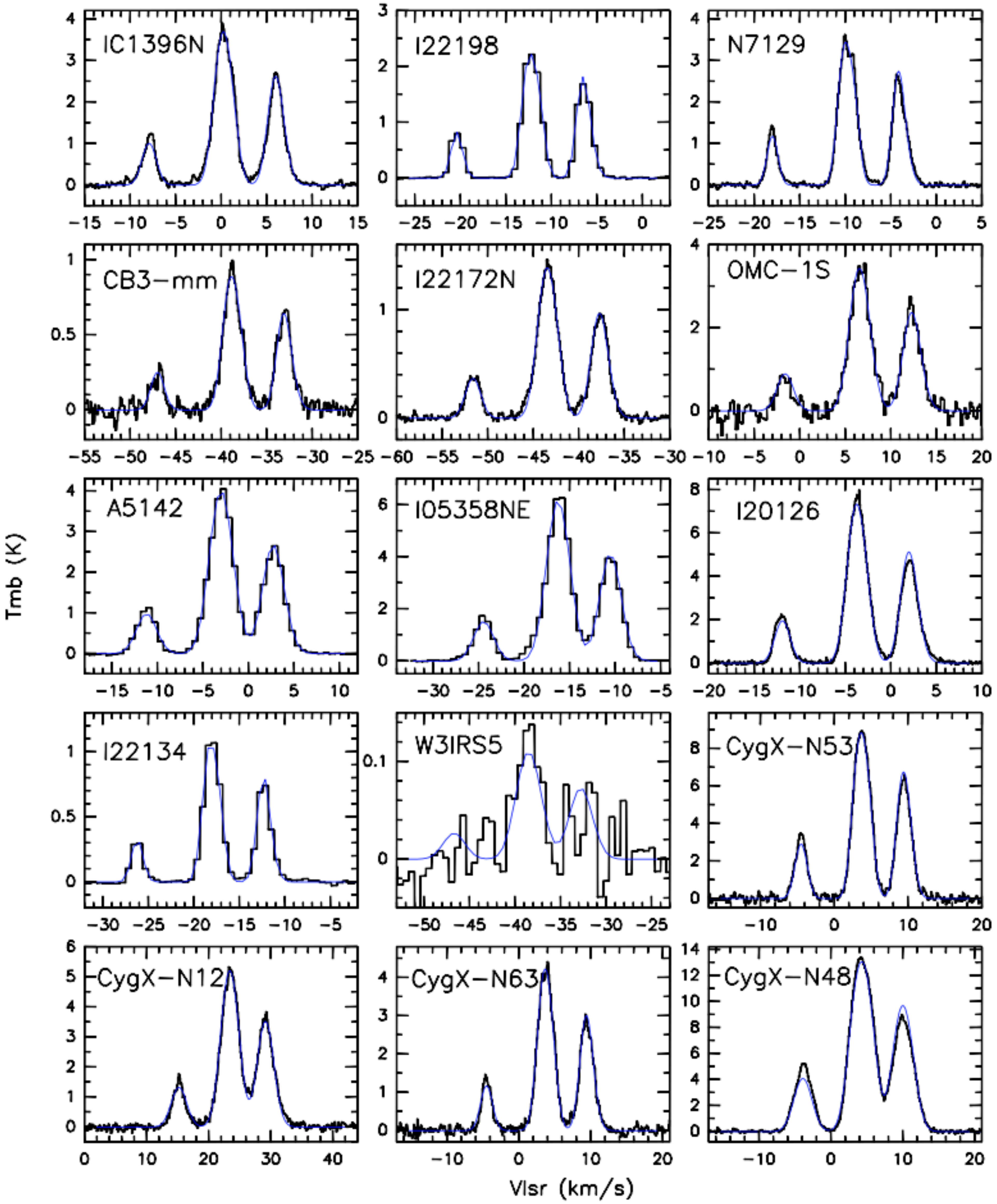

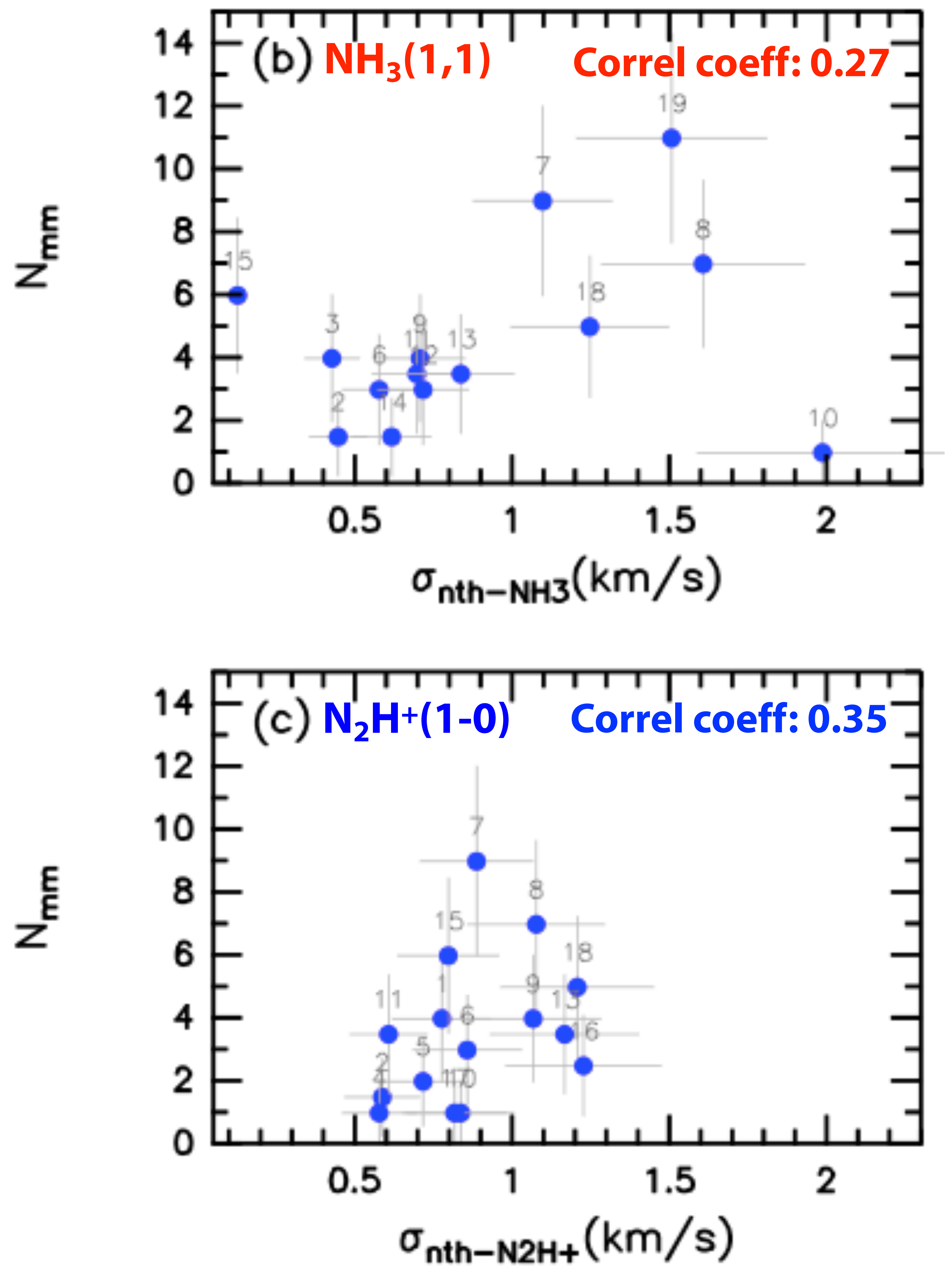

No correlation between fragmentation level and velocity dispersion of different dense gas tracers

also found by Fontani+18

not consistent with turbulent Jeans fragmentation:

$$\left[\frac{M_{\rm Jeans}^{\rm nth}}{M_\odot}\right] = 0.8255 \left[\frac{\sigma_{\rm 1D,nth}}{0.188\,{\rm km\,s^{-1}}}\right]^3 \left[\frac{n_{\rm H_2}}{10^5\,{\rm cm^{-3}}}\right]^{-1/2}$$

Palau et al. 2015, MNRAS, 453, 3785

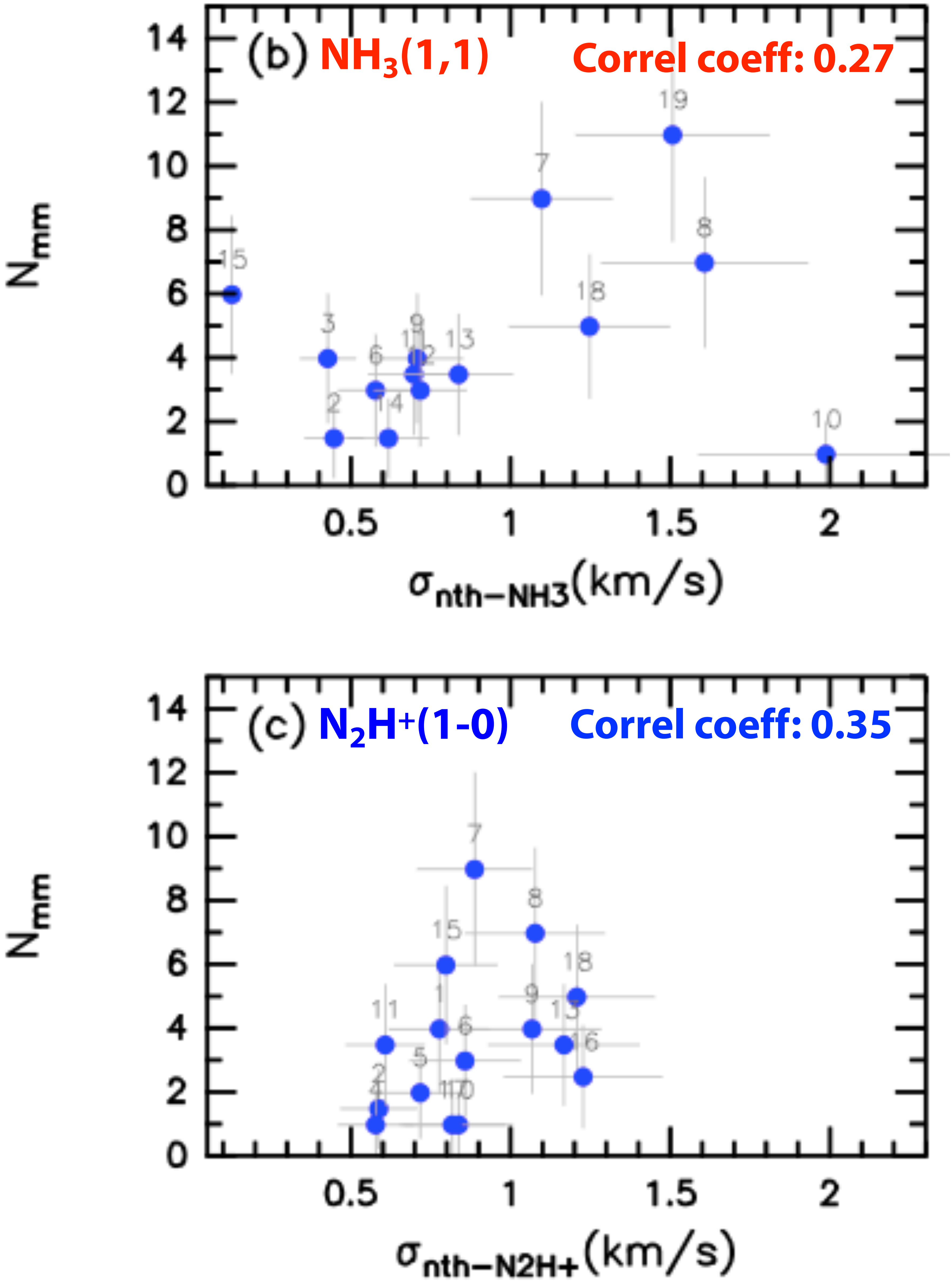

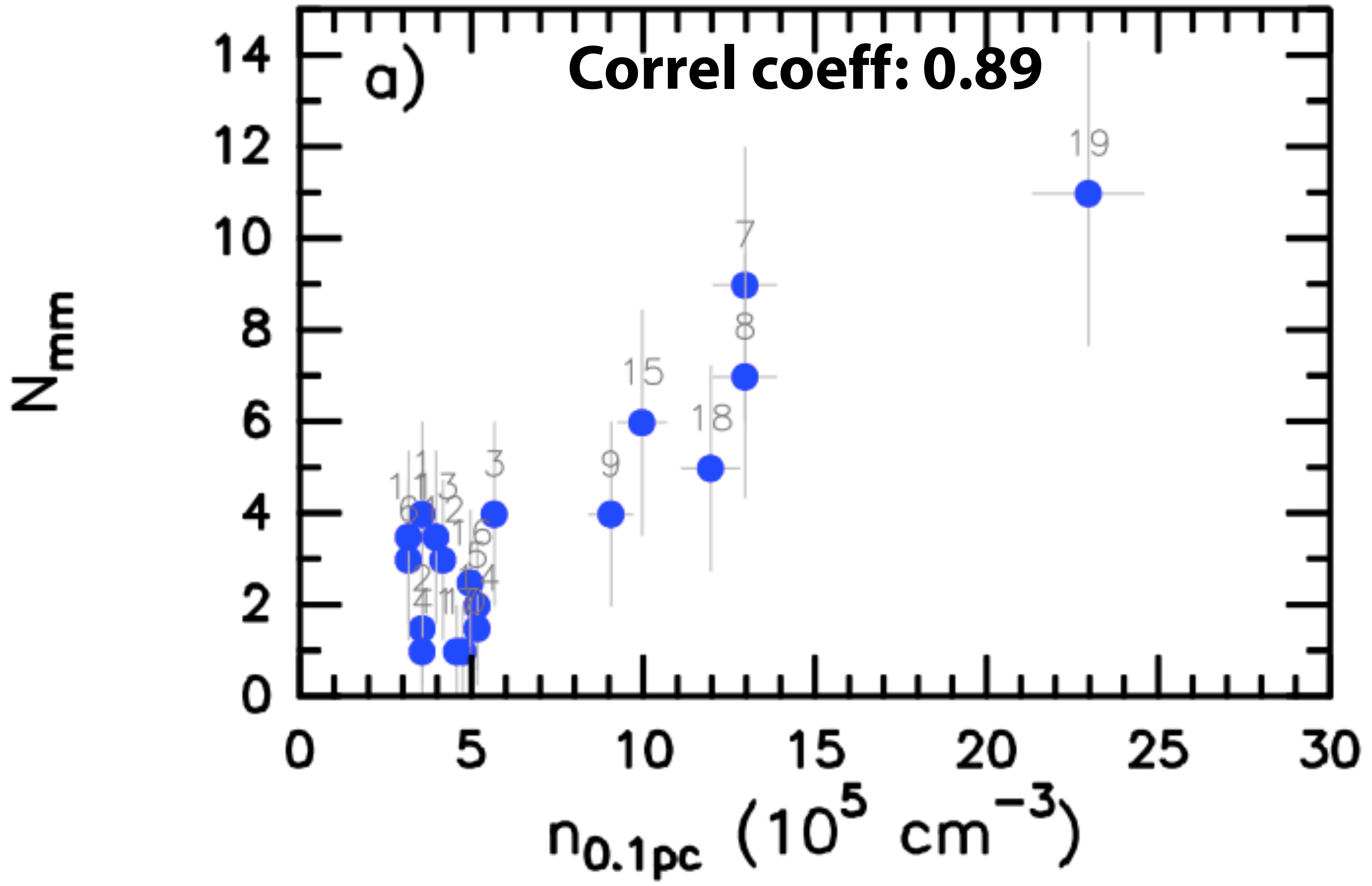

Consistent with thermal Jeans fragmentation:

$$\left[\frac{M^{\rm th}_{\rm Jeans}}{M_\odot}\right] = 0.6285 \left[\frac{T}{10\,{\rm K}}\right]^{3/2} \left[\frac{n_{\rm H_2}}{10^5\,{\rm cm}^{-3}}\right]^{-1/2}$$

Palau et al. 2015, MNRAS, 453, 3785

Magnetic field: MHD simulations including radiation transport

Commerçon et al. 2011, after Hennebelle et al. 2011

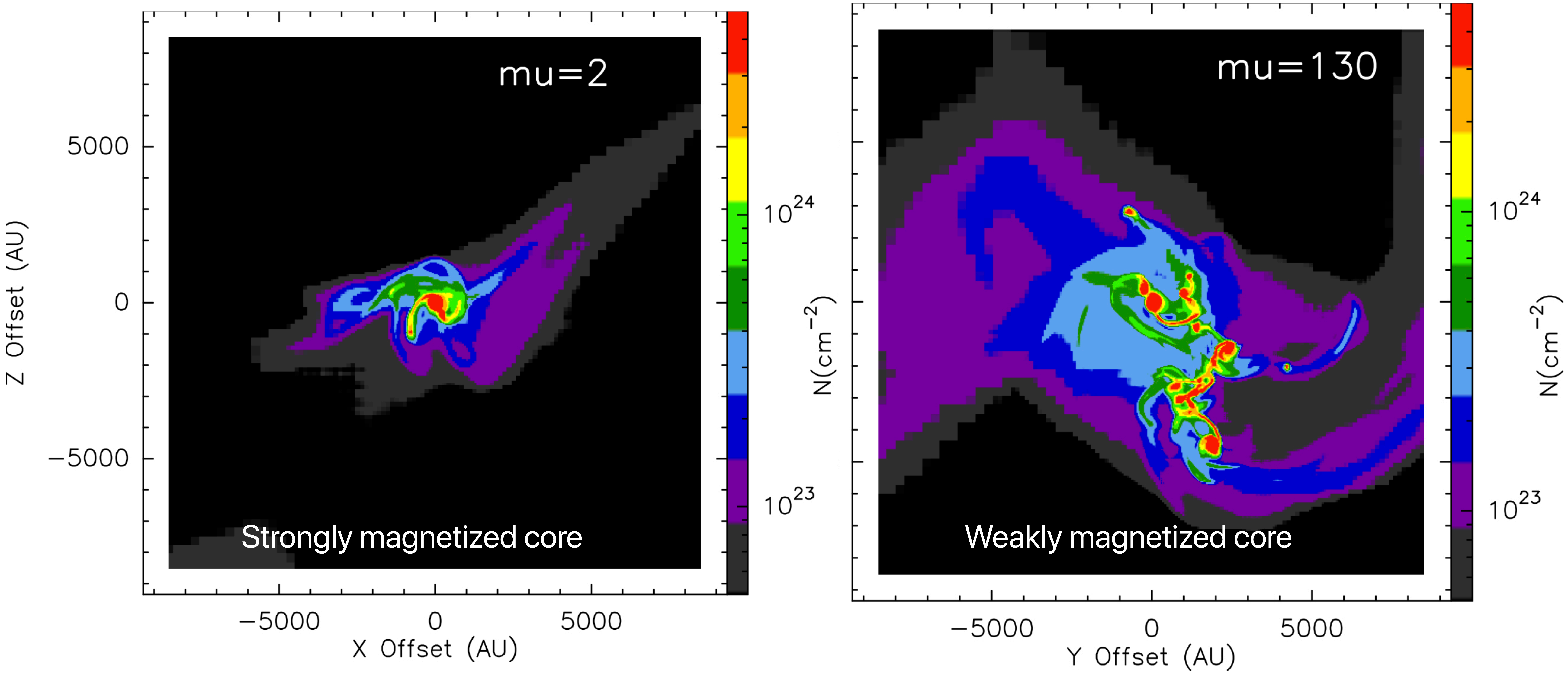

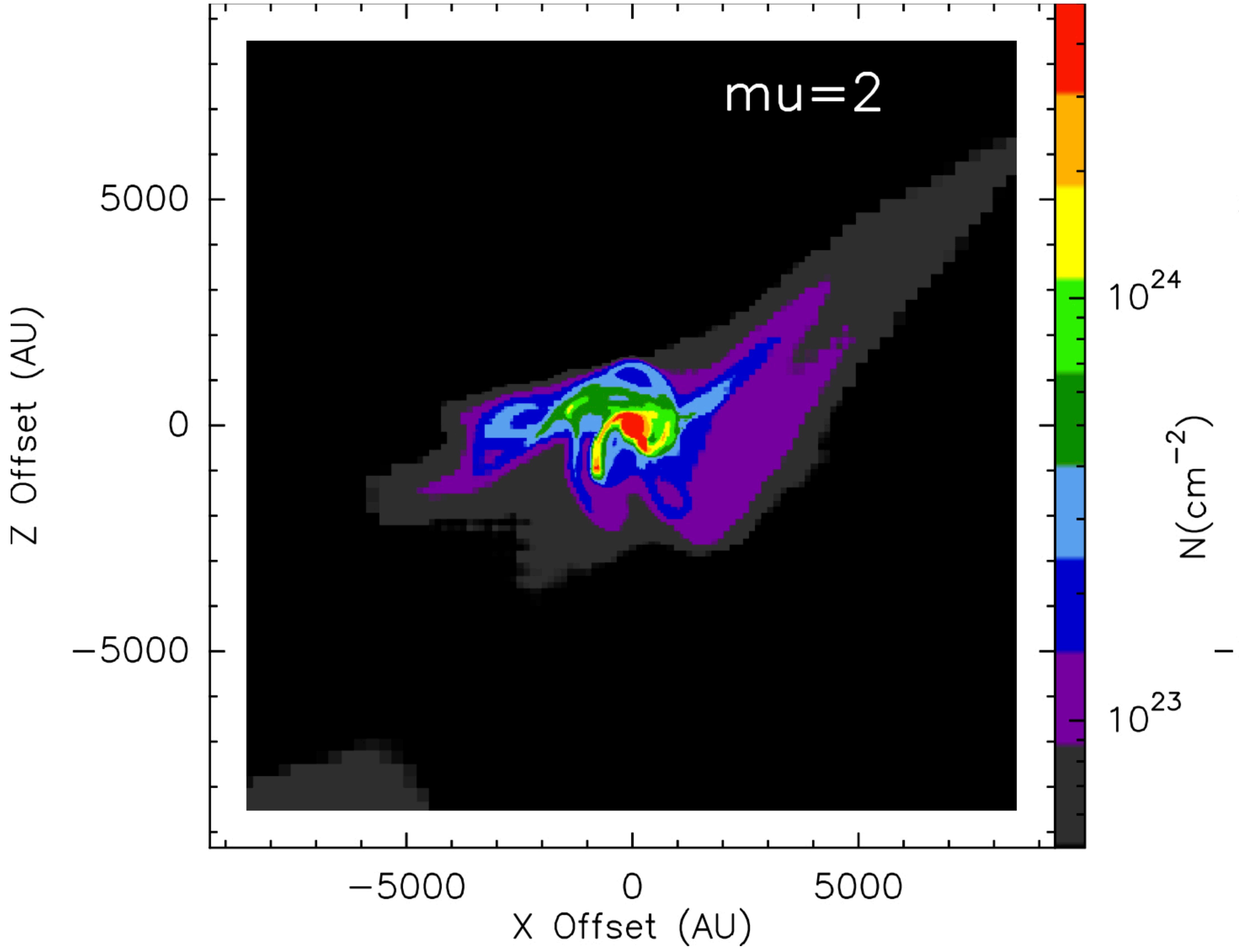

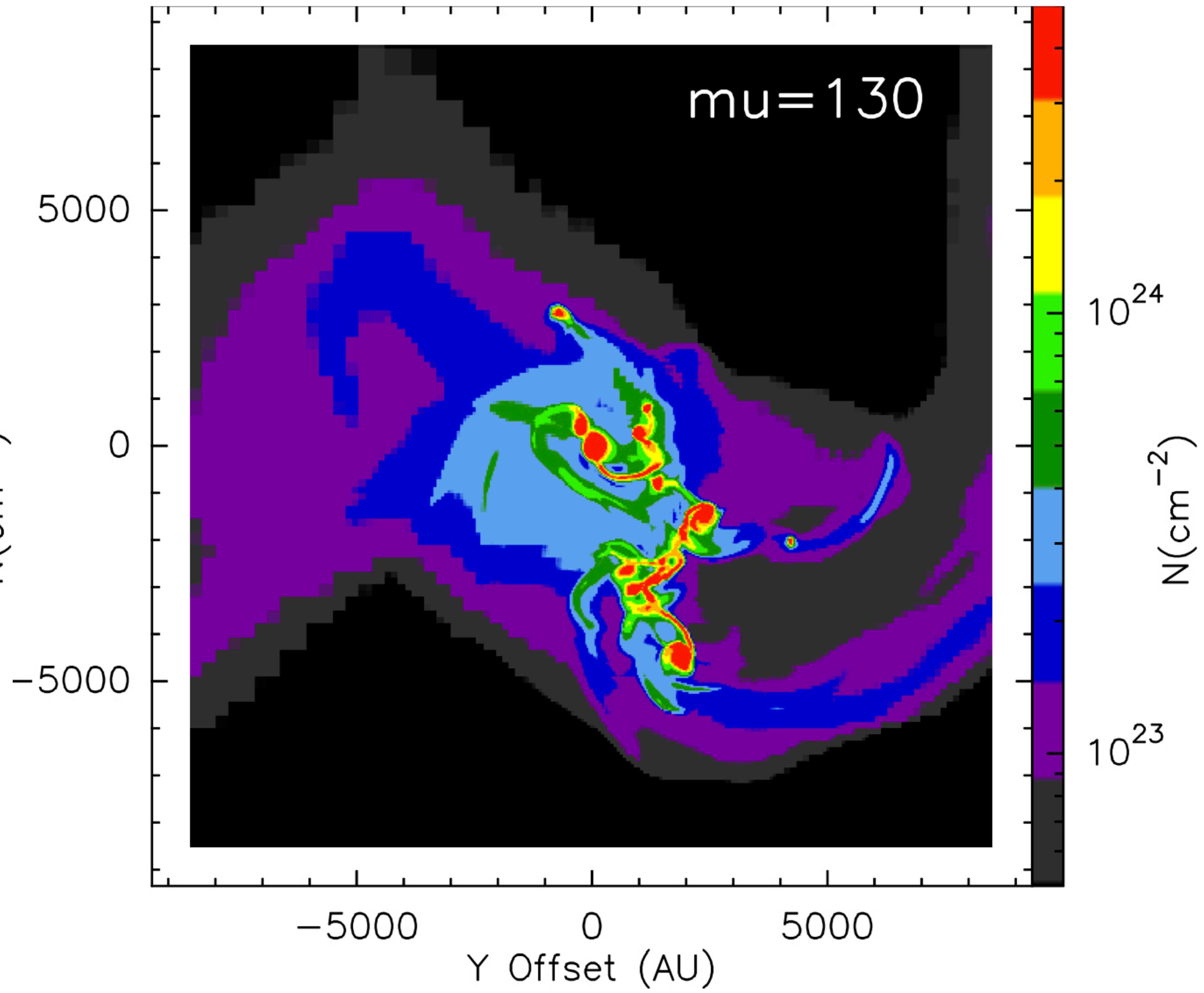

Convolution with Plateau de Bure A-config uv-coverage

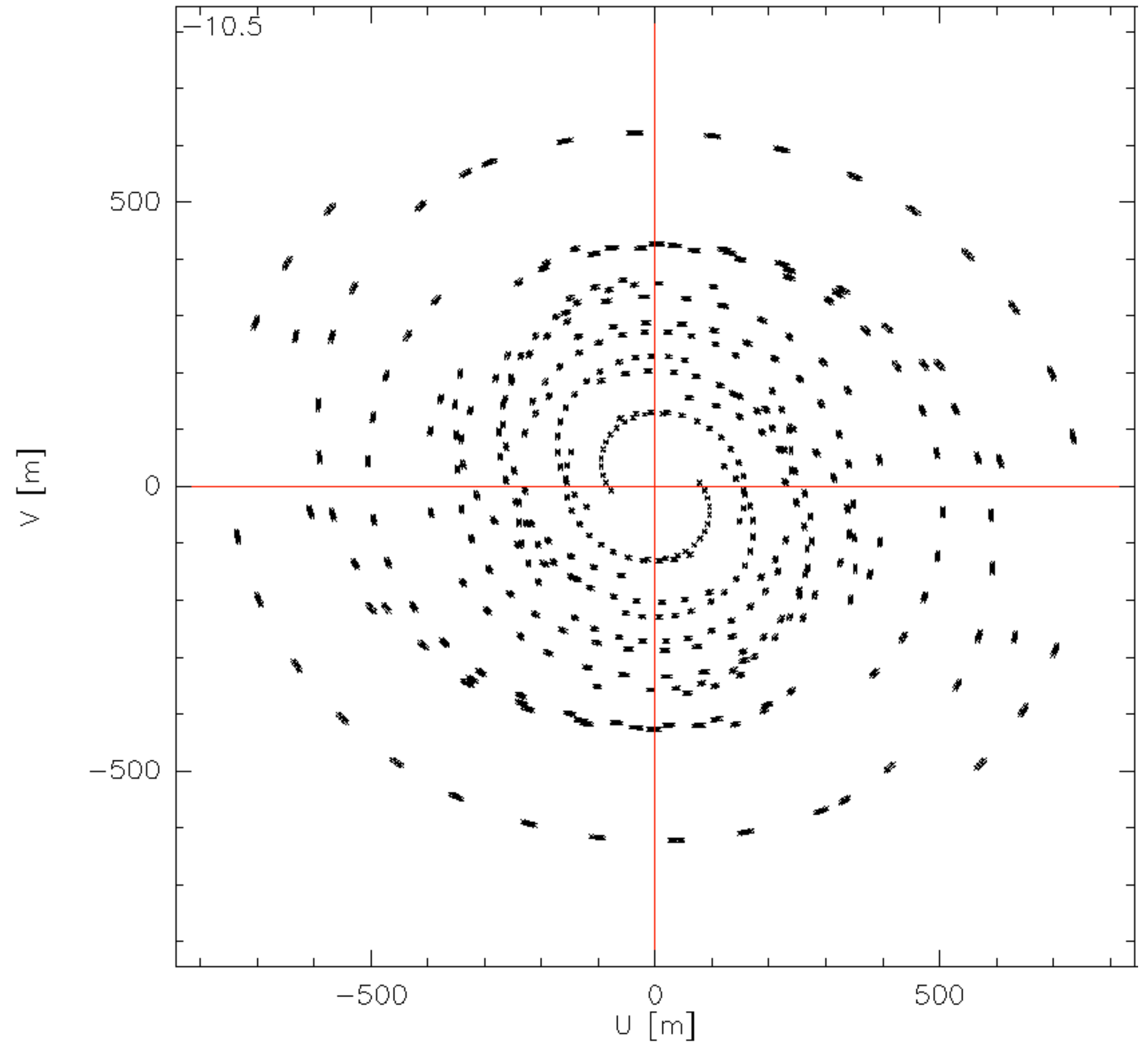

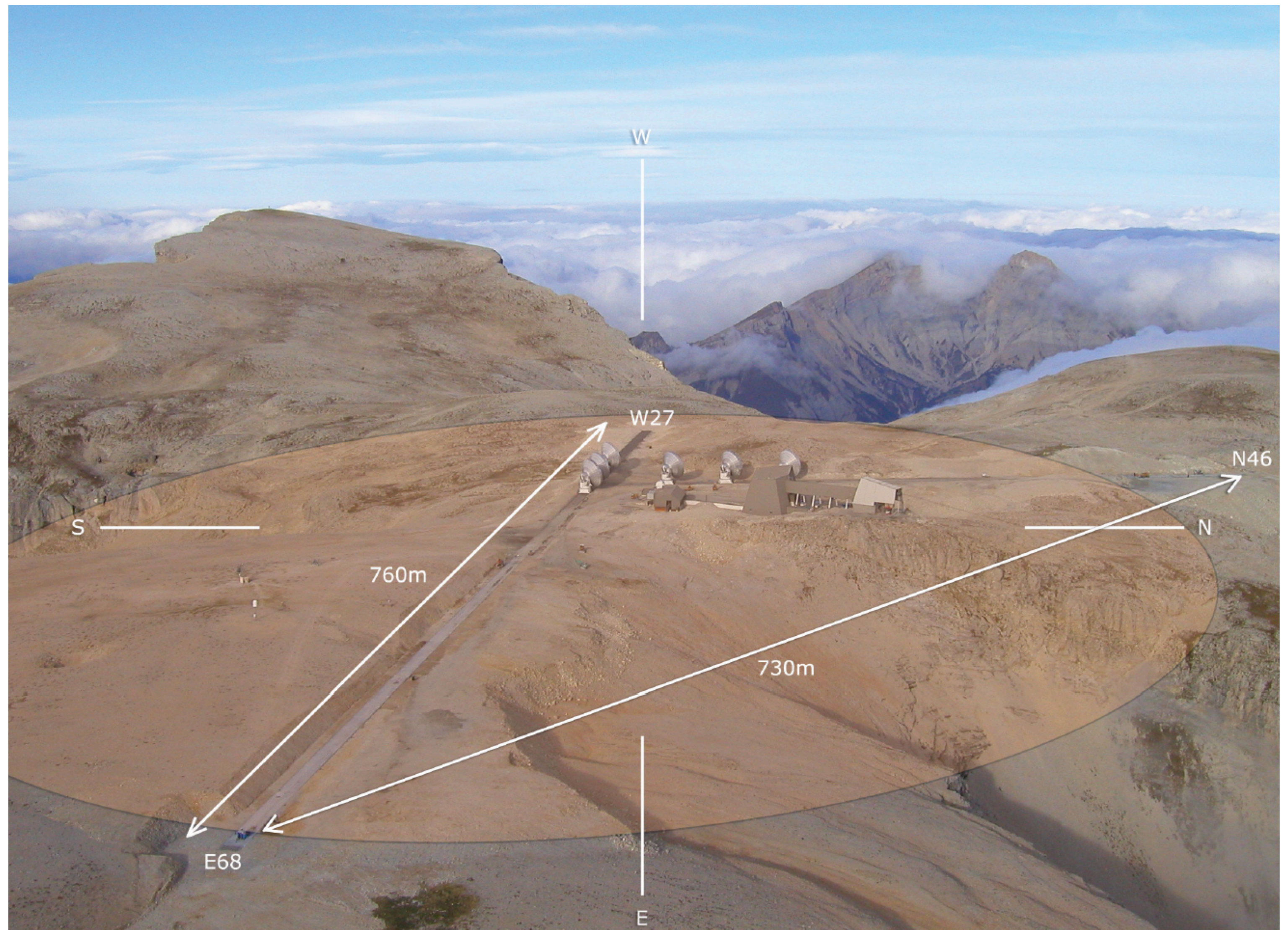

Palau et al. 2013, ApJ, 762, 120

Compare fragmentation level (Palau et al. 2013)

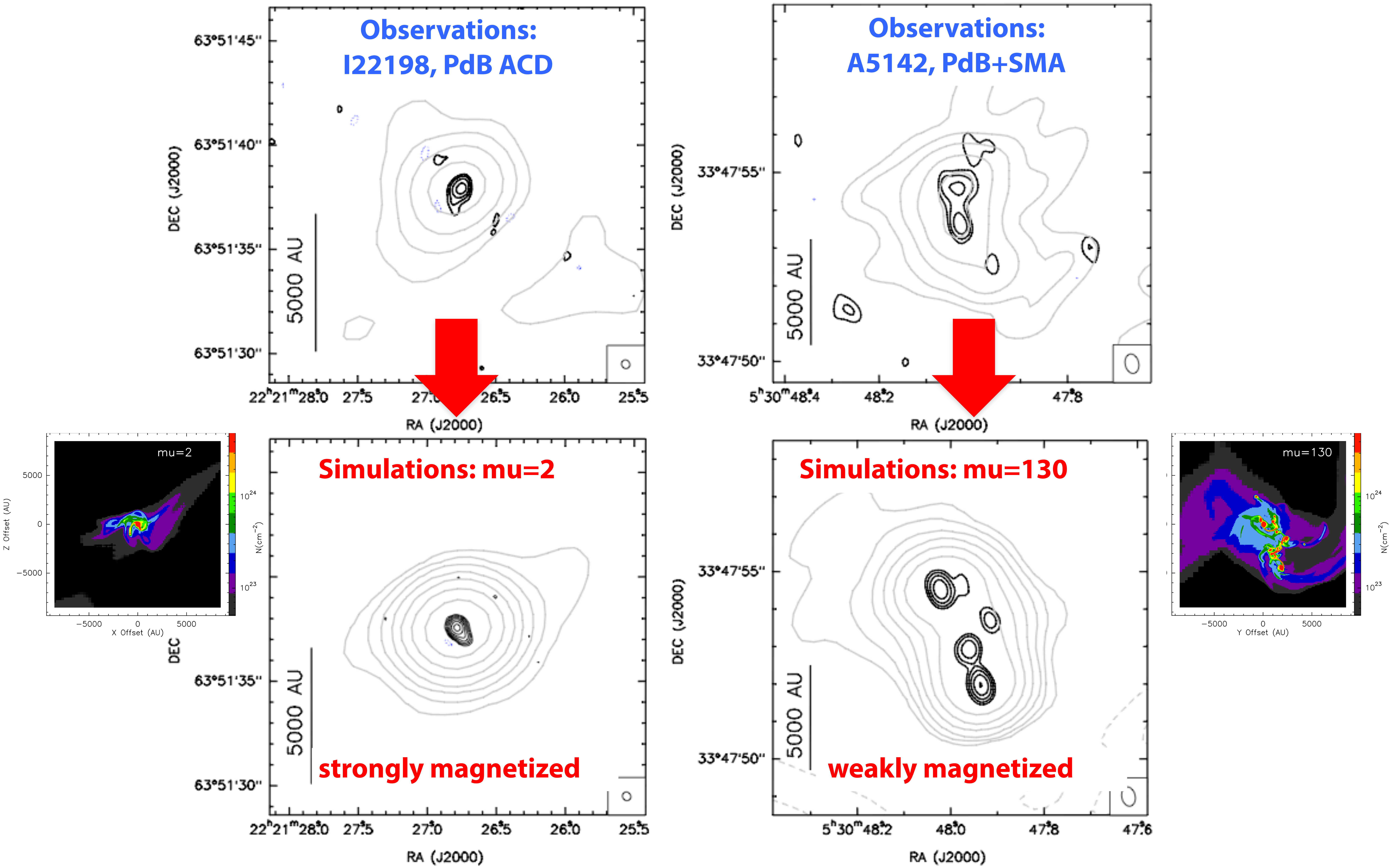

Consistent with Fontani et al. 2016, ALMA data

Magnetic field: what do observations tell us?

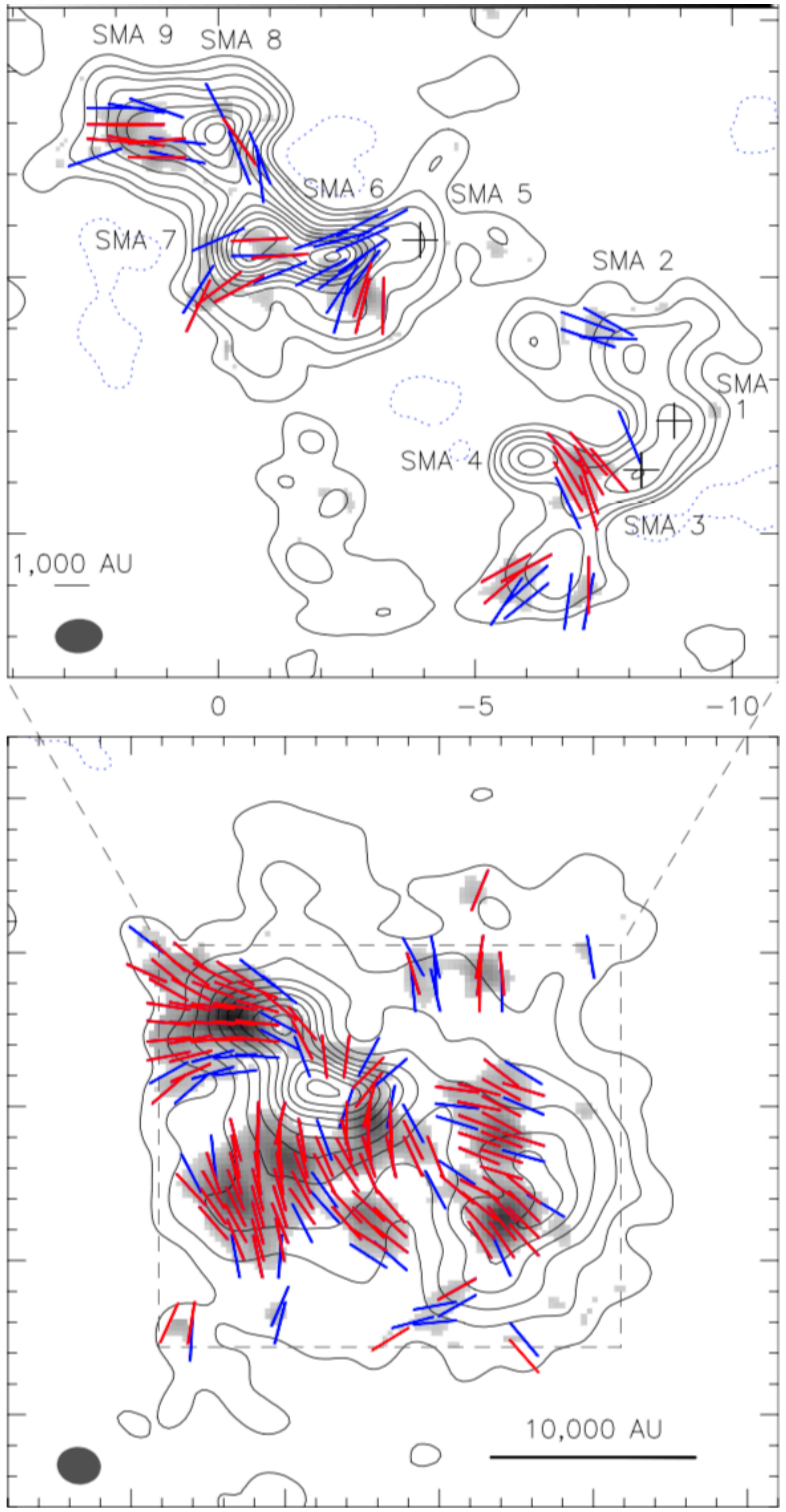

SMA Legacy (PI: Qizhou Zhang, Harvard-Smithsonian CfA)

study dust polarization properties to infer magnetic field strength

Introduction

Inside 0.1 pc: method + first results

Density and T structure

Role of rotation, turbulence and B

Inside 0.01 pc: ALMA

Select the region with highest fragmentation: OMC-1S

THE ASTROPHYSICAL JOURNAL, 785:42 (18pp), 2014 April 10 PALAU ET AL.

Table 1
Best-fit Parameters to the Radial Profiles and SED of the Massive Dense Cores

ID-Source	D (kpc)	L_{bol}[a] ($L_\odot$)	N_{mm}[a]	β[b]	T_0[b] (K)	ρ_0[b] (g cm^{-3})	p[b]	χ_r[b]	p_{lit}[c]	References[c]
1-IC1396N	0.75	290	4	1.41 ± 0.19	43 ± 4	$(2.8 \pm 0.4) \times 10^{-17}$	1.62 ± 0.08	0.580	1.2	1
2-I22198[d]	0.76	340	1.5	1.46 ± 0.31	43 ± 5	$(2.8 \pm 1.0) \times 10^{-17}$	2.45 ± 0.16	0.885	...	...
3-NGC 2071-IRS1	0.42	440	4	1.09 ± 0.21	40 ± 3	$(6.1 \pm 1.0) \times 10^{-17}$	1.83 ± 0.09	0.534	...	...
4-NGC 7129-FIRS2	1.25	460	1	1.55 ± 0.28	47 ± 4	$(5.9 \pm 1.1) \times 10^{-17}$	2.14 ± 0.11	0.454	1.4	1
5-CB3-mm	2.50	700	2	1.42 ± 0.24	58 ± 7	$(7.4 \pm 1.5) \times 10^{-17}$	2.04 ± 0.10	0.552	2.2	1
6-I22172N-IRS1	2.40	830	3	1.49 ± 0.23	75 ± 10	$(3.7 \pm 0.7) \times 10^{-17}$	1.89 ± 0.08	0.283	...	...
7-OMC-1S	0.45	2000	9	1.42 ± 0.20	86 ± 9	$(8.8 \pm 1.8) \times 10^{-17}$	1.56 ± 0.10	0.319	??	2
8-AFGL 5142	1.80	2200	7	1.25 ± 0.20	70 ± 7	$(1.8 \pm 0.2) \times 10^{-16}$	2.00 ± 0.05	0.361	...	...
9-I05358+3543NE	1.80	3100	4	1.28 ± 0.18	62 ± 6	$(6.4 \pm 1.0) \times 10^{-17}$	1.55 ± 0.05	0.229	>0.8, 1.5	3, 7
10-I20126+4104	1.64	8900	1	1.82 ± 0.24	86 ± 9	$(8.4 \pm 1.6) \times 10^{-17}$	2.21 ± 0.11	0.607	1.6, 1.8, 2.2	3, 4, 5
11-I22134-IRS1	2.60	11800	3.5	1.70 ± 0.19	82 ± 8	$(3.1 \pm 0.5) \times 10^{-17}$	1.76 ± 0.06	0.477	1.3	3
12-HH80-81	1.70	21900	3	1.56 ± 0.14	108 ± 10	$(4.2 \pm 0.6) \times 10^{-17}$	1.78 ± 0.04	0.473	...	...
13-W3IRS5	1.95	140000	3.5	1.04 ± 0.12	260 ± 30	$(2.4 \pm 0.3) \times 10^{-17}$	1.46 ± 0.04	0.602	1.5, 1.4	4, 7
14-AFGL 2591	3.00	190000	1.5	0.96 ± 0.12	250 ± 20	$(5.4 \pm 0.7) \times 10^{-17}$	1.80 ± 0.03	0.549	1.0, 2.0, 1.0	4, 6, 7
15-CygX-N53	1.40	300	6	1.55 ± 0.22	45 ± 4	$(9.7 \pm 1.8) \times 10^{-17}$	1.76 ± 0.07	0.487	...	...
16-CygX-N12[e]	1.40	320	2.5	1.75 ± 0.26	50 ± 4	$(3.3 \pm 0.3) \times 10^{-17}$	1.52 ± 0.03	0.376	...	...
17-CygX-N63[e]	1.40	470	1	1.80 ± 0.33	45 ± 3	$(6.5 \pm 1.1) \times 10^{-17}$	2.03 ± 0.07	0.570	...	...
18-CygX-N48	1.40	4400	5	1.88 ± 0.18	58 ± 5	$(1.0 \pm 0.2) \times 10^{-16}$	1.71 ± 0.05	0.459	...	...
19-DR21-OH	1.40	10000	11	1.60 ± 0.26	73 ± 7	$(3.1 \pm 0.6) \times 10^{-16}$	1.98 ± 0.08	0.808	1.8, 1.4	4, 7

Palau et al. 2014, ApJ, 785, 42


OMC-1S: ALMA@1.3mm, beam ~ 0.2''

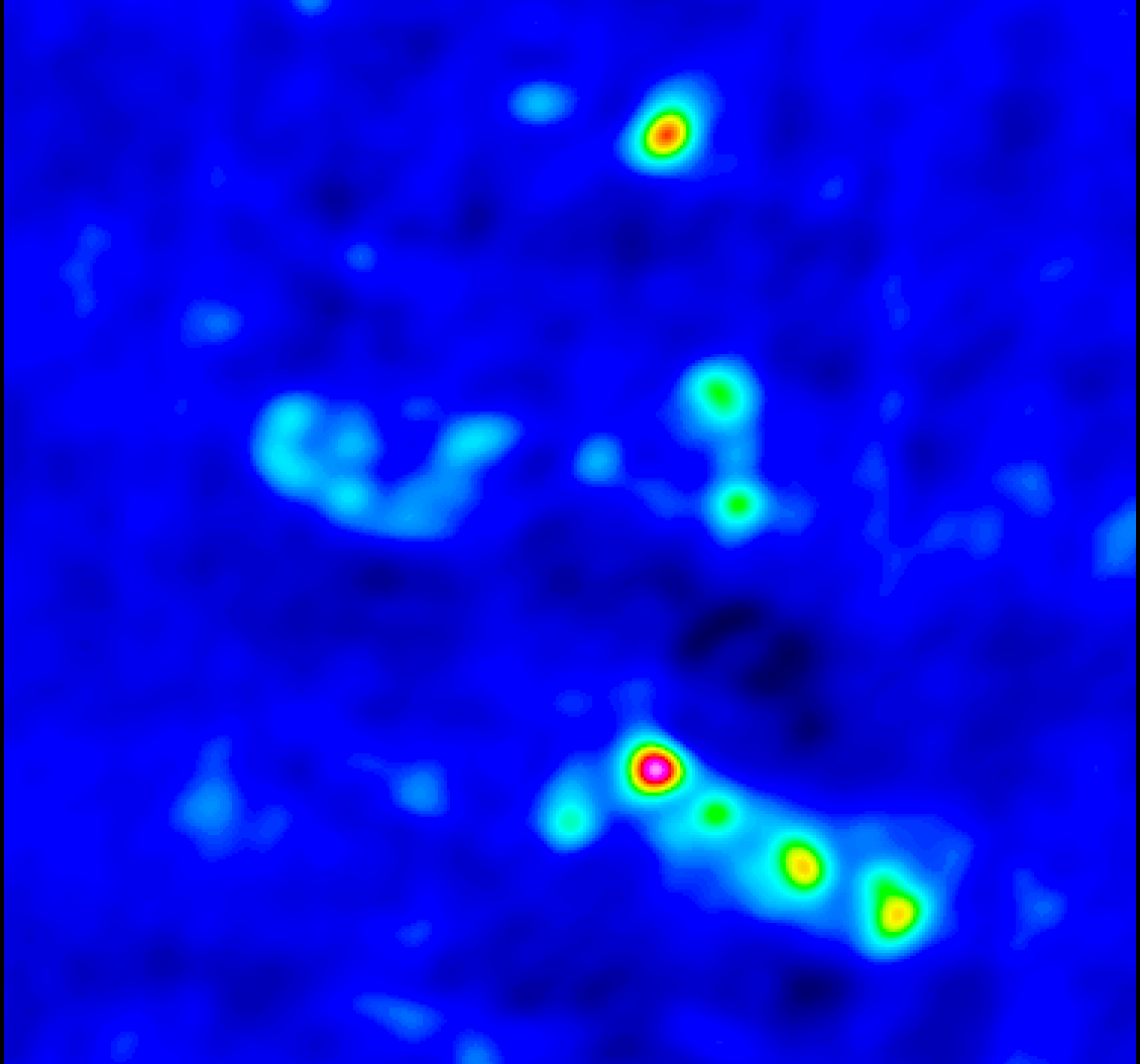

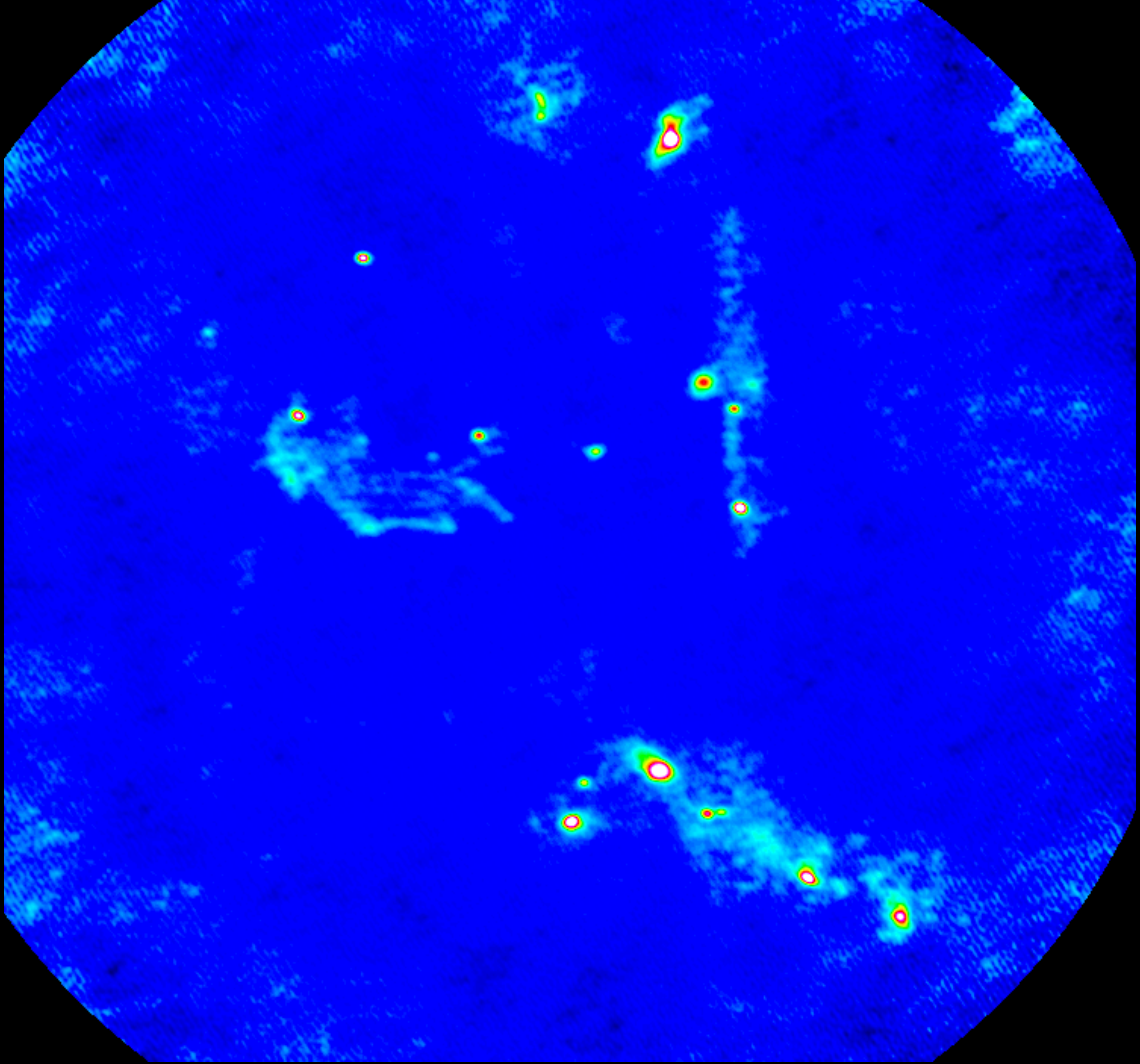

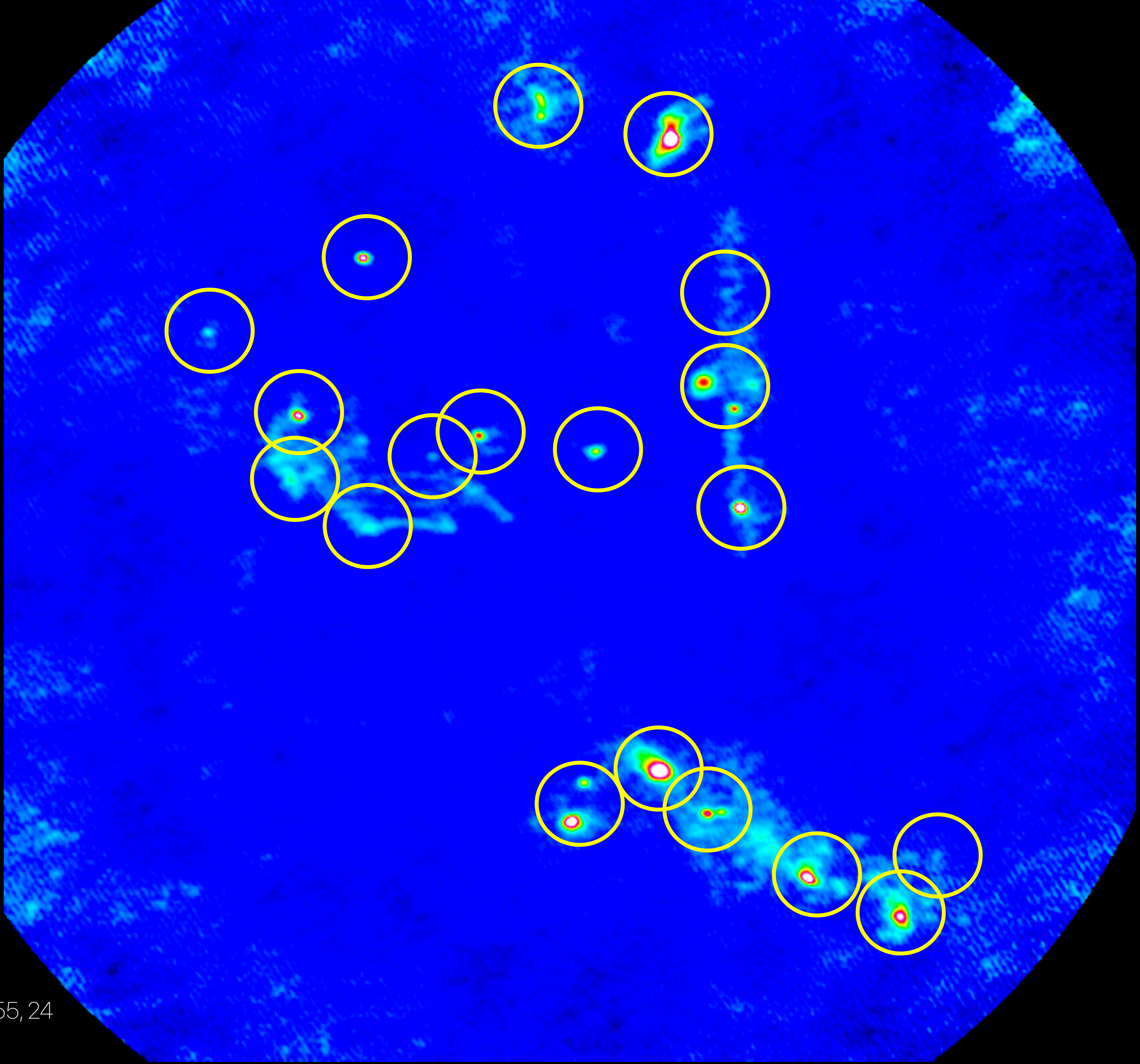

Palau et al. 2018, ApJ, 855, 24

Again, a trend of higher N_{mm} with density

Consistent with findings of Palau et al. 2014, 2015 but now at scales 1 order of magnitude smaller!

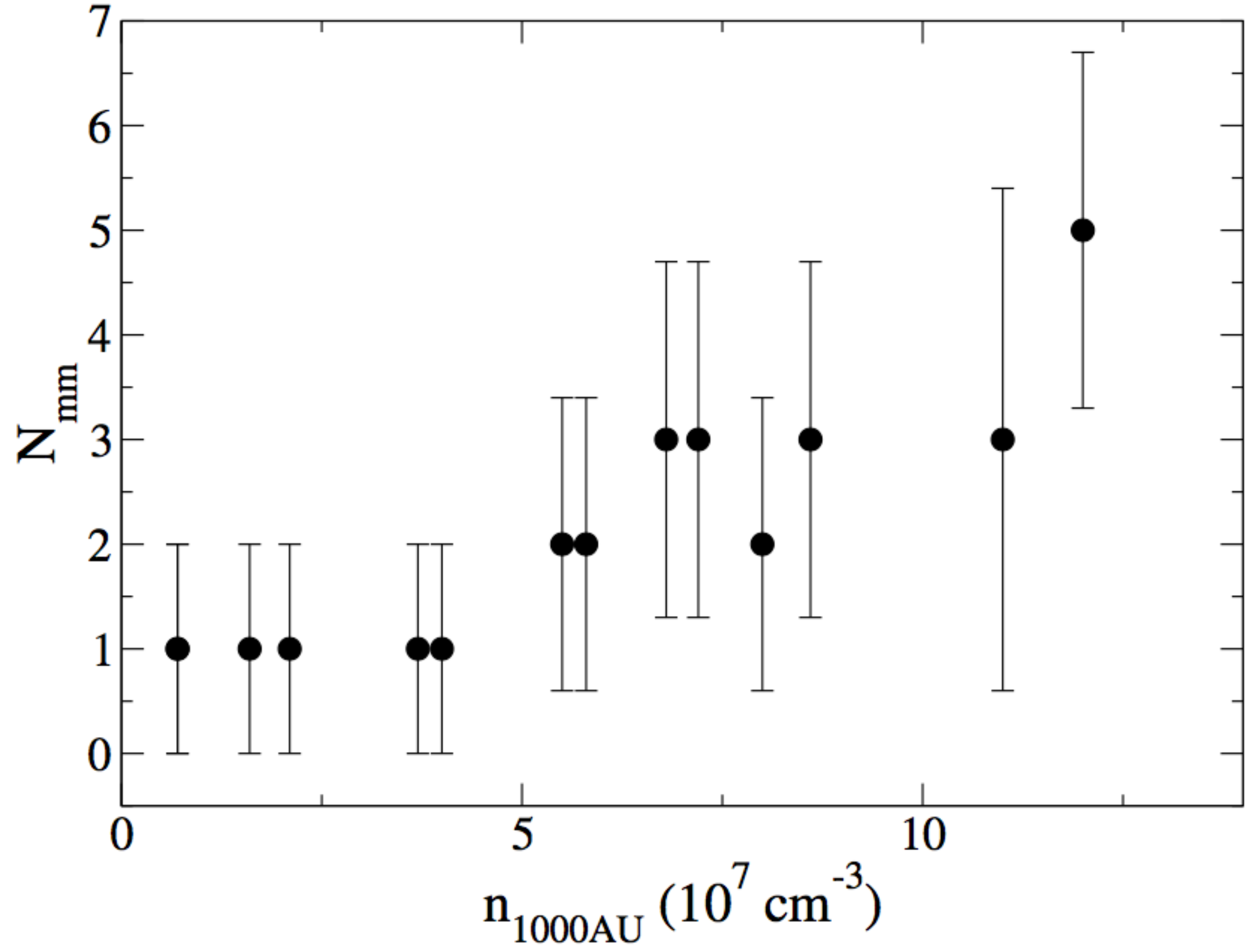

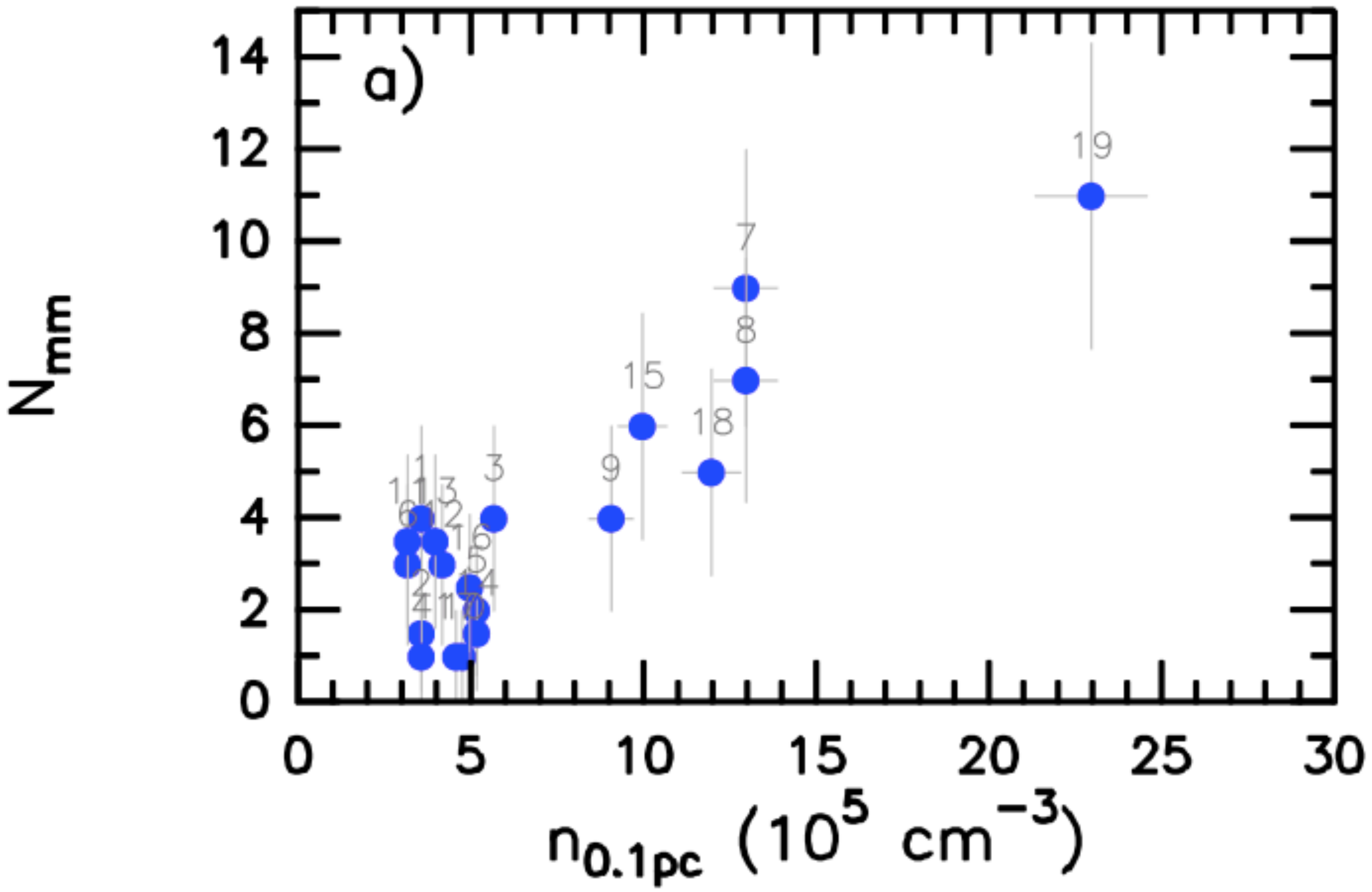

Palau et al. 2018, ApJ, 855, 24

Again, a trend of higher N_{mm} with density

Consistent with findings of Palau et al. 2014, 2015 but now at scales 1 order of magnitude smaller!

Trend also found in Perseus cloud (Pokhrel, Myers, Dunham et al. 2018)

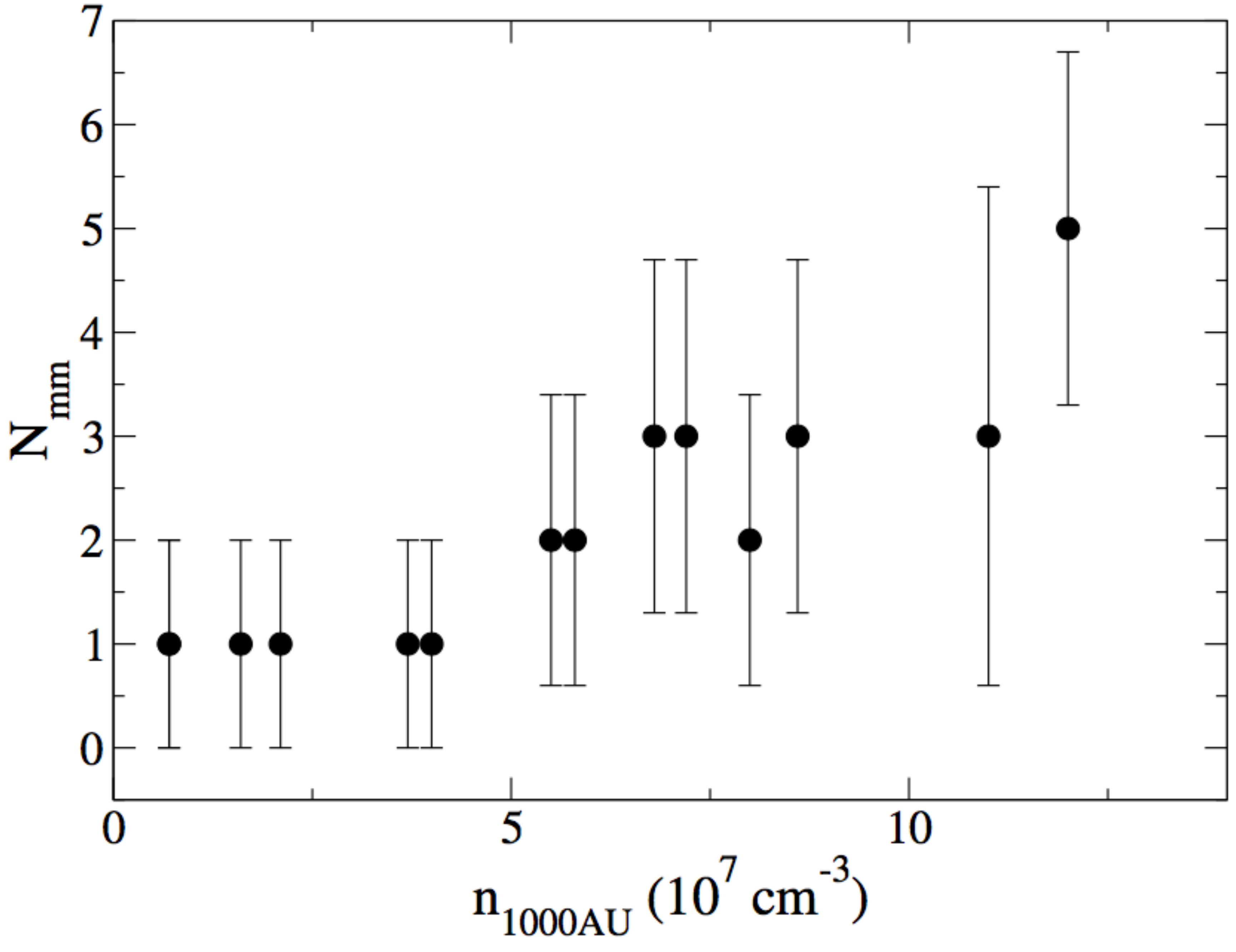

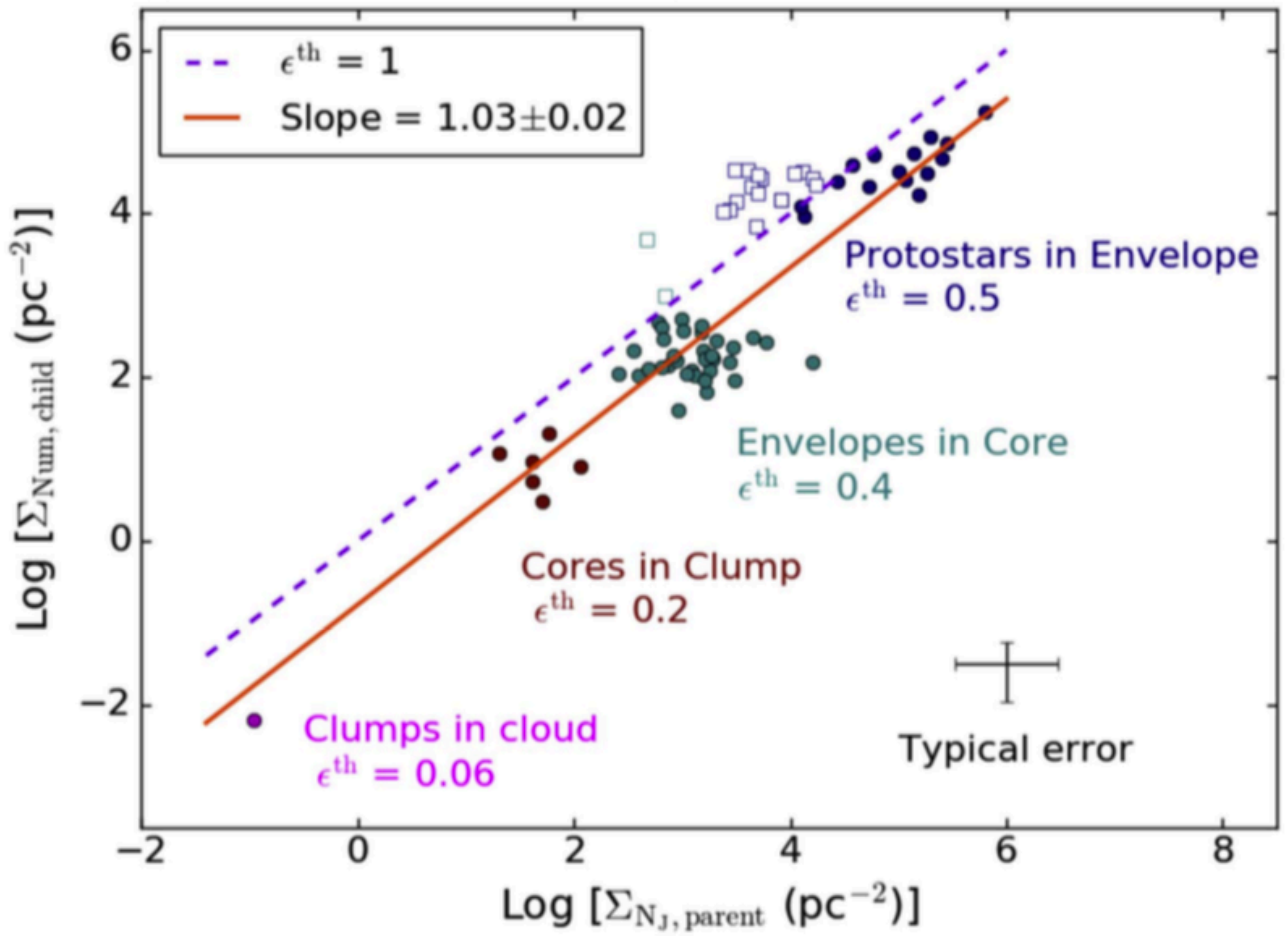

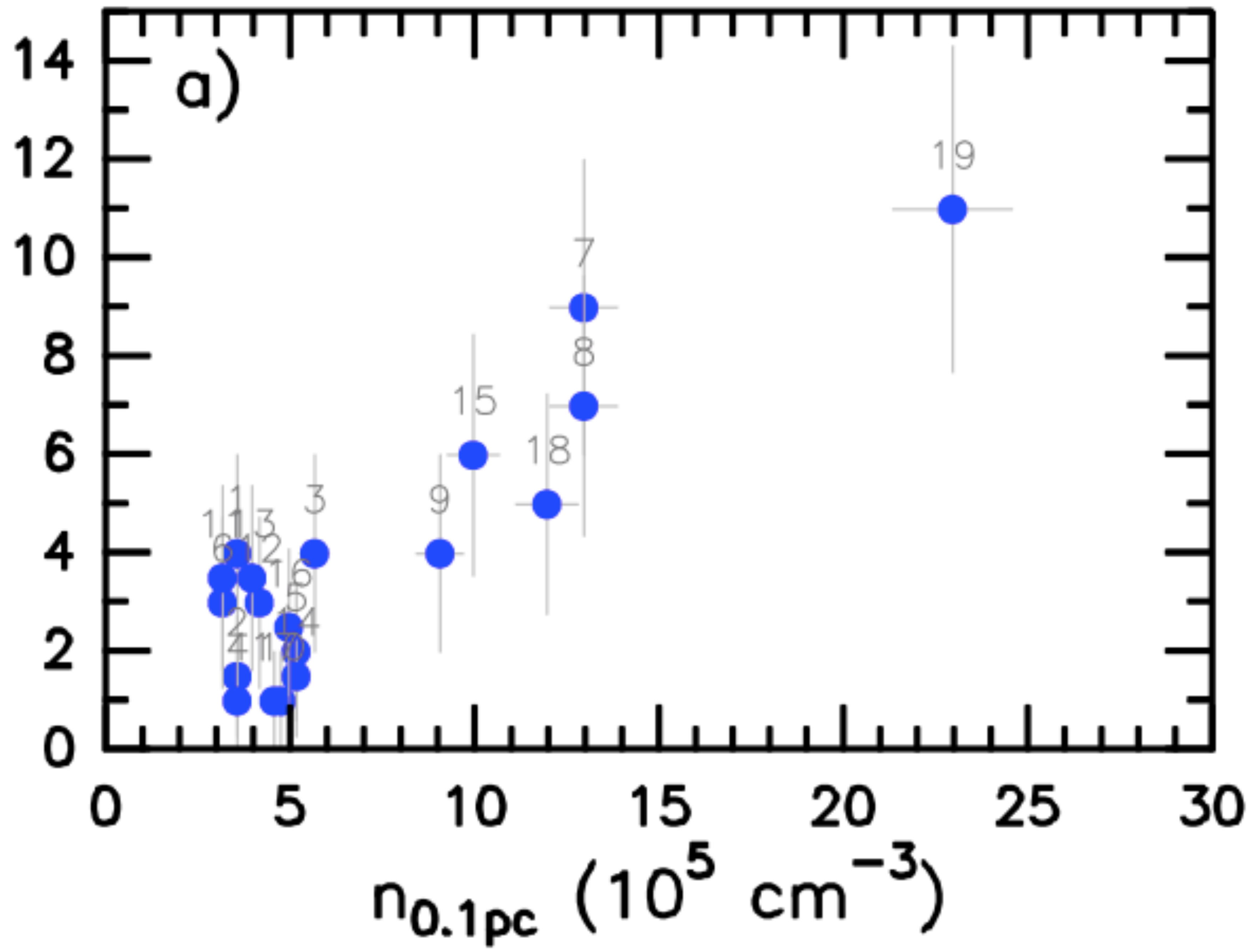

Conclusions

sample of 19 massive dense cores: study fragmentation level vs several properties of the cores

fragmentation within 0.1 pc seems to be better described by pure thermal Jeans fragmentation, compared to rotational fragmentation and turbulent support

preliminary work shows no clear correlation of dispersion in polarization angles with fragmentation

ALMA data: same conclusions at 0.001 pc as for 0.01 pc

Thanks

Masses of fragments: 75 fragments in19 massive dense cores